Introduction of Polarized Electron ion Collider in China-EicC

Aiqiang Guo (IMP, CAS)

SPIN2025 - Sep.22-26 2025 @ Qingdao

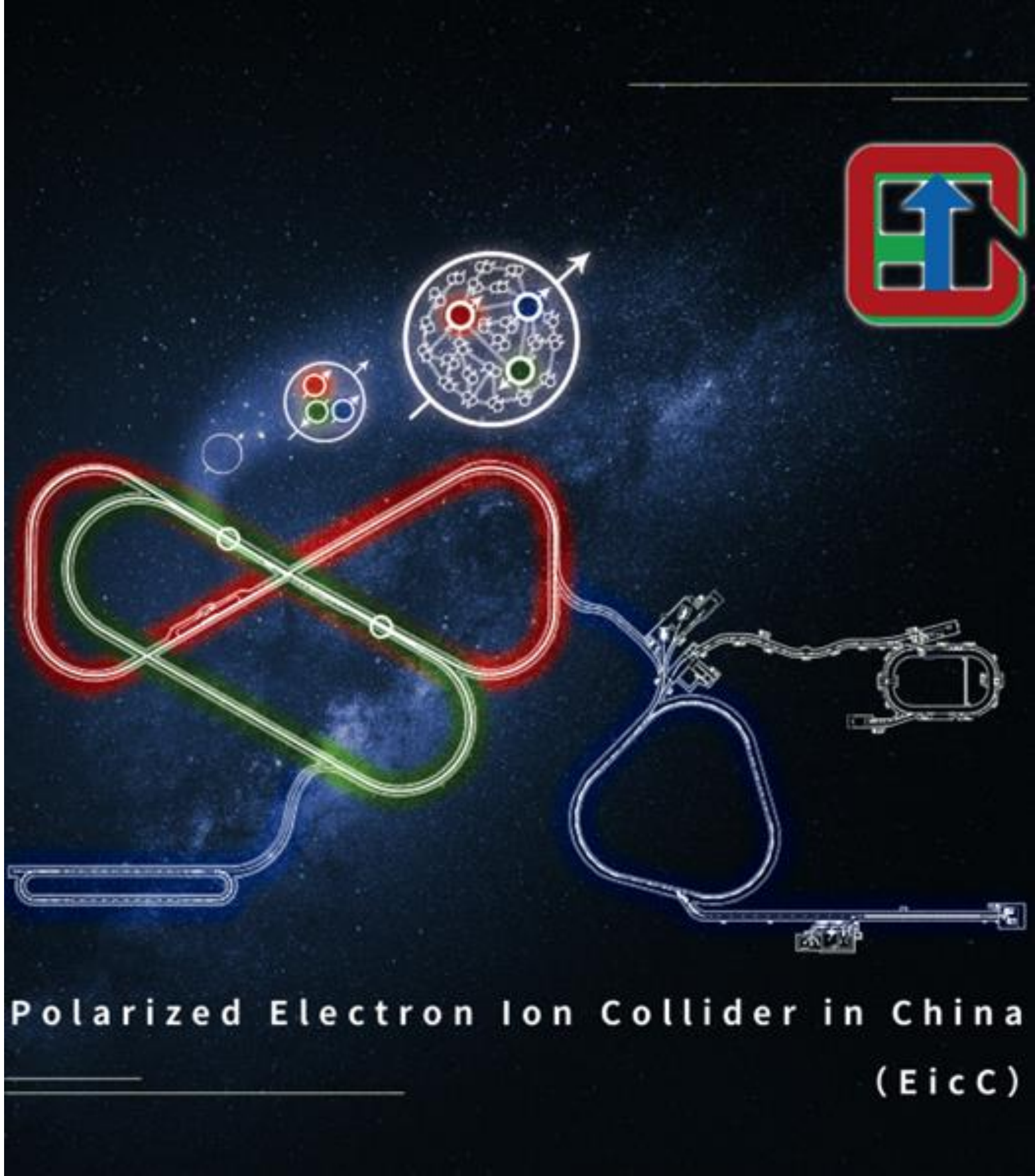

Nucleon structure

- **If we had a magical magnifying glass…**

Atom Nucleus Nucleon(Baryon) Meson

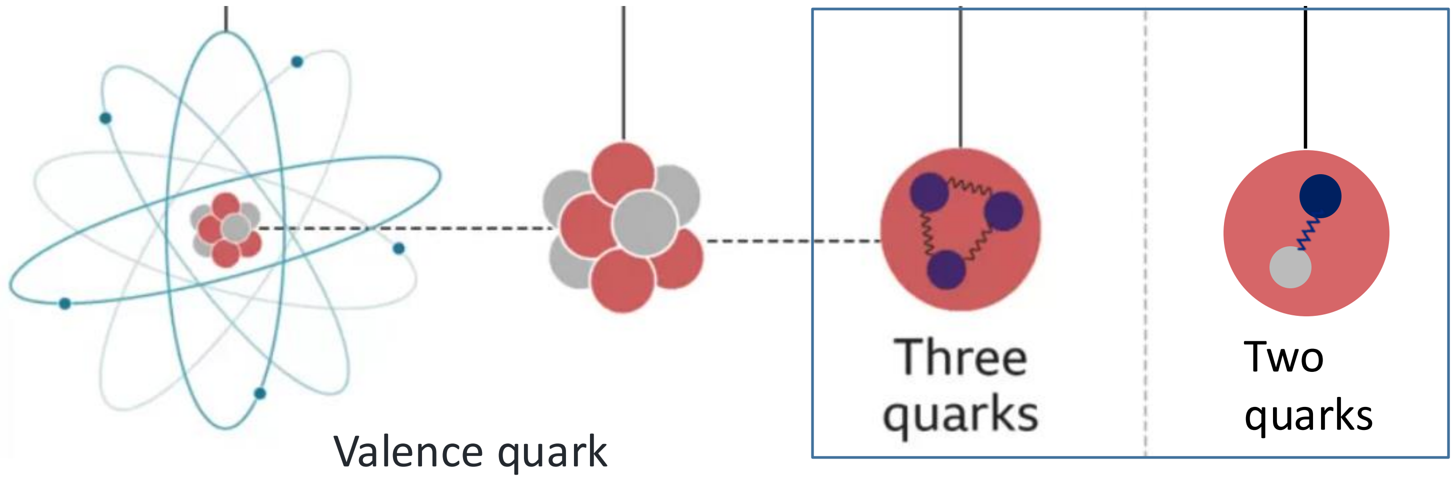

(1964-1974) hadron model

Strong force

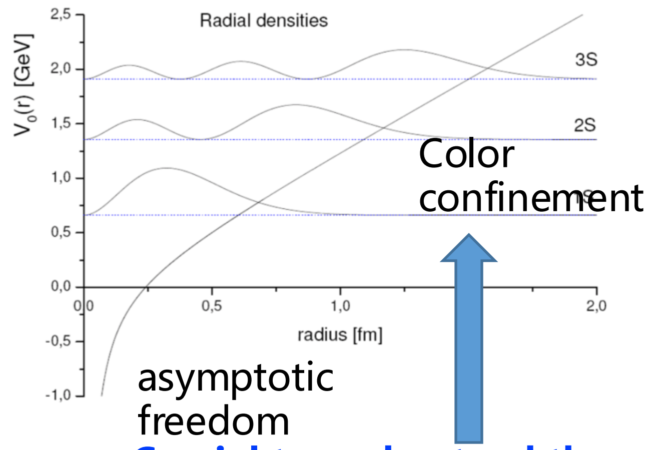

Crucial to understand the color confinement!

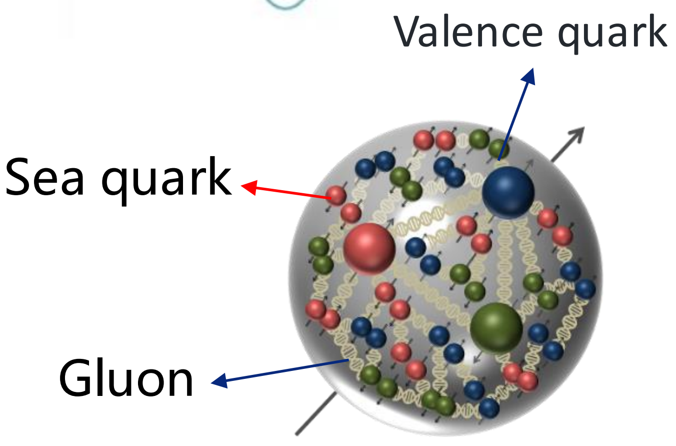

1974-1992

From DIS, more complex structure is found

From high Lum. Experiments, many exotics states are found

Challenge to hadron model !

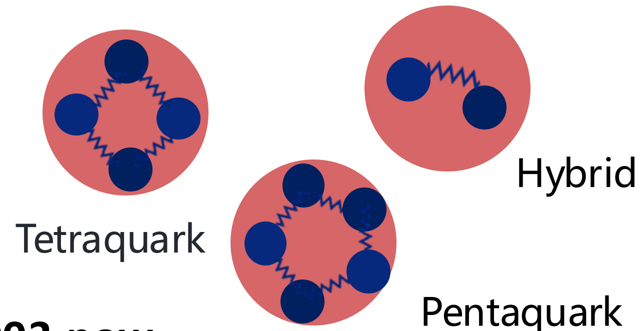

2003-now

Nucleon spin crisis

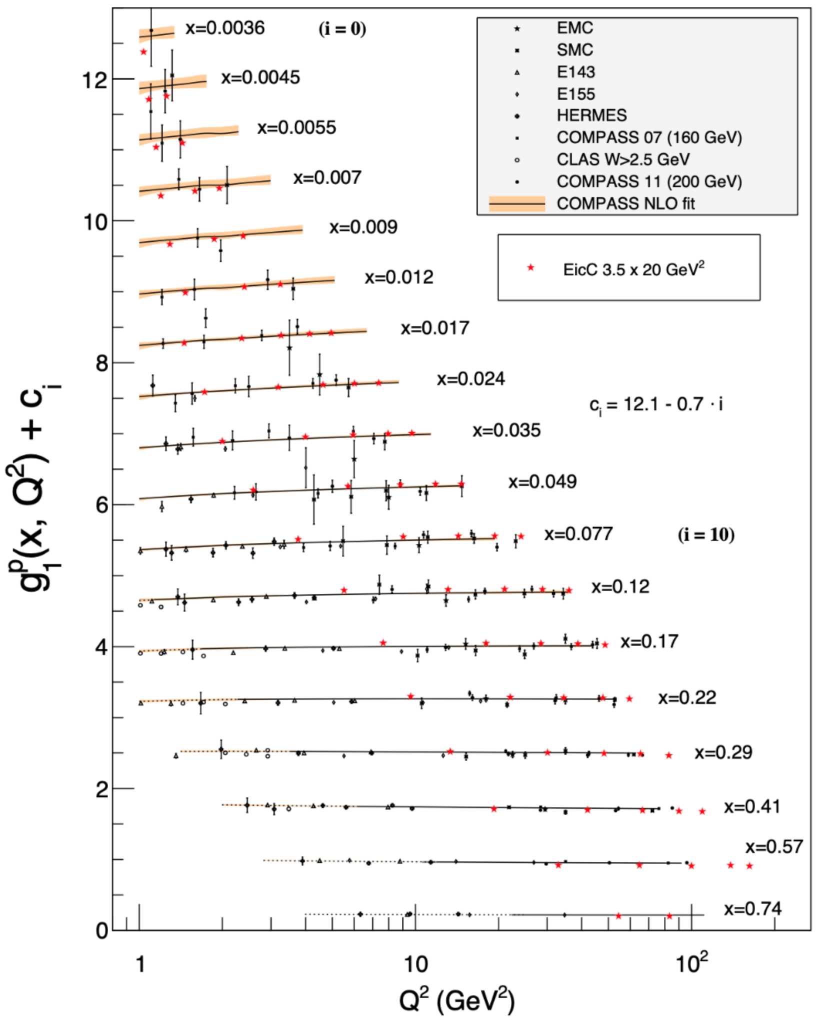

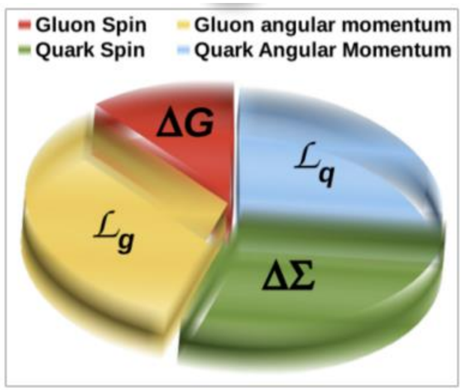

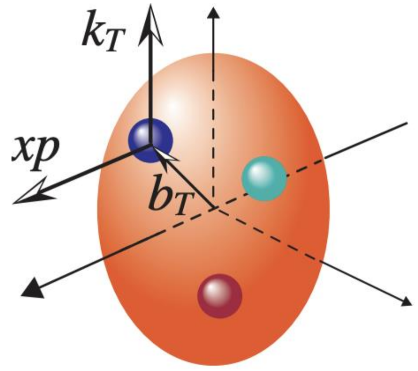

Spin decomposition: $S_{tot} = \frac{1}{2} = \frac{1}{2}\Delta\boldsymbol{\Sigma} + \Delta\boldsymbol{G} + \boldsymbol{\mathcal{L}}_q + \boldsymbol{\mathcal{L}}_g$

Quark spin | Gluon spin | Quark angular momentum | Gloun angular momentum

- **Accurate measurement of the nucleon polarization structure functions to determine the contributions of quark and gluon spins.**
- **Through three-dimensional tomographic imaging studies of the nucleon structure, researchers probe the transverse motion of quarks and gluons to investigate their orbital angular momentum.**

➢ ***Understand the origin of the nucleon spin!***

Lepton-Nucleon Scatterings

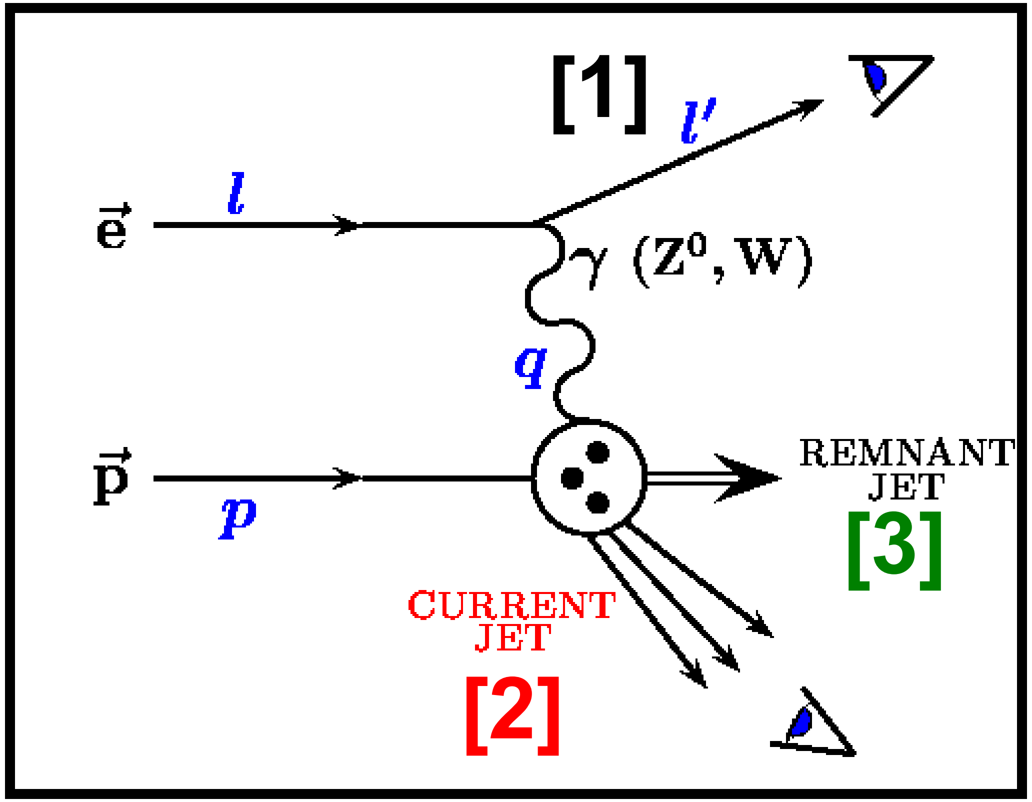

QED tool to study QCD nature of the nucleon

$$Q^2 = -q^2 = sxy$$

$$x = \frac{Q^2}{2p \cdot q}$$

$$y = \frac{p \cdot q}{p \cdot l}$$

$$s = 4E_e E_p$$

$$W = (q+p)^2$$

- QED probe is clean
- α_{EM} ~1/137 with broad Q coverage
- One-photon exchange approximation: ~1% accuracy
- Detection scale is determined by Q^2: 1GeV^2 ~ nucleon size

- **Observe scattered electron/muon** **[1] → inclusive**
- **Observe current jet/hadron** **[1]+[2] → semi-inclusive**
- **Observe remnant jet/hadron as well** **[1]+[2]+[3] → exclusive**
- **Electron Ion Collider (EIC), regarded as a "super electron microscope"**

Status of development in US

Electron-ion collider (EIC)

center-mass-energy~100 GeV

2005: discussion in community
2007, 2015: Long Range Plan in the US
2015: EIC white paper
2019.12: EIC approved (BNL)
2020: EIC CDR
2021: EIC TDR
2022: Detector Design Fixed
2024: Start to build
2030: Data taking

~1200 reserchers, ~230 institutes, 31 contries

US national labs: ANL/BNL/JLAB/LANL/LBNL/ORNL

Development in China-HIAF&EicC

中国电子－离子对撞机(EicC)

2012:Discussion in community
2020.2,2021.6:white paper(CN,EN)
2021-2023:CDR
Institutes：~45

As part of the long-term planning project for major scientific and technological infrastructure in particle physics and nuclear physics, the project has undergone two international expert reviews and one domestic expert review.

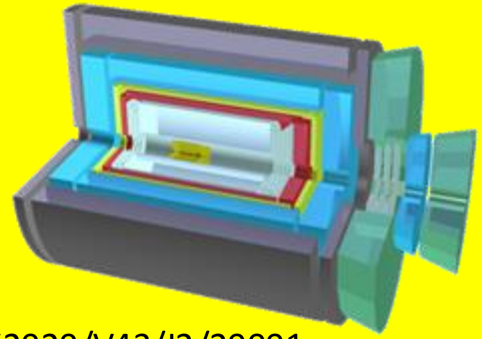

http://www.j.sinap.ac.cn/hjs/CN/Y2020/V43/I2/20001
https://journal.hep.com.cn/fop/EN/10.1007/s11467-021-1062-0

EicC's advantages (to EIC-US)：

1) The energy is in the sea quark region, closer to nuclear physics
2) Nearer to the threshold for the production of heavy quarkonium

HIAF:

Completed by the end of 2025, it will provide the world's highest-intensity pulsed heavy ion beams, creating unique conditions for the construction of the EicC

Relation between EicC and EIC

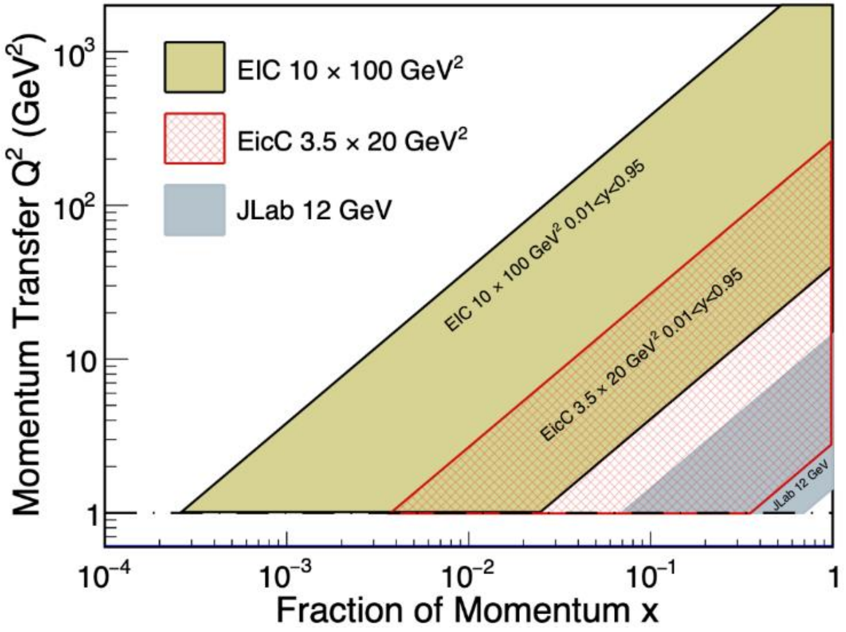

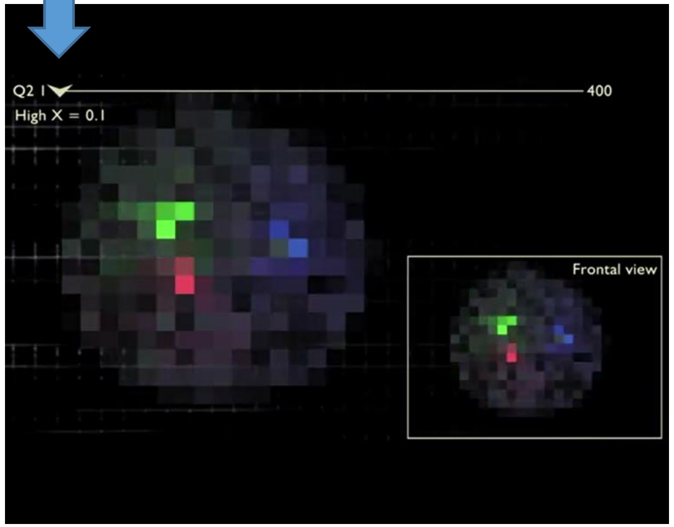

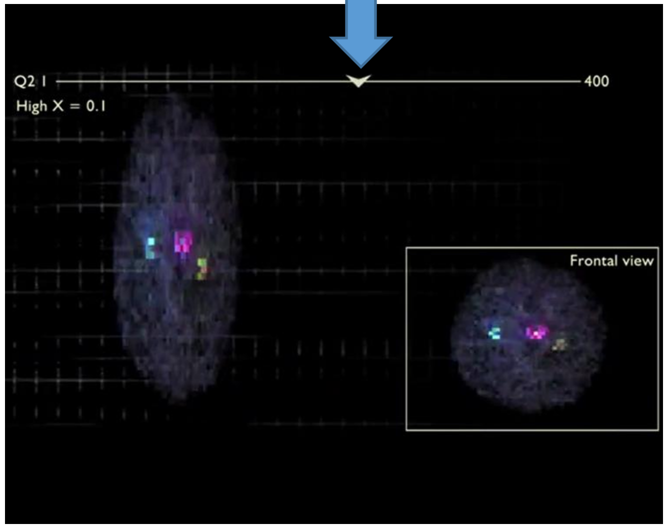

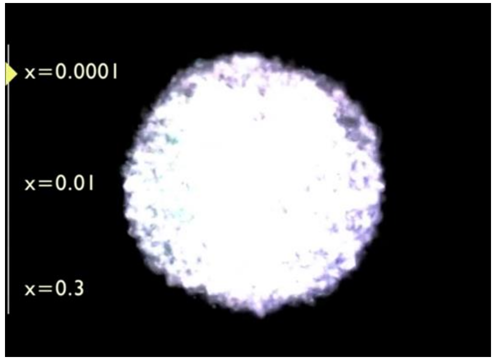

Gluon-dominated

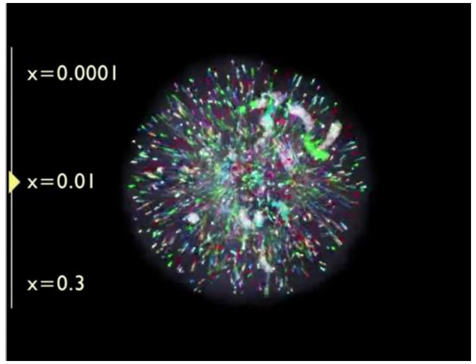

Gluon + sea quark

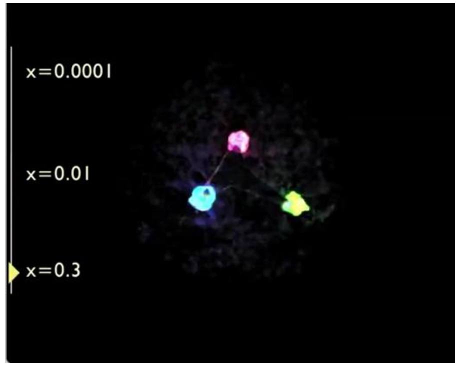

Flavor quark

- Different x, different inner plot
- Wild Q^2 coverage:
  - ➢ QCD evolution
  - ➢ Non-perturbative →perturbative

Unified view of nucleon structure

$W_p^u(x,k_T,r)$ *Wigner distributions* **(X. Ji)**

5D Dist.

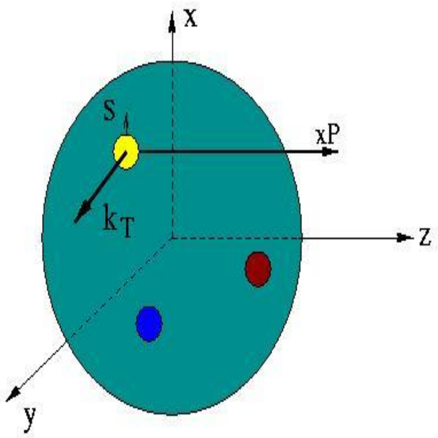

d^3r → **TMD PDFs**: $f_1^u(x,k_T)$, .. $h_1^u(x,k_T)$

$d^2k_T\,dr_z$ → **GPDs/IPDs**

3D imaging

TMD PDFs → d^2k_T → **PDFs**

GPDs/IPDs → d^2r_T → **PDFs**

GPDs/IPDs → *dx & Fourier Transformation* → **Form Factors**

PDFs: $f_1^u(x)$, .. $h_1^u(x)$

1D

Form Factors: $G_E(Q^2)$, $G_M(Q^2)$

Unified view of nucleon structure

$W_p^u(x,k_T,r)$ *Wigner distributions* **(X. Ji)**

5D Dist.

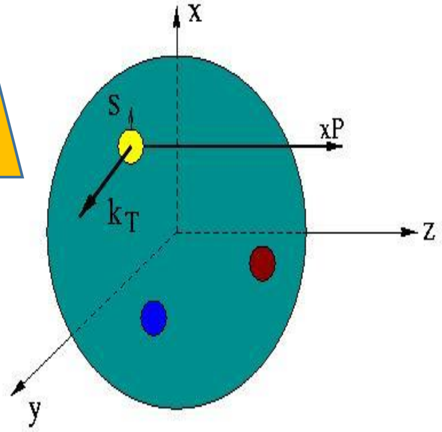

d^3r → *TMD PDFs* $f_1^u(x,k_T)$, .. $h_1^u(x,k_T)$

$d^2k_T\, dr_z$ → *GPDs/IPDs*

3D imaging

TMD PDFs —d^2k_T→ *PDFs*

GPDs/IPDs —d^2r_T→ *PDFs*

GPDs/IPDs —*dx & Fourier Transformation*→ *Form Factors*

PDFs
$f_1^u(x)$, .. $h_1^u(x)$

1D

Form Factors
$G_E(Q^2)$,
$G_M(Q^2)$

Experimentally

Highlighted physics topics

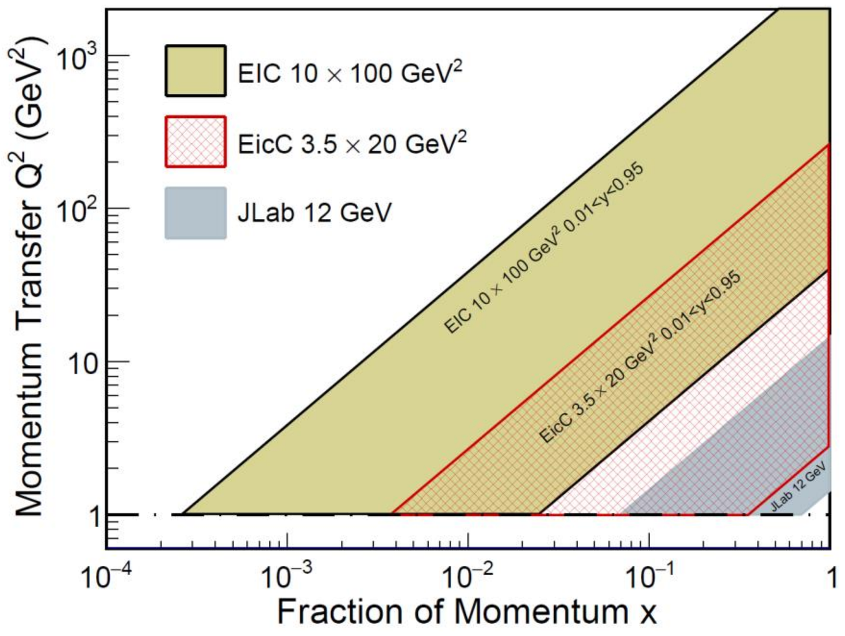

- Spin of the nucleon: 1D, 3D
  - polarized electron + polarized proton/light nuclei
- Partonic structure of nuclei and the parton interaction with the nuclear environment
  - unpolarized electron + unpolarized various nuclei
- Exotic states with c/cbar, b/bbar (BESIII community in China)
- Mass of the nucleon

Highlighted physics topics

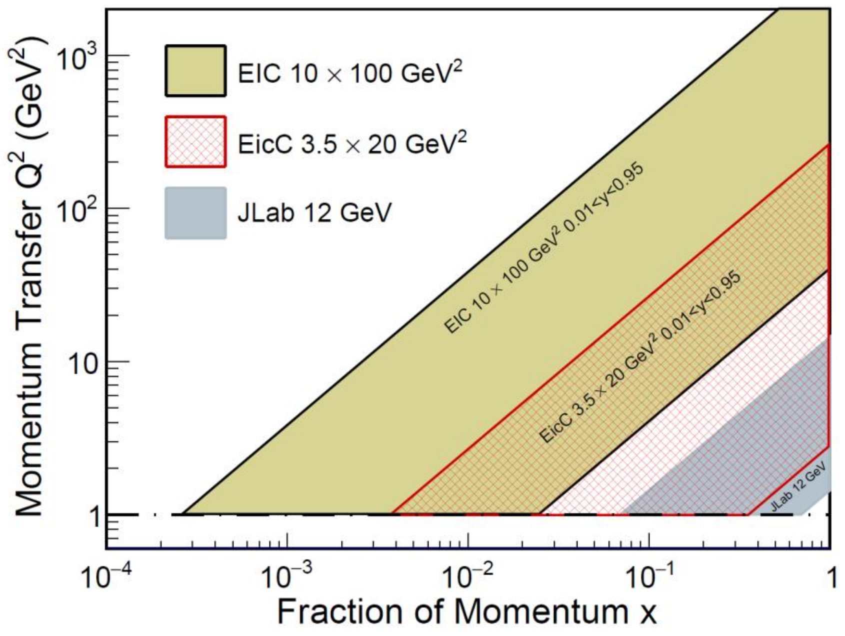

- Spin of the nucleon: 1D, 3D
  - polarized electron + polarized proton/light nuclei
- Partonic structure of nuclei and the parton interaction with the nuclear environment
  - unpolarized electron + unpolarized various nuclei
- Exotic states with c/cbar, b/bbar (BESIII community in China)
- Mass of the nucleon

SIDIS processes for flavor decompositions

Electron-proton scattering

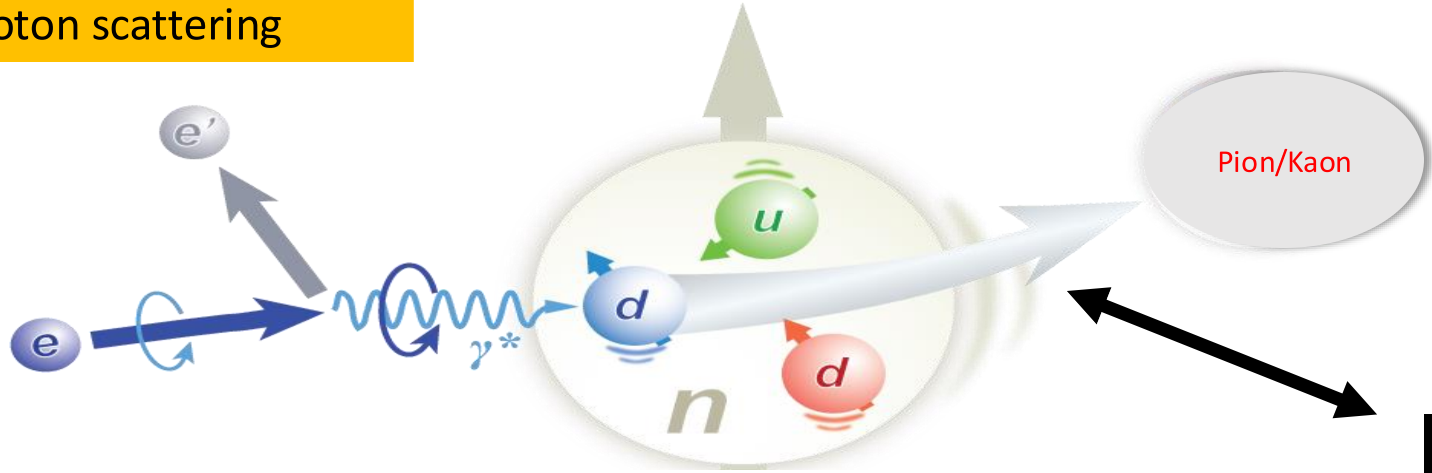

Fragmentation Functions

input

input

Experimental observable: polarized structure functions g1

$$g_1^h(x,Q^2,z) = \frac{1}{2}\sum_q e_q^2 \left[\Delta q(x,Q^2) D_q^h(z,Q^2) + \Delta \bar{q}(x,Q^2) D_{\bar{q}}^h(z,Q^2)\right]$$

Leading Order picture

Extracted nucleon structure information: polarized PDFs (helicity distribution)

Spin of the nucleon-helicity distribution

A NLO impact study
See arXiv:2103.10276
JHEP08(2021)034

EicC white paper

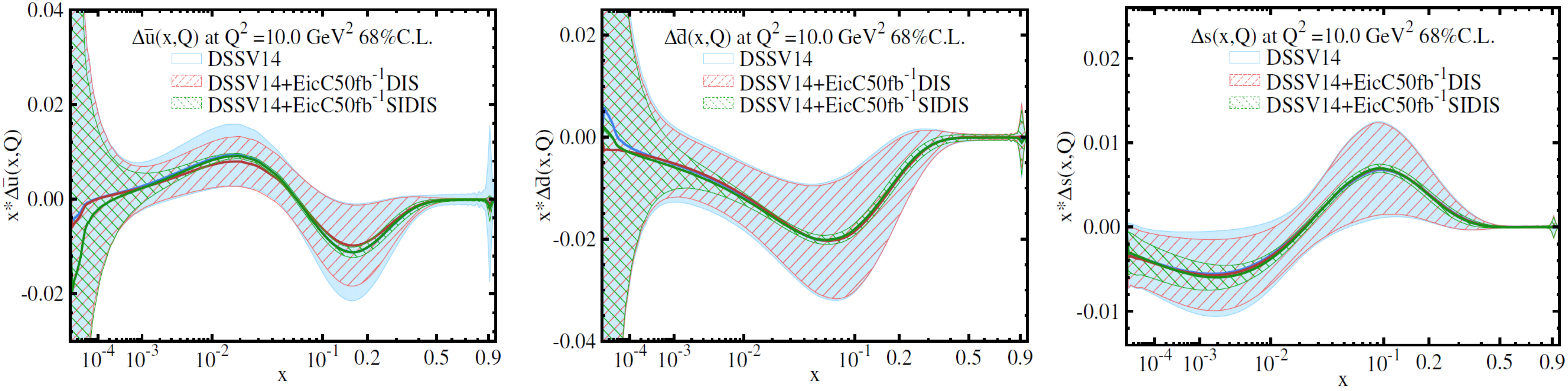

Gluon helicity distribution

One can perform double spin asymmetry ALL measurements in the e+p → e′ +D^0 +X process to access the gluon helicity distribution:

$$A_{LL}^{\vec{e}+\vec{p}\to e'+D^0+X} = \frac{1}{P_e P_p}\frac{N^{++}-N^{+-}}{N^{++}+N^{+-}},$$

$$= \frac{\Delta g(x,Q) * f(g \to D\text{^}0\,)}{g(x,Q) * f(g \to D\text{^}0\,)} = \Delta g/g$$

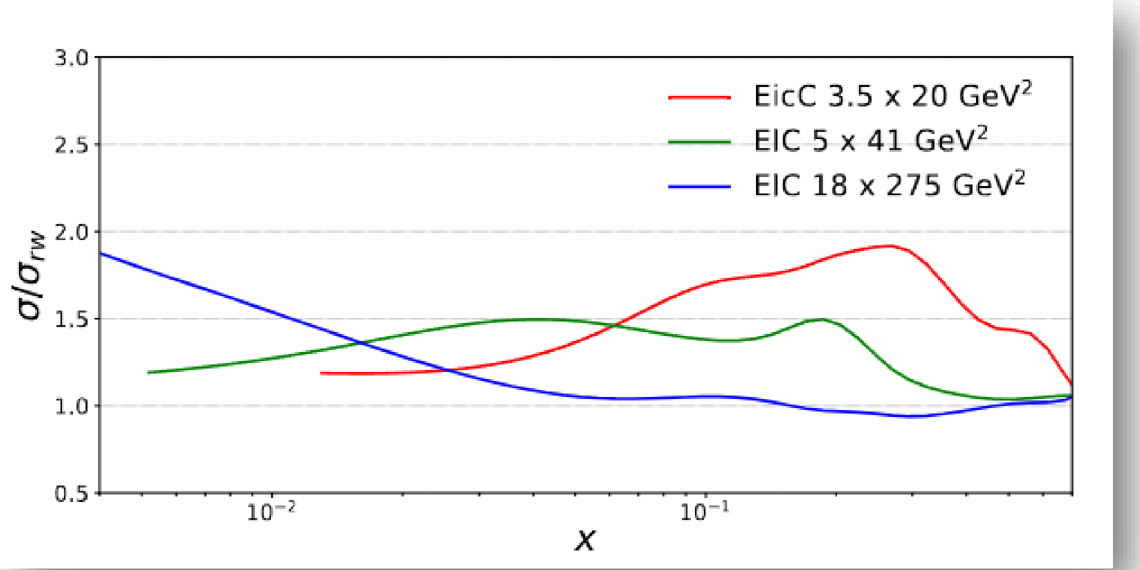

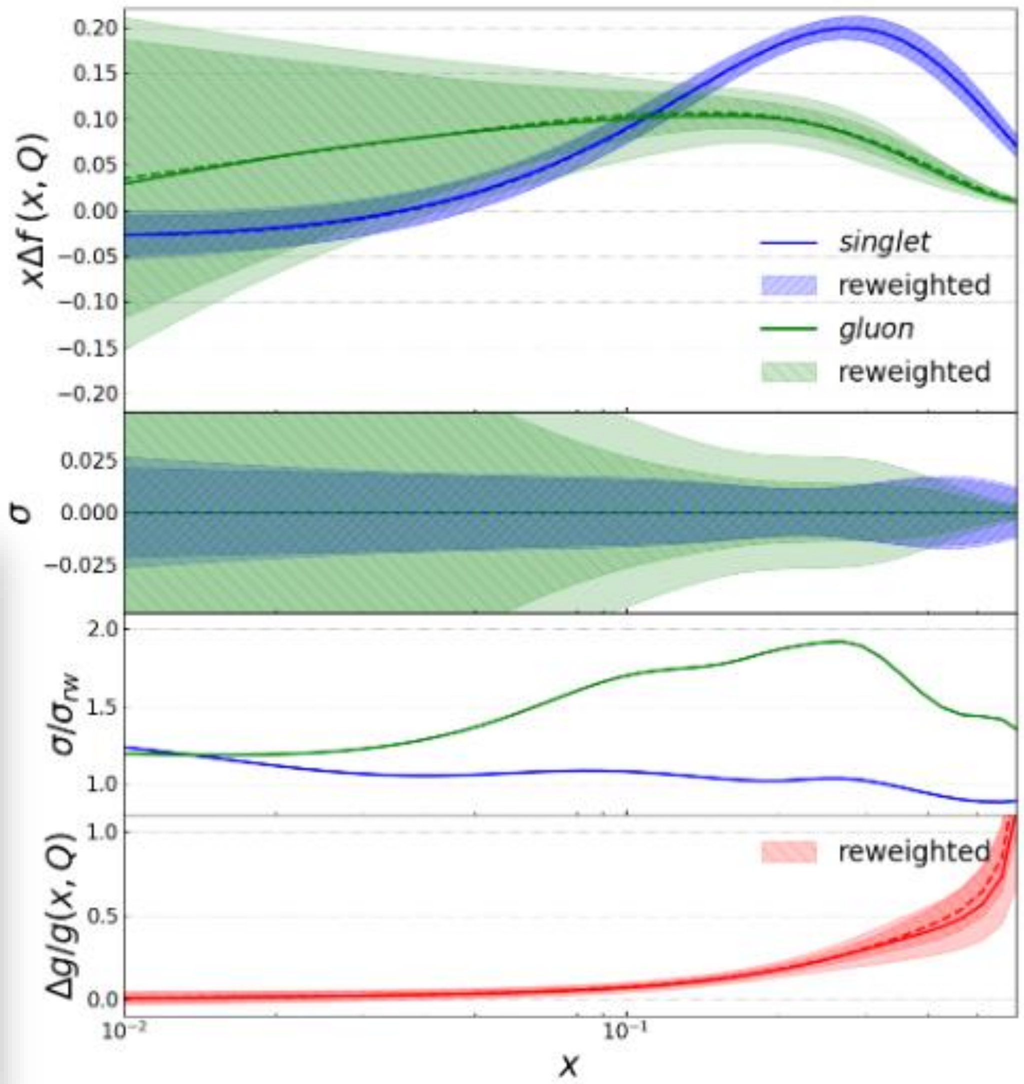

Spin-dependent TMDs (Leading-Twist)

Nucleon Polarization	Quark polarization: Unpolarized (U)	Quark polarization: Longitudinally Polarized (L)	Quark polarization: Transversely Polarized (T)
U	$f_1 =$		$h_1^{\perp} =$ Boer-Mulders
L		$g_1 =$ Helicity	$h_{1L}^{\perp} =$ Worm Gear
T	$f_{1T}^{\perp} =$ Sivers	$g_{1T} =$ Worm Gear	$h_1 =$ Transversity $h_{1T}^{\perp} =$ Pretzelosity

Nucleon Spin *Quark Spin*

Survive the k_T integration, yield 1D pdfs

Left items: The correlation between parton transverse momentum and the spin of quarks

A.Kotzinian, Nucl. Phys. **B441**, 234 (1995). *Bacchetta, Diehl, Goeke, Metz, Mulders and Schlegel JHEP 0702:093 (2007)*

TMDs in SIDIS Cross Section

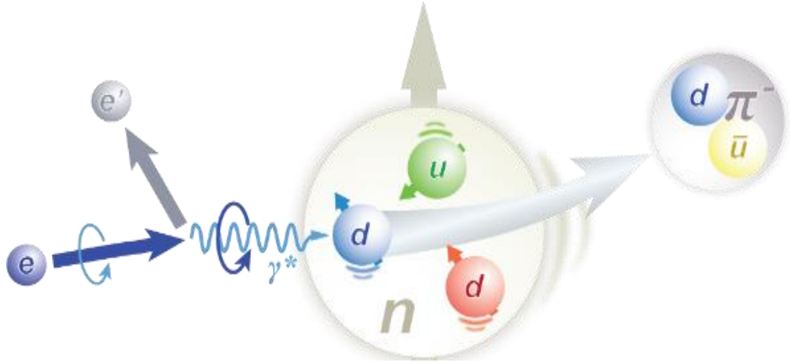

$$\frac{d\sigma}{dx\,dy\,d\phi_S\,dz\,d\phi_h\,dP_{h\perp}^2} = \frac{\alpha^2}{xyQ^2}\frac{y^2}{2(1-\varepsilon)}\cdot$$

Unpolarized

$$\{F_{UU,T} + \ldots$$

$$+\,\varepsilon\cos(2\phi_h)\cdot F_{UU}^{\cos(2\phi_h)} + \ldots$$

Polarized Target

$$+\,S_L[\varepsilon\sin(2\phi_h)\cdot F_{UL}^{\sin(2\phi_h)} + \ldots]$$

$$+\,S_T[\varepsilon\sin(\phi_h+\phi_S)\cdot F_{UT}^{\sin(\phi_h+\phi_S)}$$

$$+\sin(\phi_h-\phi_S)\cdot(F_{UT}^{\sin(\phi_h-\phi_S)} + \ldots)$$

$$+\,\varepsilon\sin(3\phi_h-\phi_S)\cdot F_{UT}^{\sin(3\phi_h-\phi_S)} + \ldots]$$

Polarized Beam and Target

$$+\,S_L\lambda_e[\sqrt{1-\varepsilon^2}\cdot F_{LL} + \ldots]$$

$$+\,S_T\lambda_e[\sqrt{1-\varepsilon^2}\cos(\phi_h-\phi_S)\cdot F_{LT}^{\cos(\phi_h-\phi_S)} + \ldots]\}$$

- f_1 =
- Boer-Mulder $h_1^\perp$ =
- $h_{1L}^\perp$ =
- Transversity h_{1T} =
- Sivers $f_{1T}^\perp$ =
- Pretzelosity $h_{1T}^\perp$ =
- g_1 =
- $g_{1T}^\perp$ =

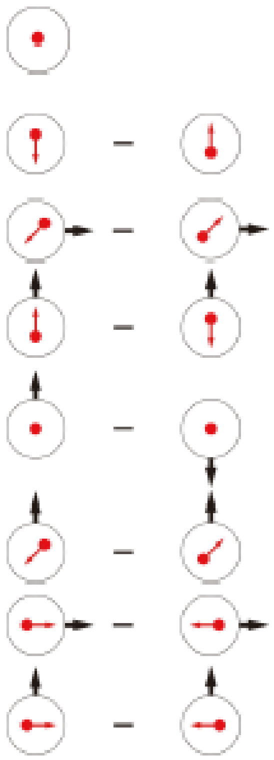

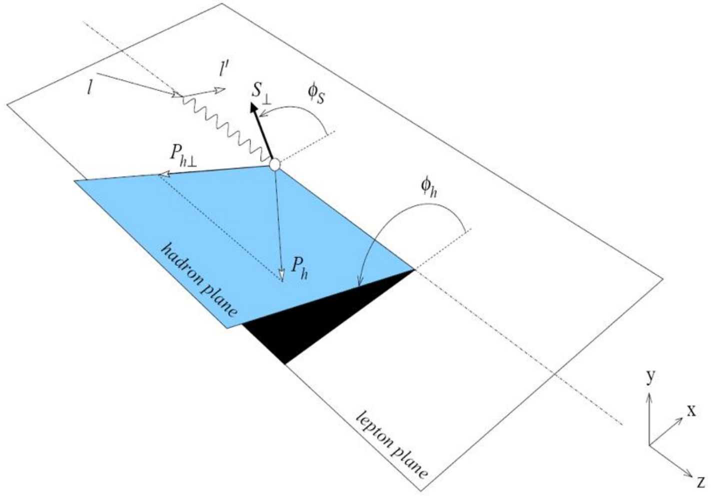

S_L, S_T: Target Polarization; λ_e: Beam Polarization

Target SSA, beam-target DSA measurements

Spin structure of the nucleon-TMDs

u/d Sivers EicC vs world data

LO analysis

EicC SIDS data:

- Pion(+/-), Kaon(+/-)
- ep: 3.5 GeV X 20 GeV
- eHe-3: 3.5 GeV X 40 GeV
- Pol.: e(80%), p(70%), He-3(70%)
- Lumi: ep 50 fb^{-1}, eHe-3 50 fb^{-1}

EicC, precise measurements.

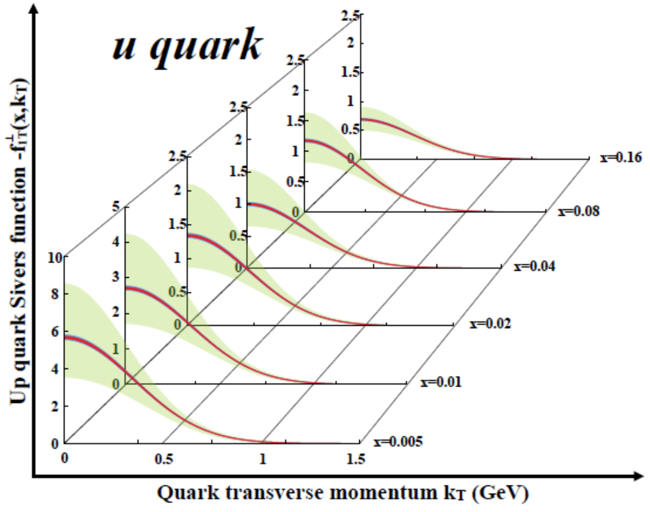

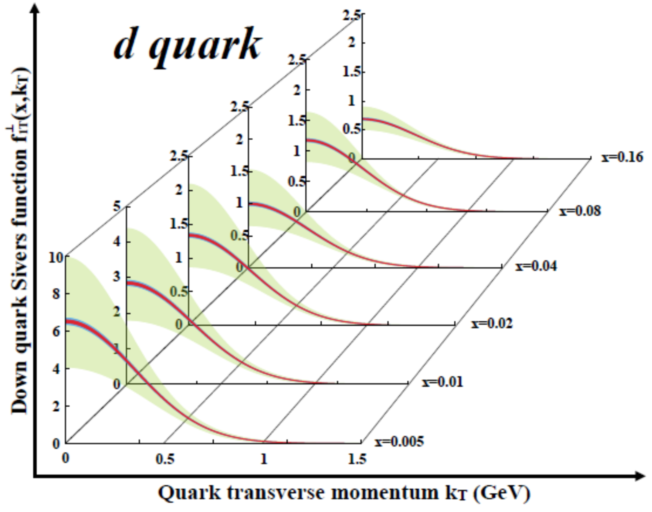

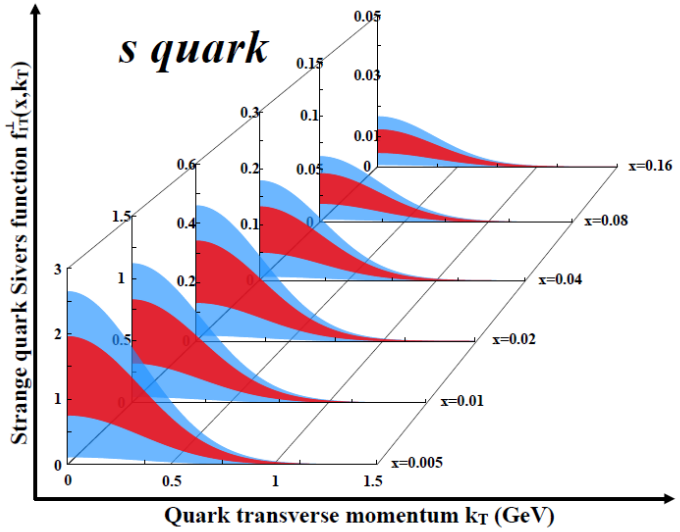

Green: Current accuracy
Red: stat. error only
Blue: sys. Error included

- sea quark Sivers function dynamically generated via Spin depenendent odderon
- leads to a unique predication for s-quark: quark and anit-quark Sivers functions flip sign

H. Dong, D. X. Zheng, J. Zhou, 2018

Highlighted physics topics

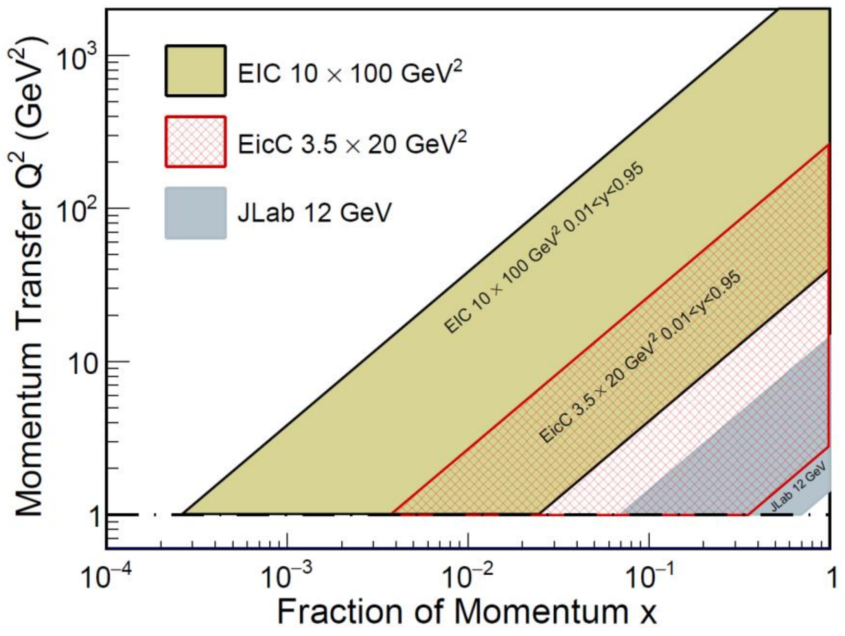

- Spin of the nucleon: 1D, 3D
  - polarized electron + polarized proton/light nuclei
- Partonic structure of nuclei and the parton interaction with the nuclear environment
  - unpolarized electron + unpolarized various nuclei
- Exotic states with c/cbar, b/bbar (BESIII community in China)
- Mass of the nucleon

Problems for cold nuclear matter effect

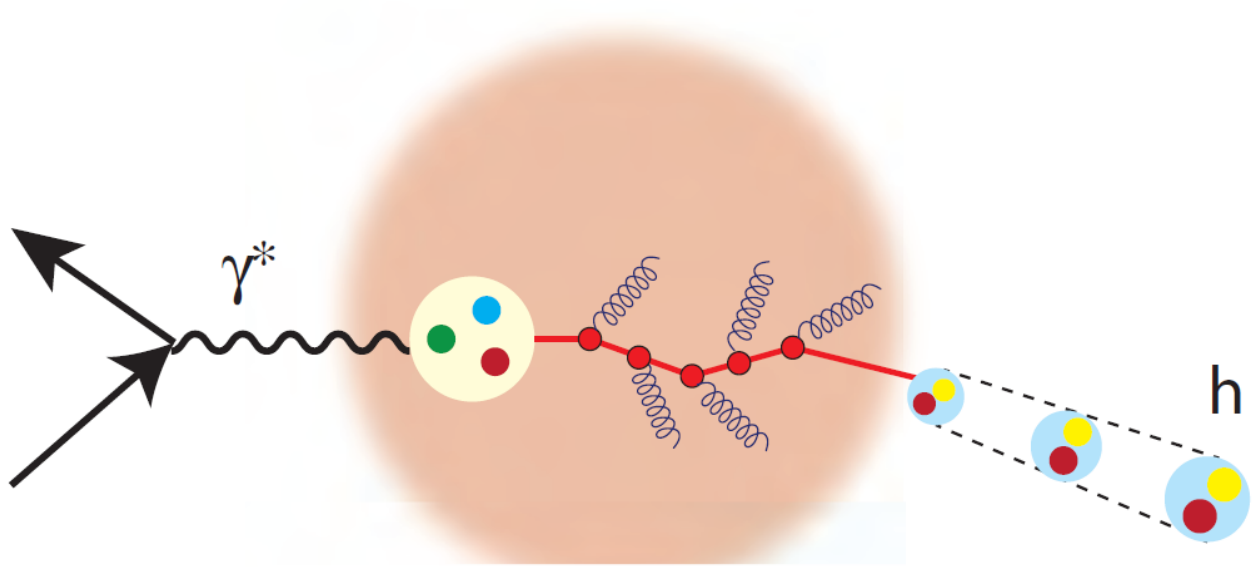

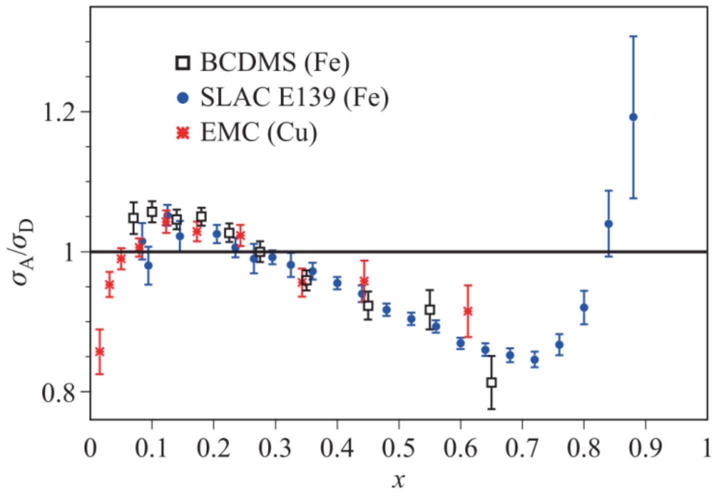

$$R_{u/p}^{\mathrm{Au}}(x, k_\perp, Q_0) = \frac{f_{u/p}^{\mathrm{Au}}(x, k_\perp, Q_0)}{f_{u/p}(x, k_\perp, Q_0)}$$

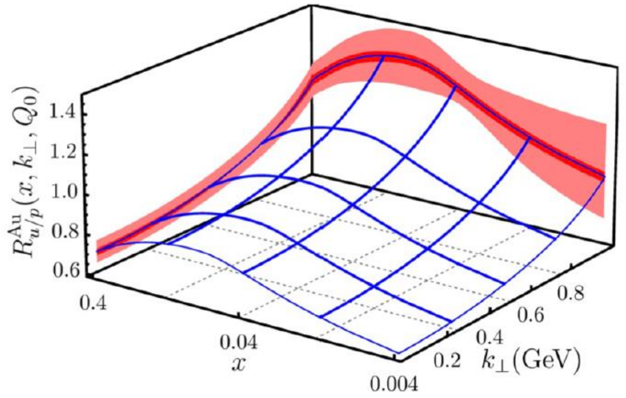

- Initial state parton distribution in nucleus (nPDFs)
- Intermediate state parton propagating in nuclear medium (energy loss, broadening…)
- Final state hadronization (hadron transport, FFs…)

arXiv:2107.12401

Problems for cold nuclear matter effect

Particle	Momentum (GeV/c/u)	CM energy (GeV/u)	Average polarization	Luminosity at the nucleon level ($cm^{-2} \cdot s^{-1}$)	Integrated luminosity (fb^{-1})
e	3.5		80%		
p	20	16.76	70%	2.00×10^{33}	50.5
d	12.90	13.48	Yes	8.48×10^{32}	21.4
$^{3}He^{++}$	17.21	15.55	Yes	6.29×10^{32}	15.9
$^{7}Li^{3+}$	11.05	12.48	No	9.75×10^{32}	24.6
$^{12}C^{6+}$	12.90	13.48	No	8.35×10^{32}	21.1
$^{40}Ca^{20+}$	12.90	13.48	No	8.35×10^{32}	21.1
$^{197}Au^{79+}$	10.35	12.09	No	9.37×10^{32}	23.6
$^{208}Pb^{82+}$	10.17	11.98	No	9.22×10^{32}	23.3
$^{238}U^{92+}$	9.98	11.87	No	8.92×10^{32}	22.5

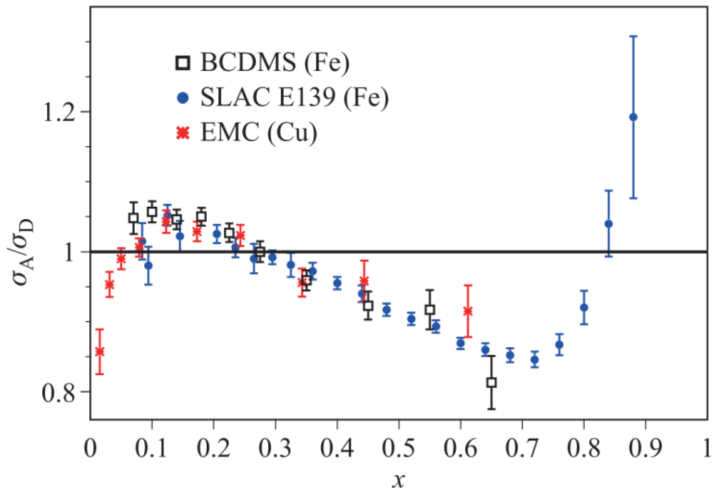

$$R_{u/p}^{Au}(x, k_\perp, Q_0) = \frac{f_{u/p}^{Au}(x, k_\perp, Q_0)}{f_{u/p}(x, k_\perp, Q_0)}$$

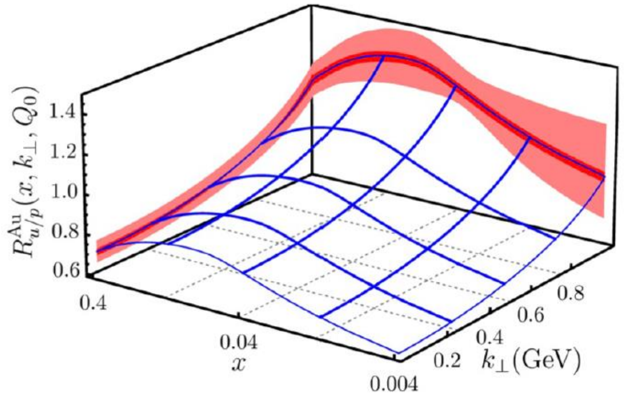

- Initial state parton distribution in nucleus (nPDFs)
- Intermediate state parton propagating in nuclear medium (energy loss, broadening…)
- Final state hadronization (hadron transport, FFs…)

arXiv:2107.12401

Nuclear PDFs study with ion beam

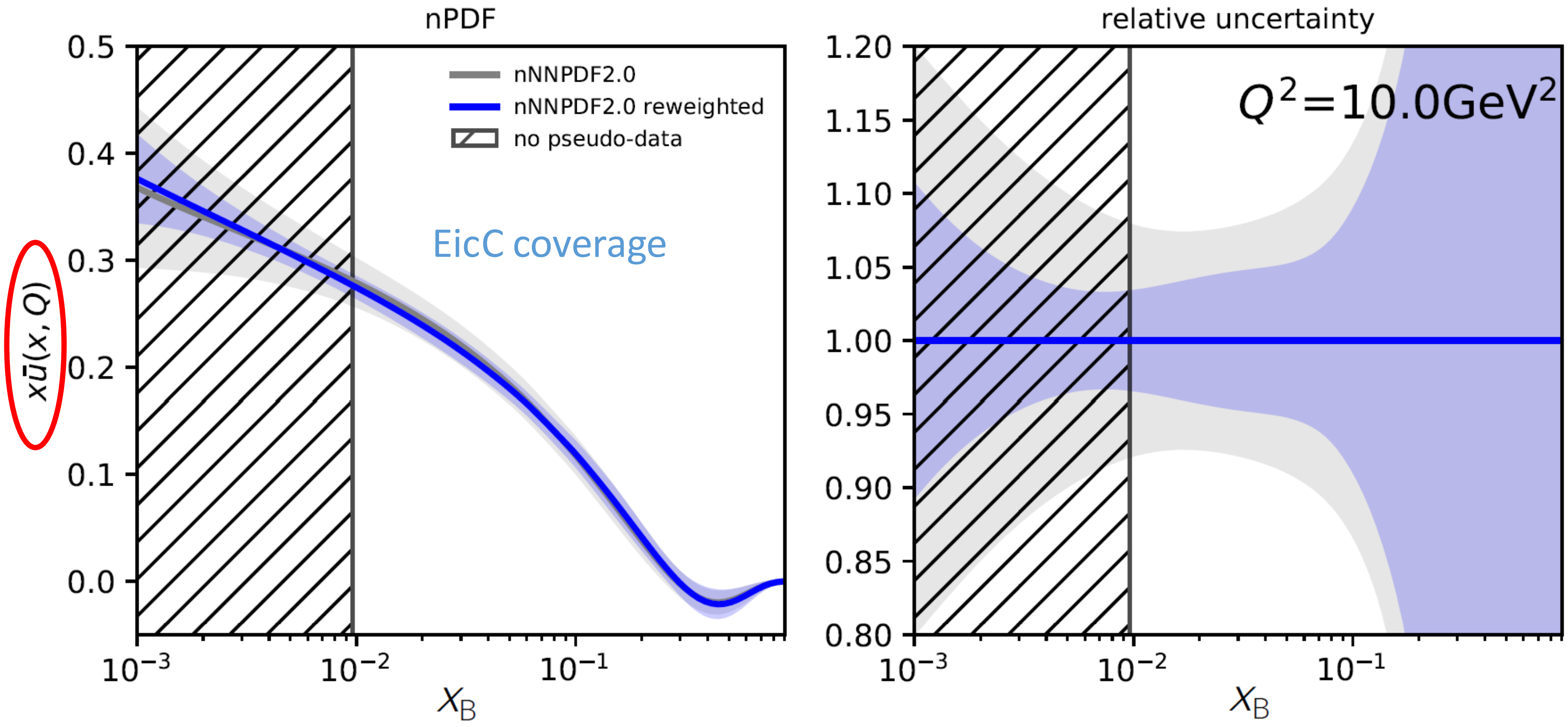

With only a few hours of running

Charm in-medium modification and hadronization at the EicC

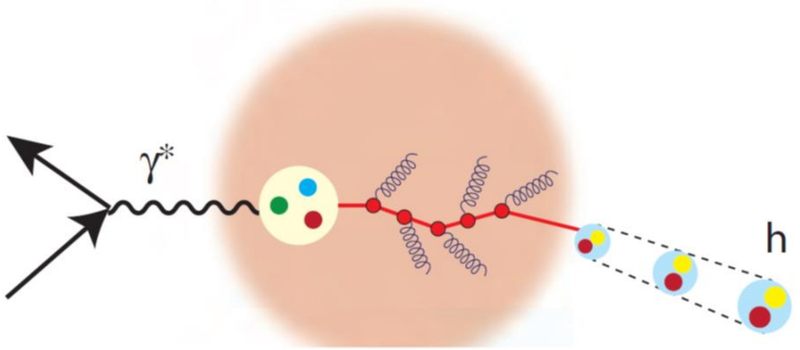

- Fragmentation and hadronization can be very different in different system.
- Because of the shorter formation time of heavy flavor mesons, they have stronger interaction with nuclear matter than light mesons.
- Their measurement at the EIC is expected to avoid most of the heavy-ion background
- Baryon-to-meson ratio $R = \frac{\Lambda_c^+}{D^0}$ can be studied at Eicc to investigate the effect of cold nuclear medium

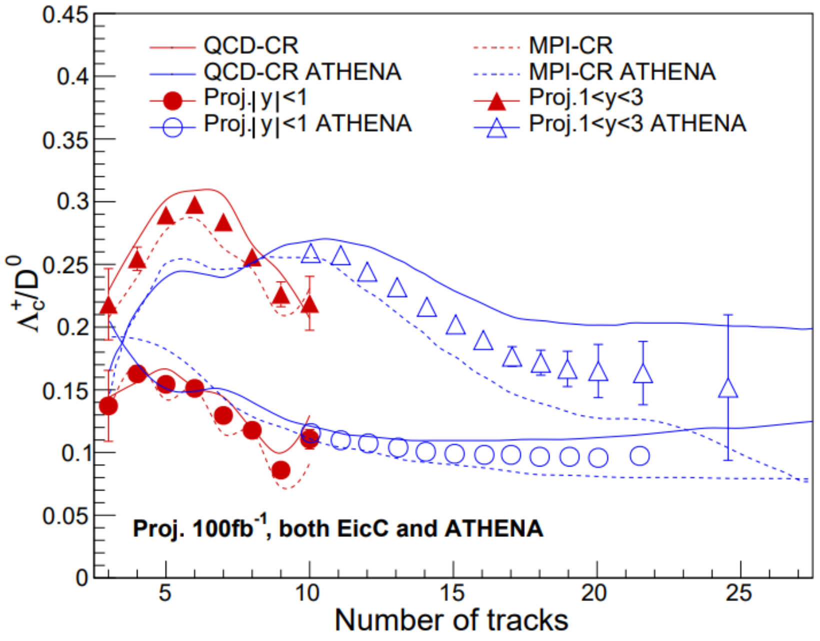

- Patron fragmentation varies with different system.
- Data is produced by pythia8 and two fragmentation model (QCD-CR and MPI-CR) are used.

Highlighted physics topics

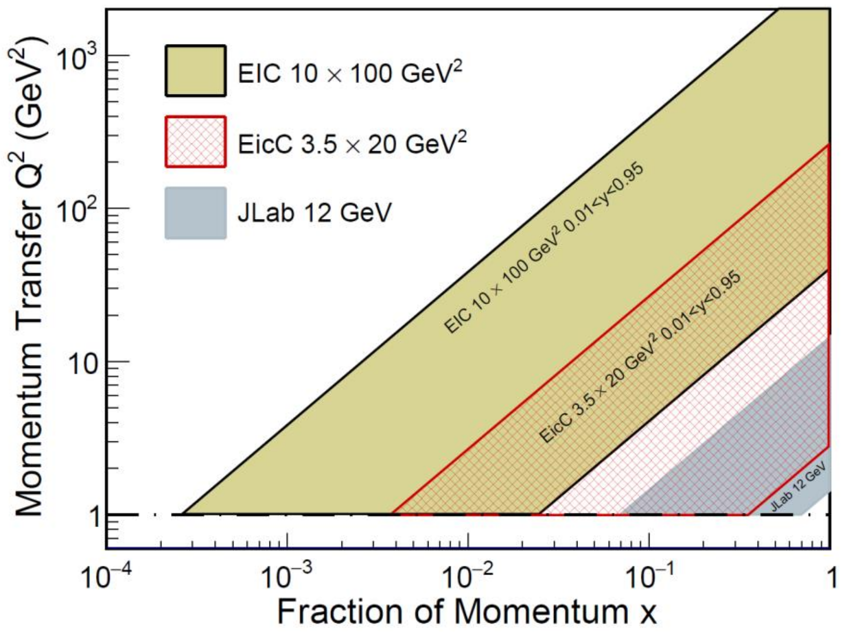

- Spin of the nucleon: 1D, 3D
  - polarized electron + polarized proton/light nuclei
- Partonic structure of nuclei and the parton interaction with the nuclear environment
  - unpolarized electron + unpolarized various nuclei
- Exotic states with c/cbar, b/bbar (BESIII community in China)
- Mass of the nucleon

Study of quarkonium at EicC

- Study the exotic states from **new production mechanism** is crucial to pin down their nature
- EicC as a unique electron-ion collider has many advantages
  - ➢ Larger cross section compared to e^+e^- collision
  - ➢ Smaller background compared to pp and pp collisions
  - ➢ Polarized beams: pin down the quantum numbers J^P
  - ➢ **No triangle singularity**

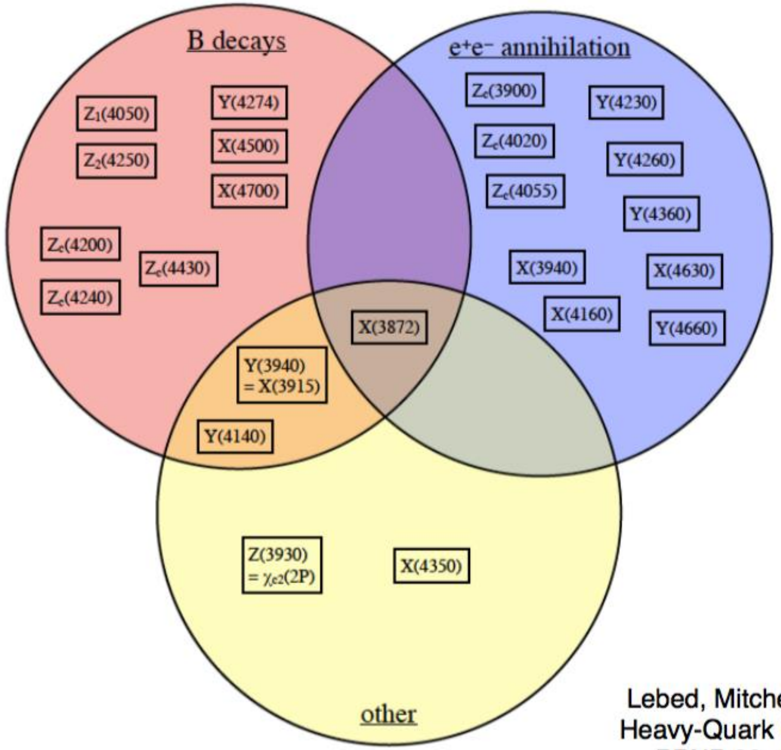

Lebed, Mitchell, Swanson, Heavy-Quark QCD Exotica, PPNP 93, 143 (2017)

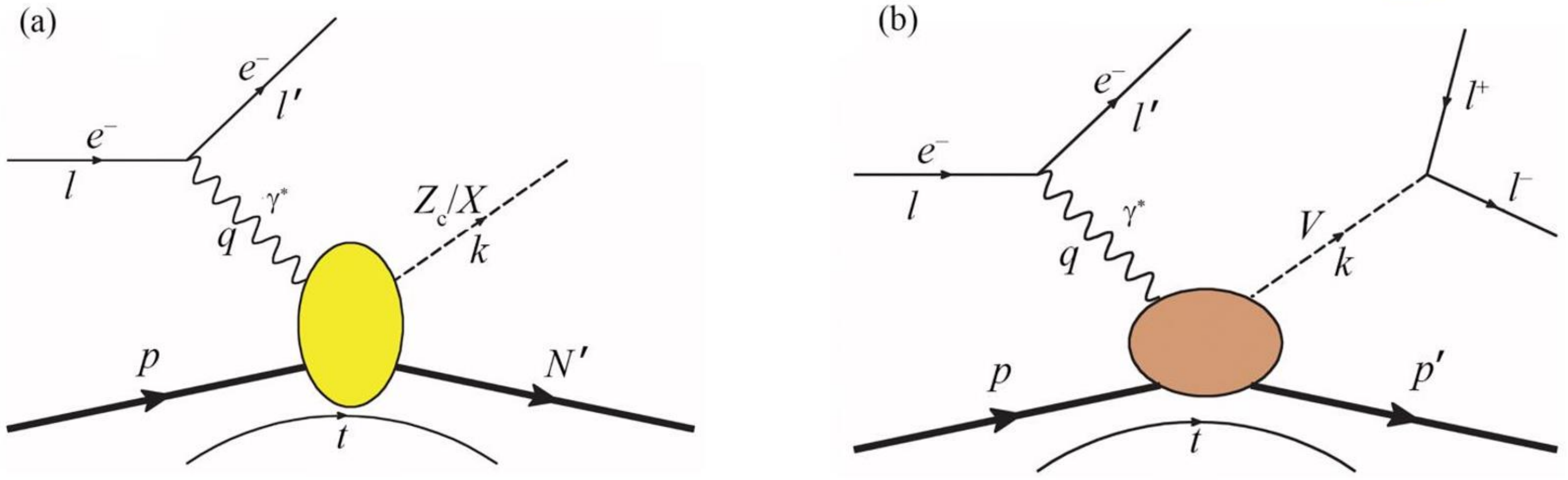

Physical projection at EicC

(arXiv:2009.08345)

- There is cusp structures at $\Lambda_c \bar{D}^*$ the thresholds in the energy dependence cross section.

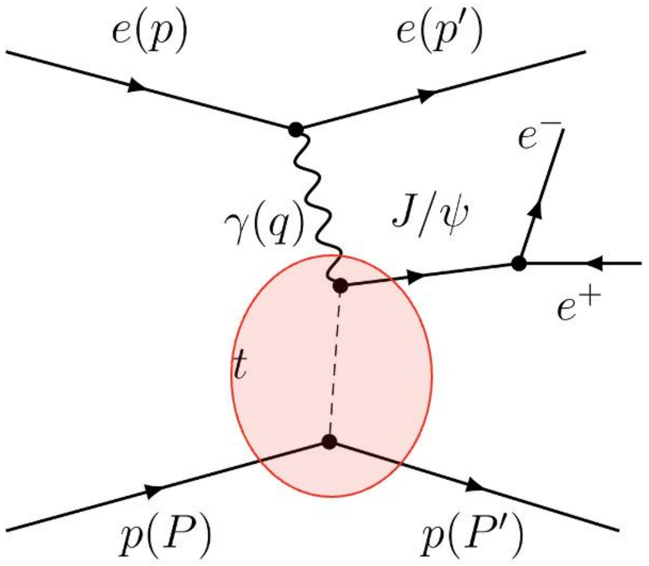

ep →epJ/ψ → e^+e^- or ($\mu^+\mu^-$)

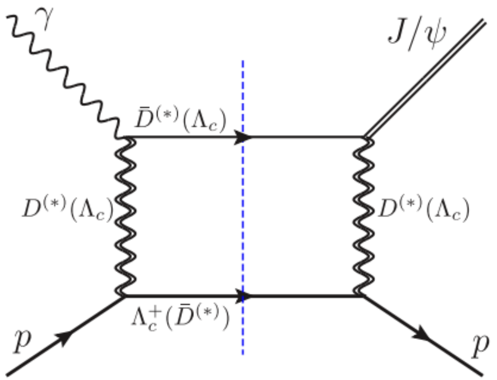

? ?

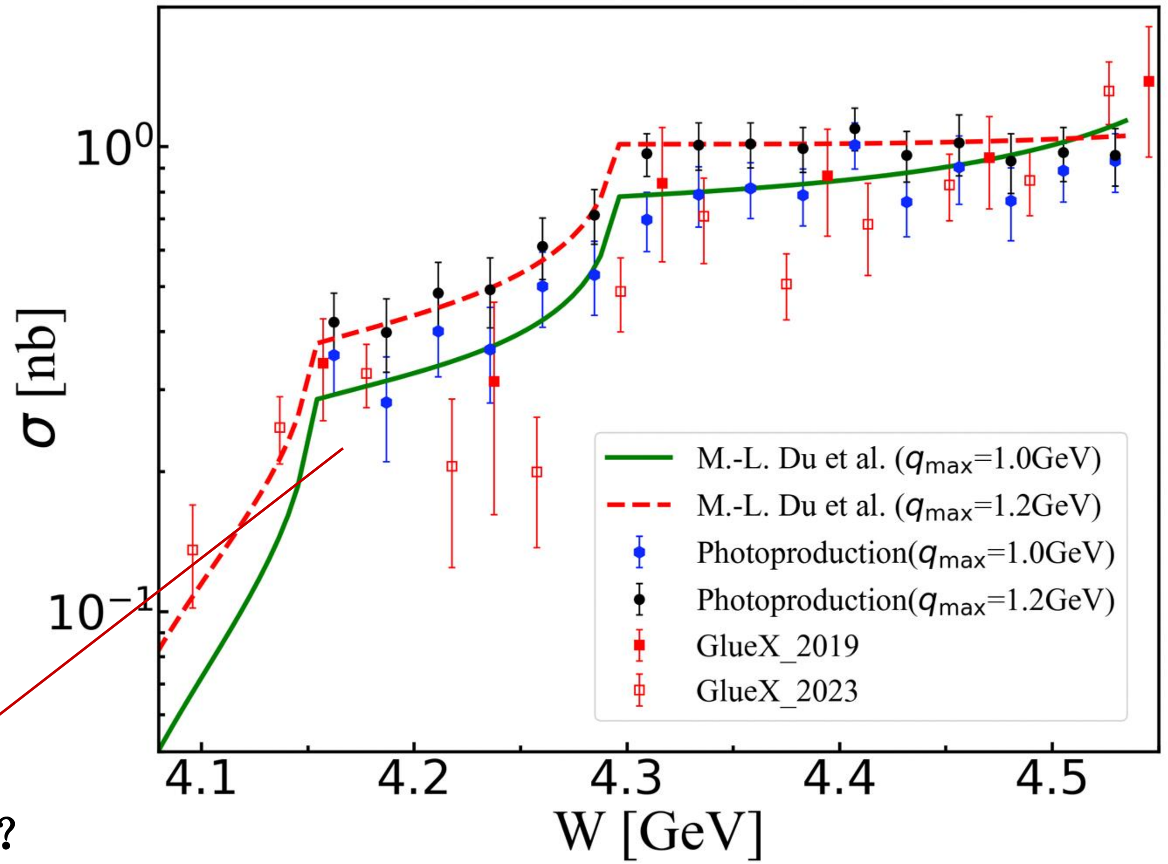

Spectrometer of EicC

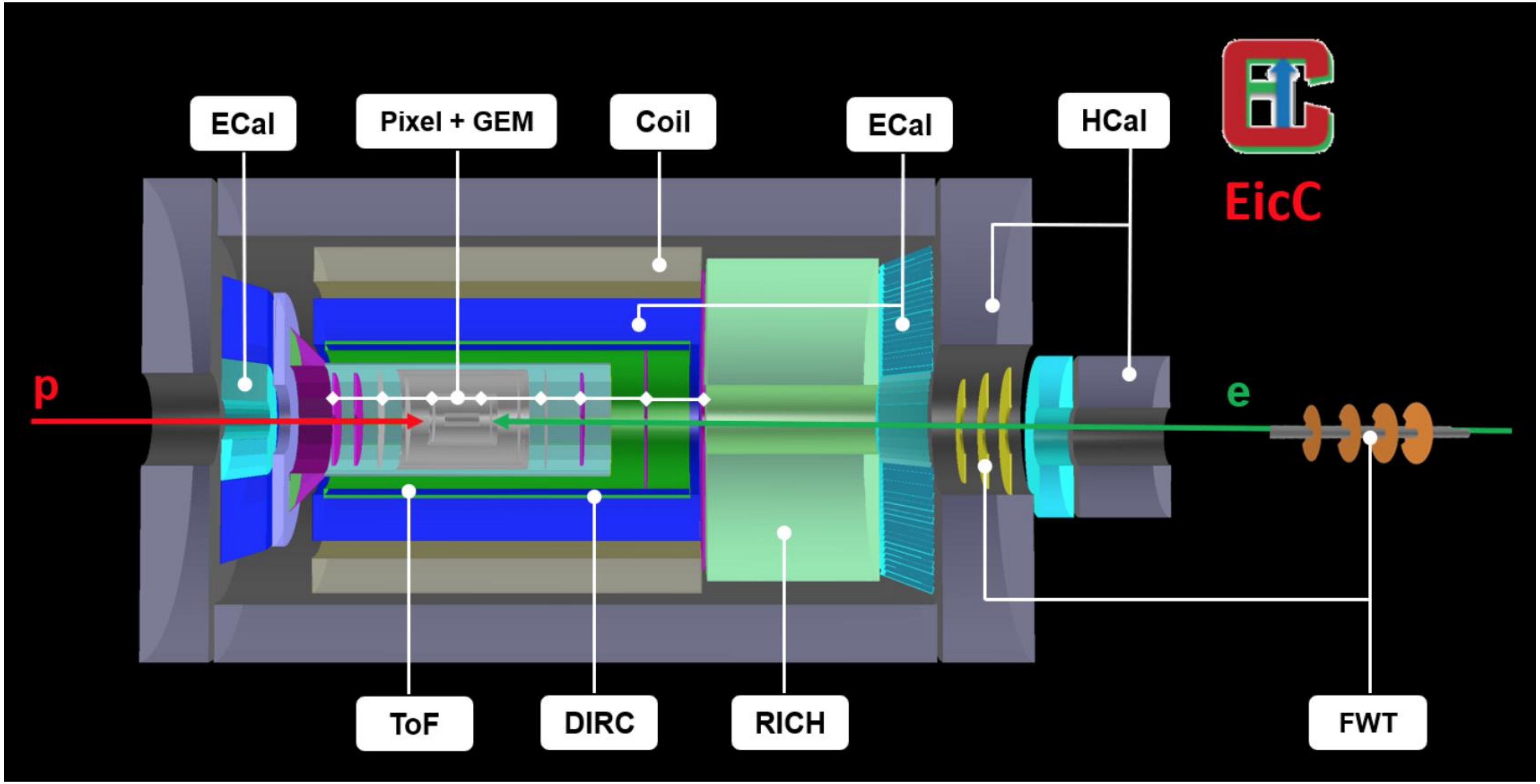

- Baseline design of EicC: 3.5 GeV electron beam and 20 GeV proton beam,
- Mian parts of the spectrometer: Vertex, Tracking, PID, Calorimeter, FWT, ...,

Spectrometer of EicC

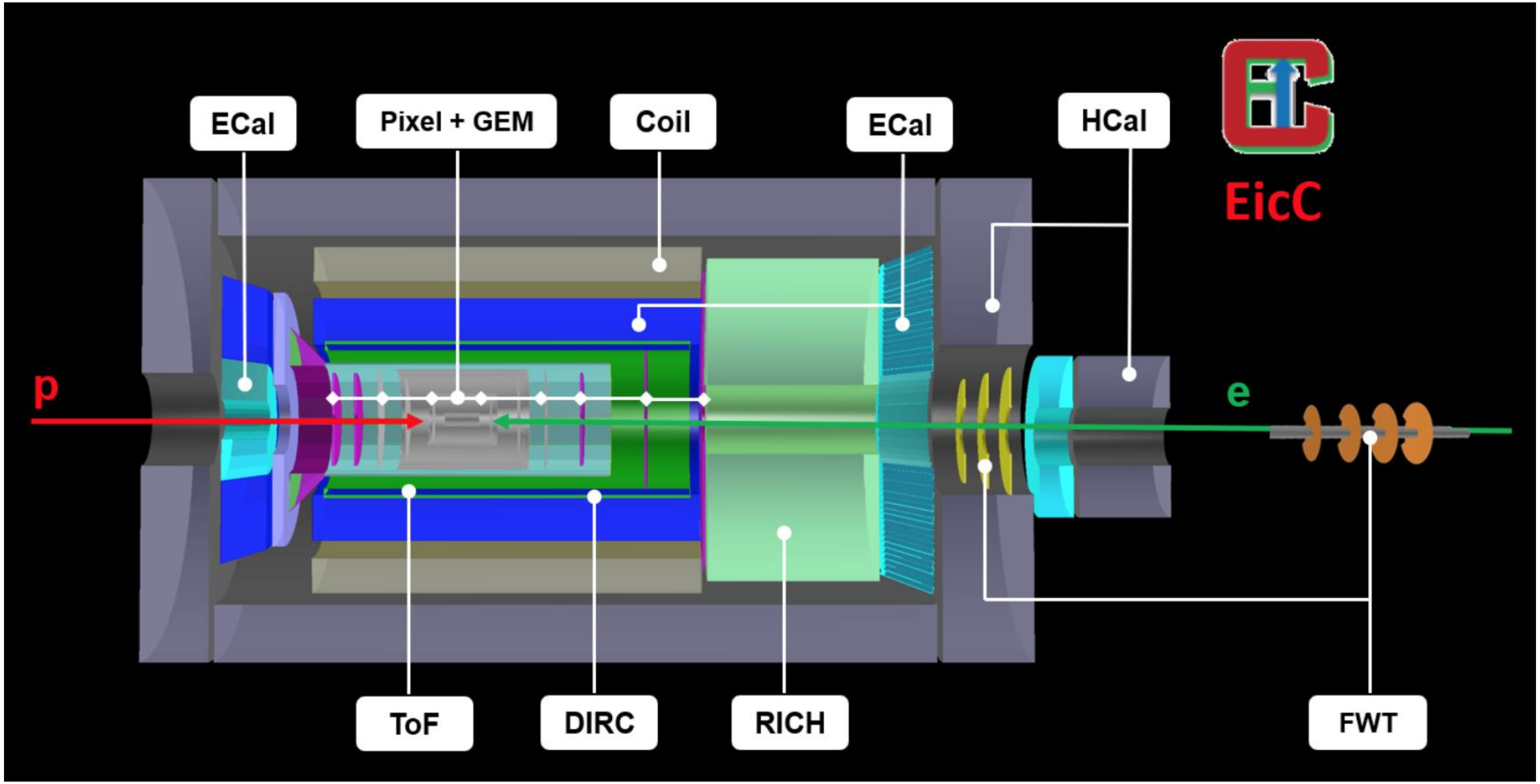

- Baseline design of EicC: 3.5 GeV electron beam and 20 GeV proton beam,
- Mian parts of the spectrometer: Vertex, Tracking, PID, Calorimeter, FWT, ...,

Spectrometer of EicC

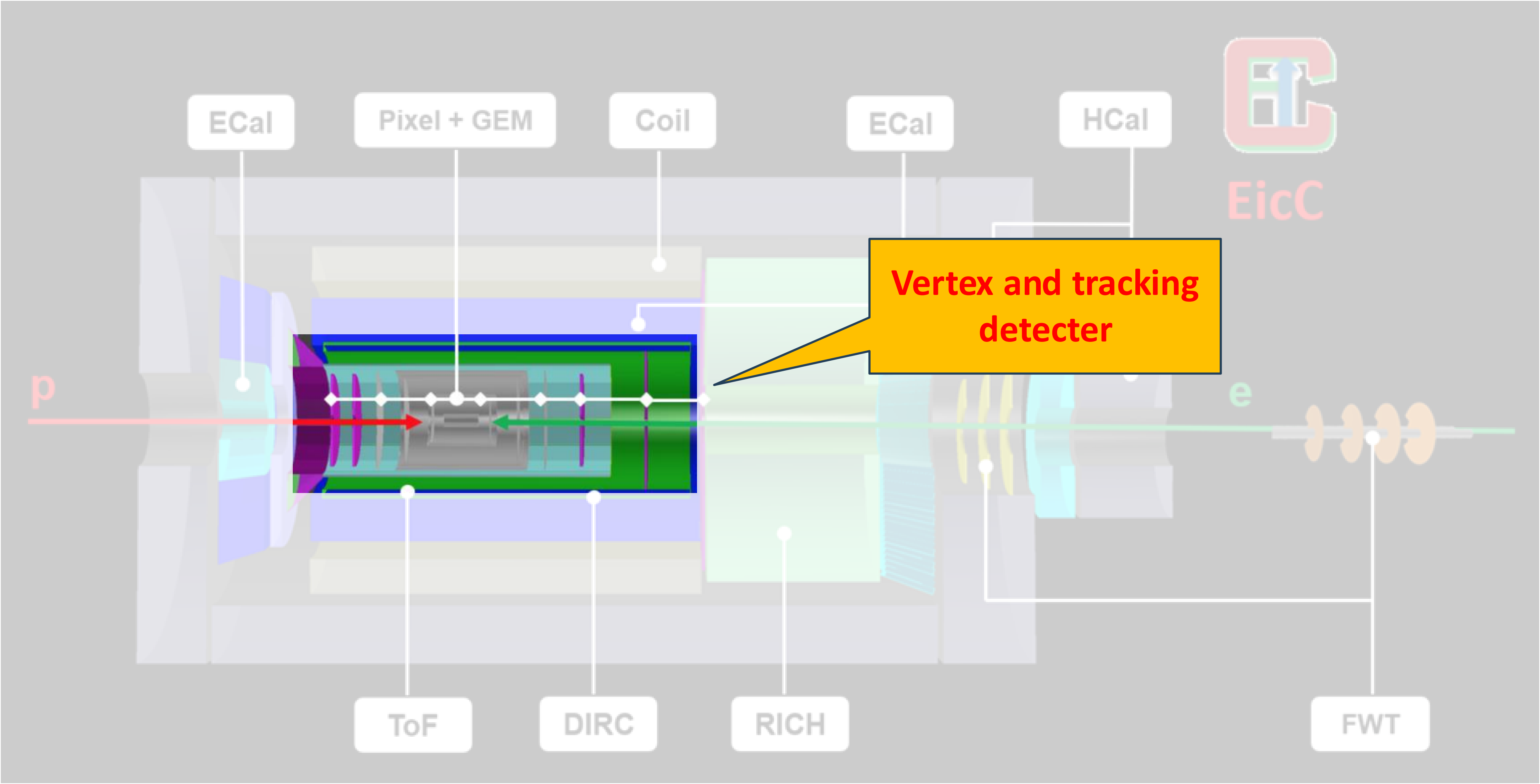

- Baseline design of EicC: 3.5 GeV electron beam and 20 GeV proton beam,
- Mian parts of the spectrometer: Vertex, Tracking, PID, Calorimeter, FWT, …,

EicC vertex&tracking detector design

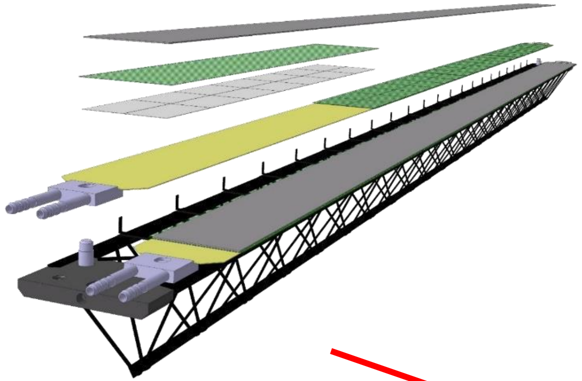

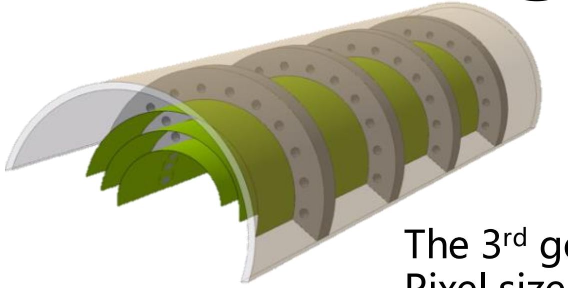

The 3[rd] generation MAPS
Pixel size: ~20x20 μm
Material budget: 0.05%

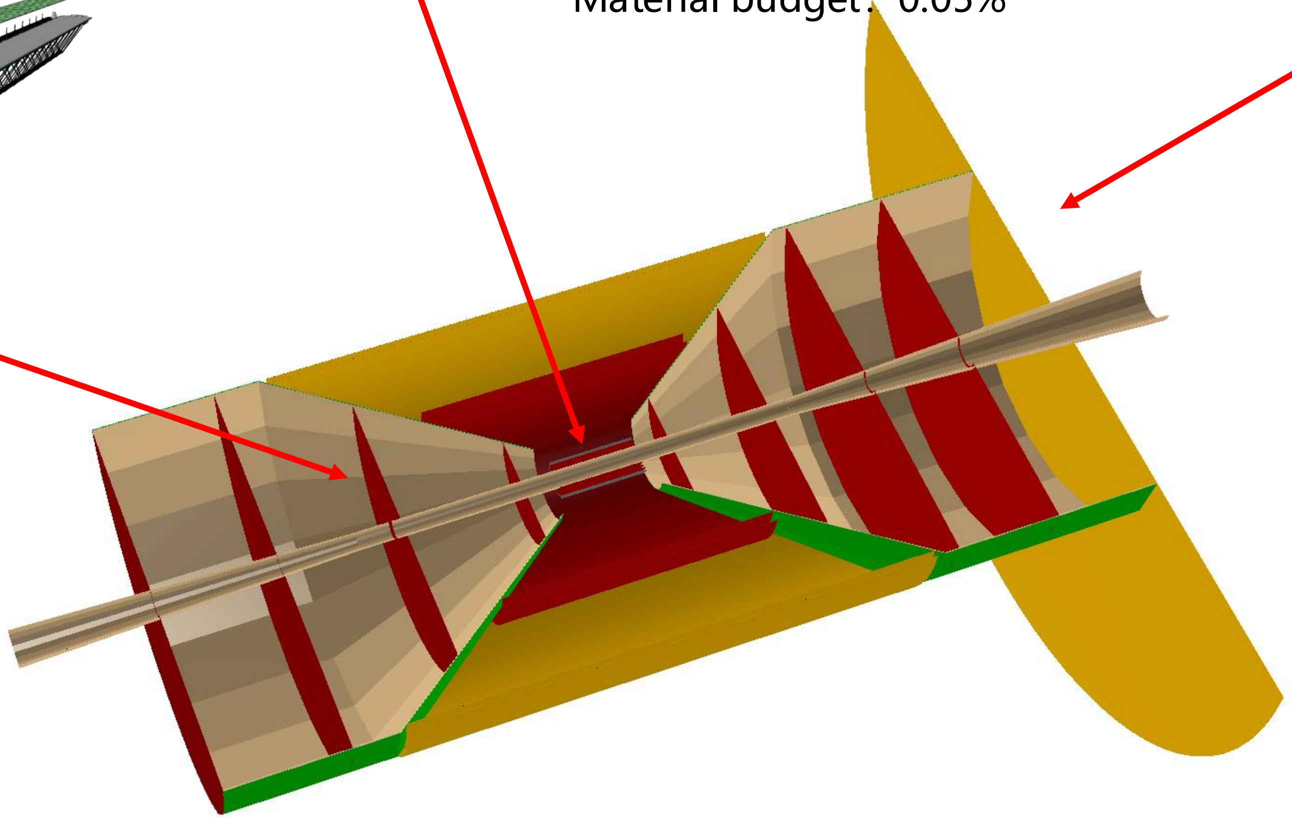

The 1[st] generation MAPS
Pixel size : ~30x30 μm
Material budget: 0.85%

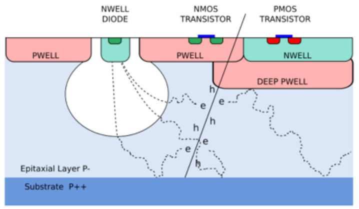

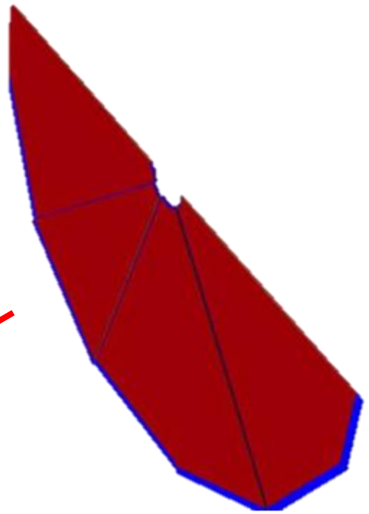

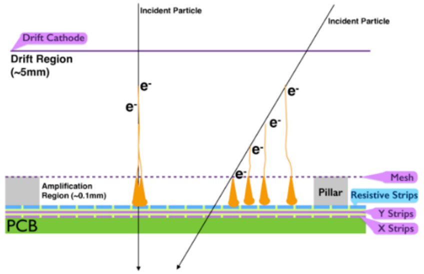

MPGD
Pitch size: ~150 μm
Material budget: 1%

The Monolithic Active Pixel Sensors (MAPS).

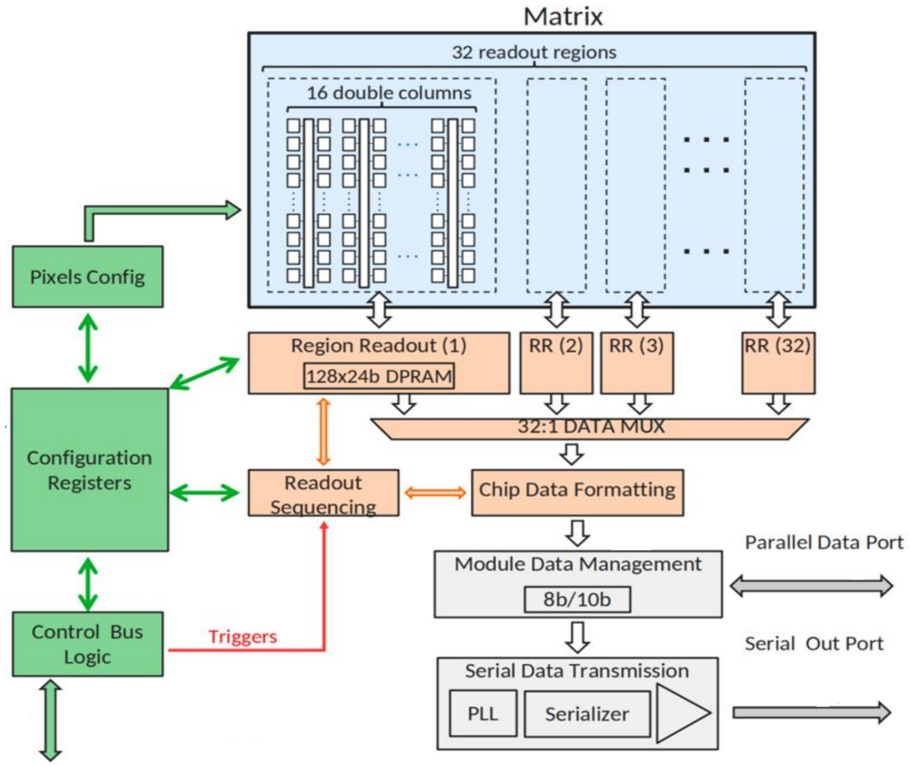

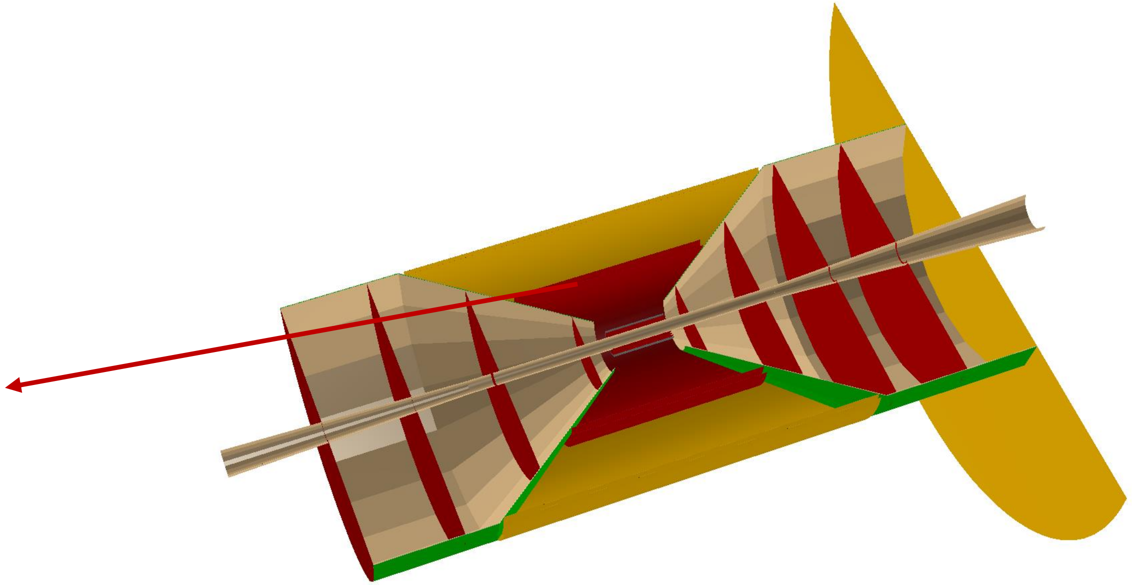

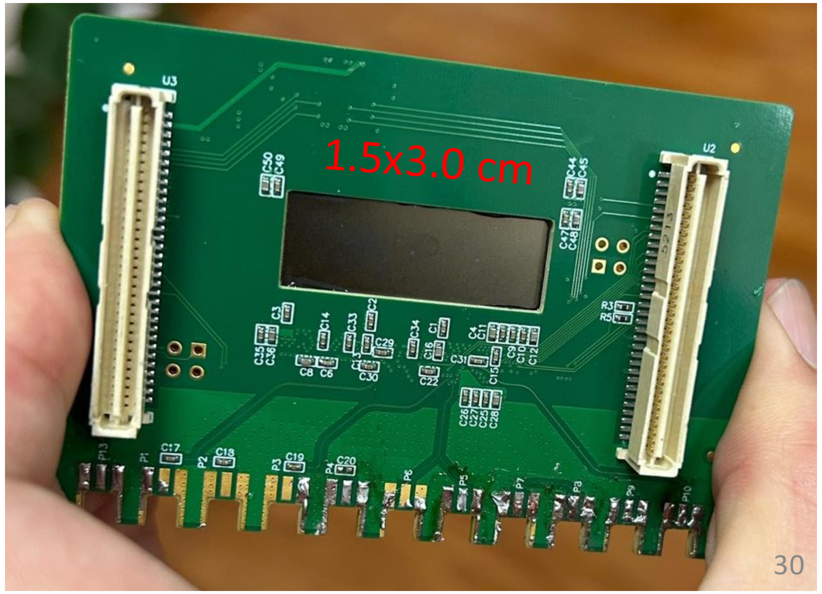

- Based on domestically developed technology, we have developed the fully-functional MAPS chip MIC6_V3 with similar performance as ALPIDE chip.
- Key features:
  - high granularity: pixel size: ~30 μm
  - High speed: integration time: 5~10 μs
  - Low Power Consumption： ～30mW/cm^2 ~low material

Modularized structure

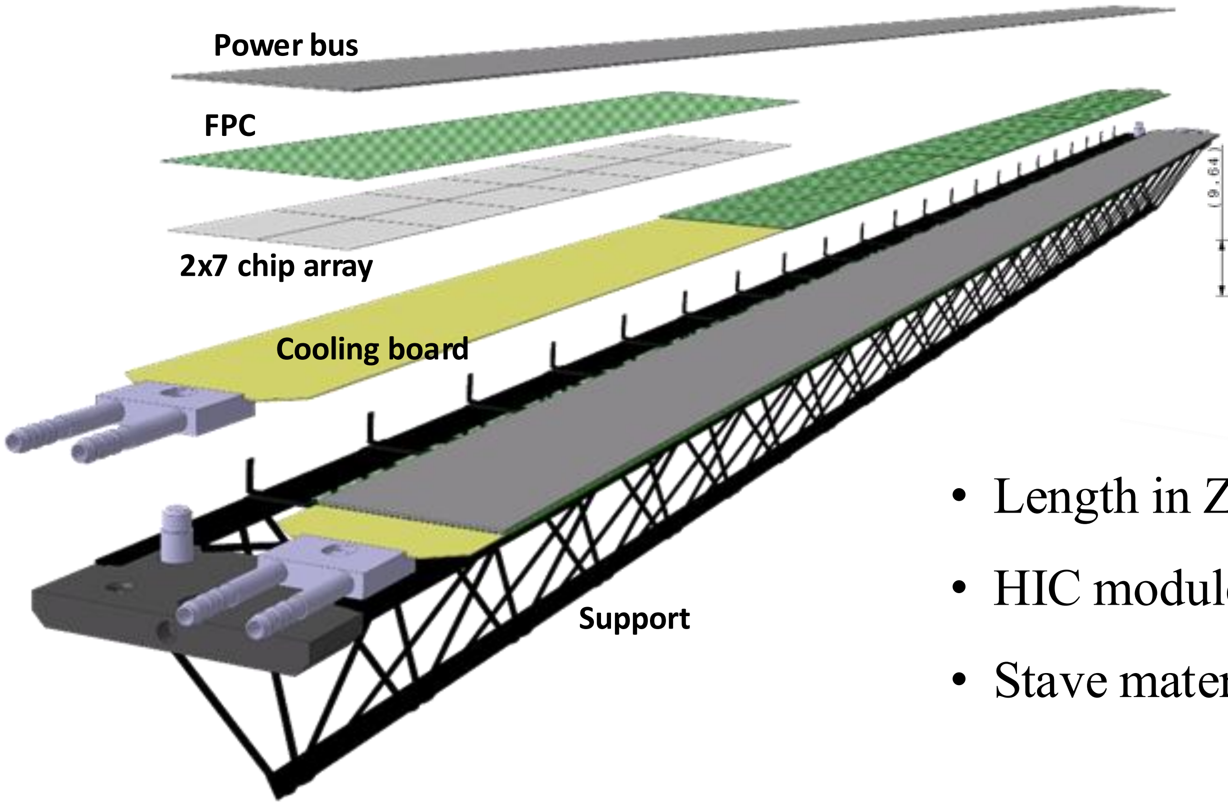

Stave module structure

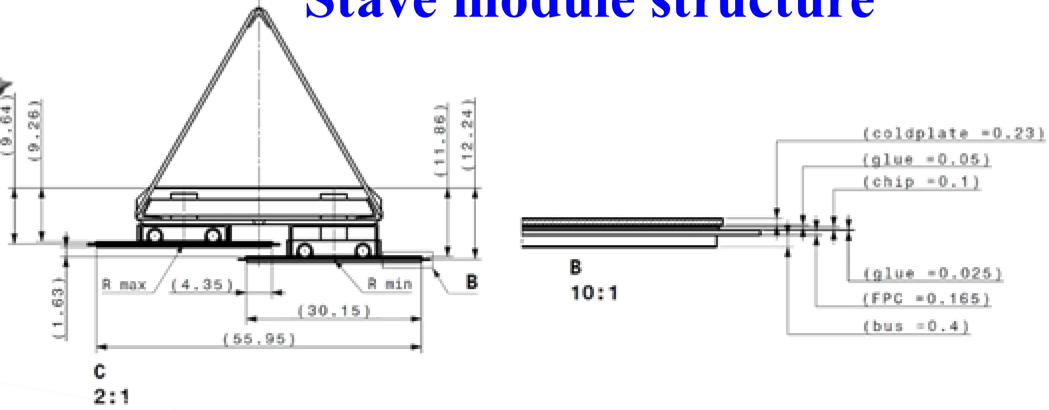

- Length in Z (mm): 1477.5 mm (NICA ITS outer layer)
- HIC module No. in stave: 2 × 7 (NICA ITS outer layer)
- Stave material budget: ~0.85% X_0

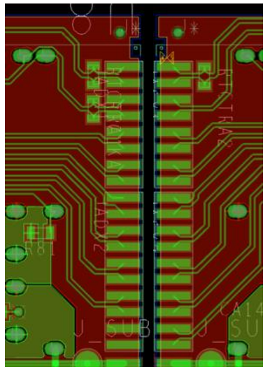

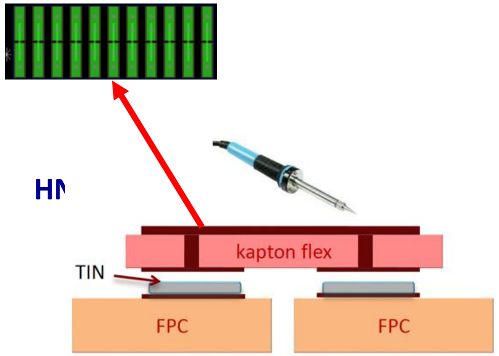

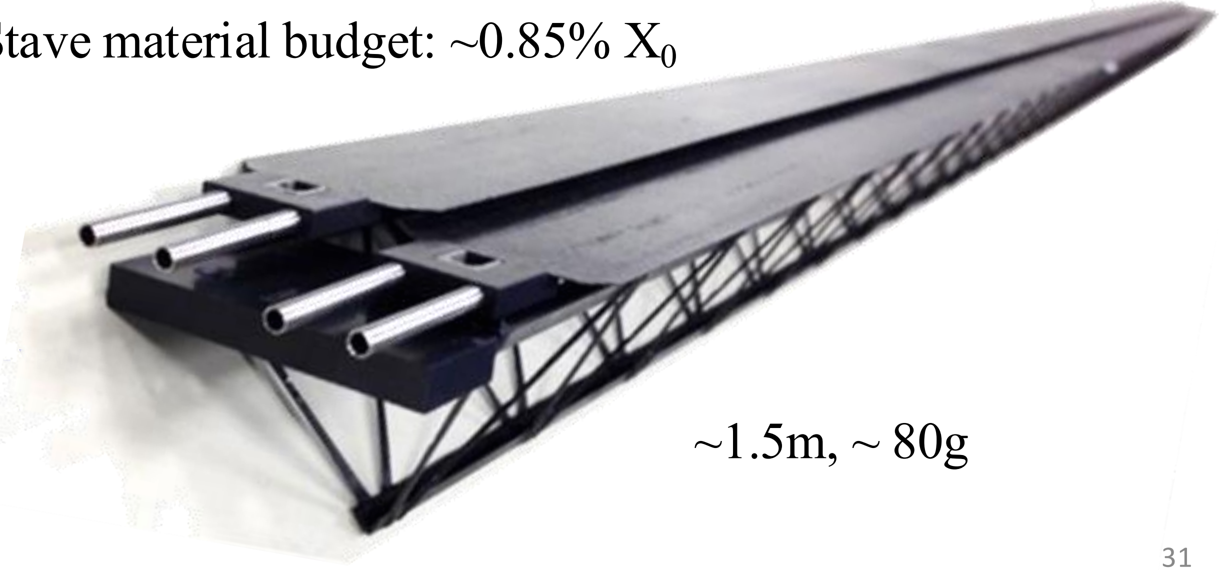

~1.5m, ~ 80g

Micromegas detector

Feature

- high granularity: spatial resolution: ~ 65 μm
- High speed: 100~200 kHz/cm^2

Electron beam test（5GeV at DESY）

- X-Y 2D readout
- Efficiency： >98%

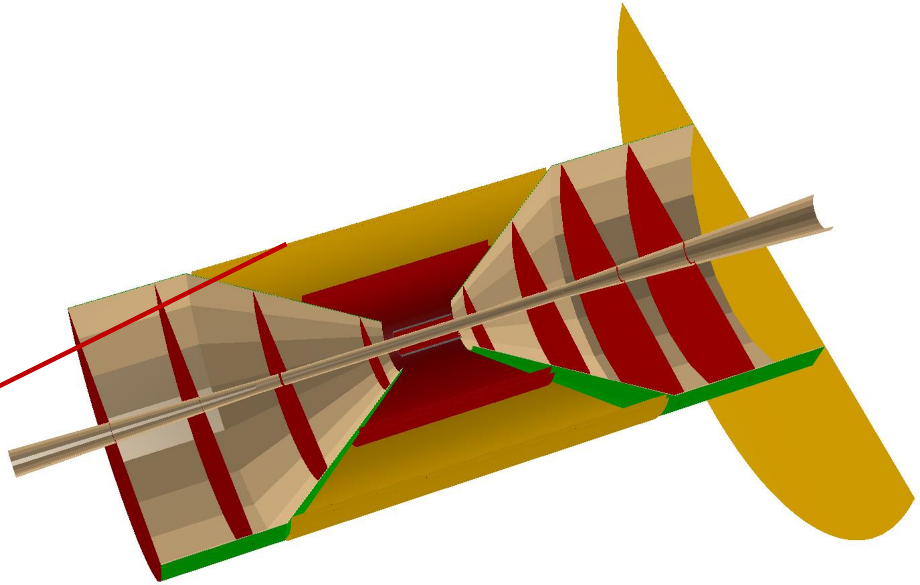

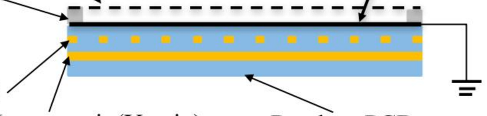

Jianxin Feng, Zhiyong Zhang, Jianbei Liu et al., NIM-A 989 (2021) 164958.

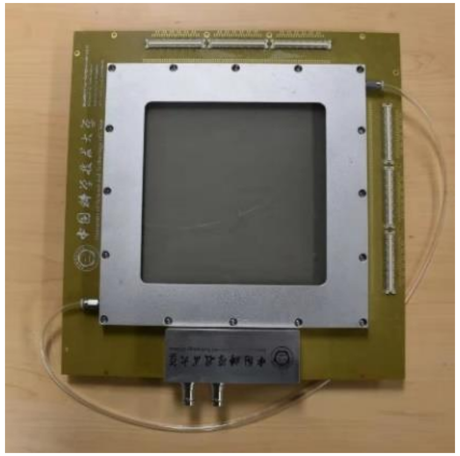

Micromegas prototype
40x40 cm

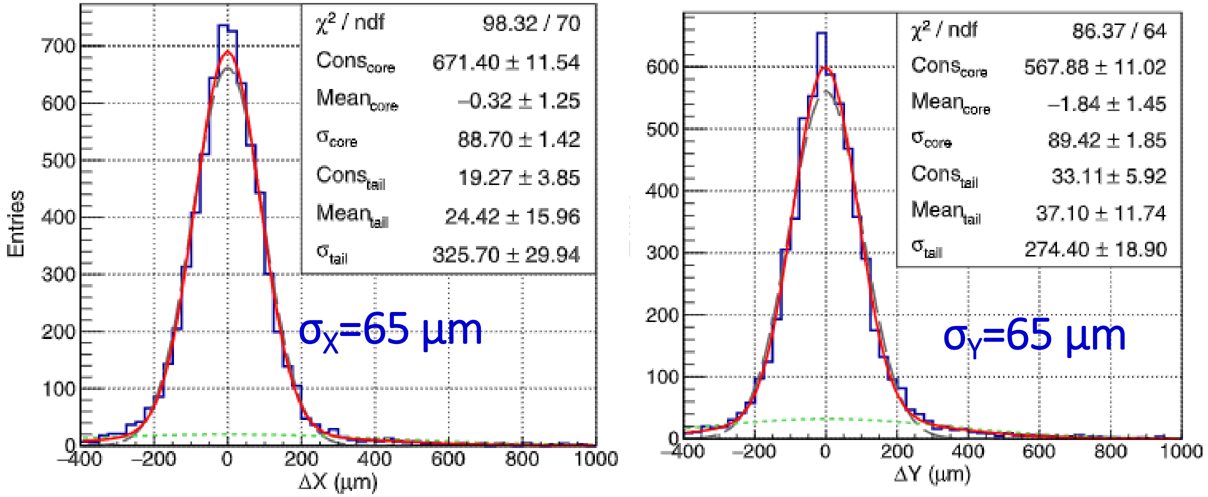

The performance

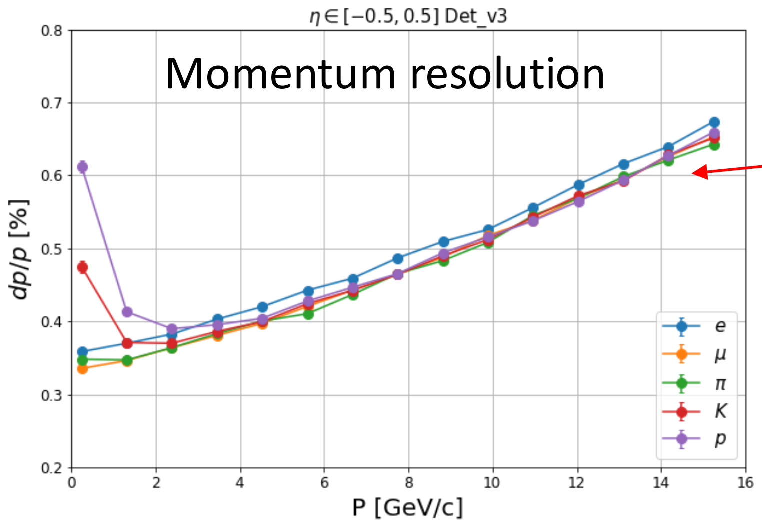

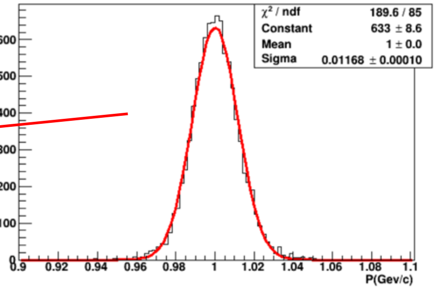

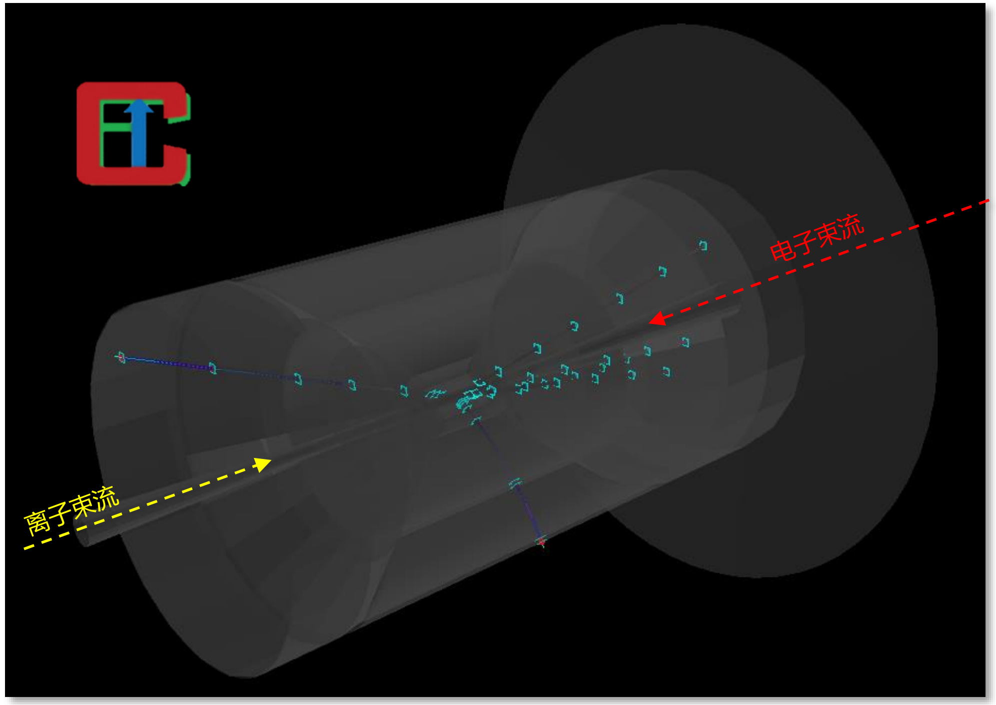

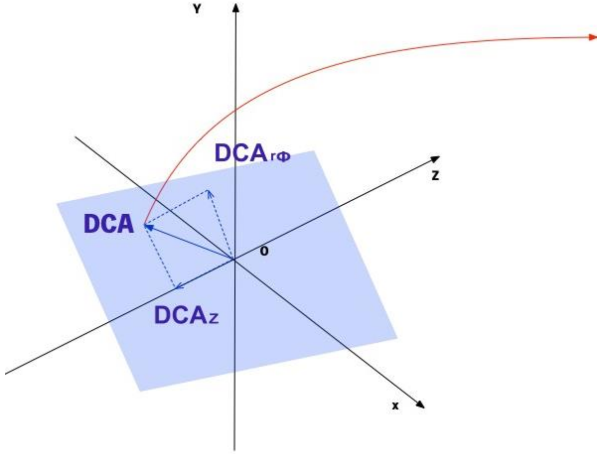

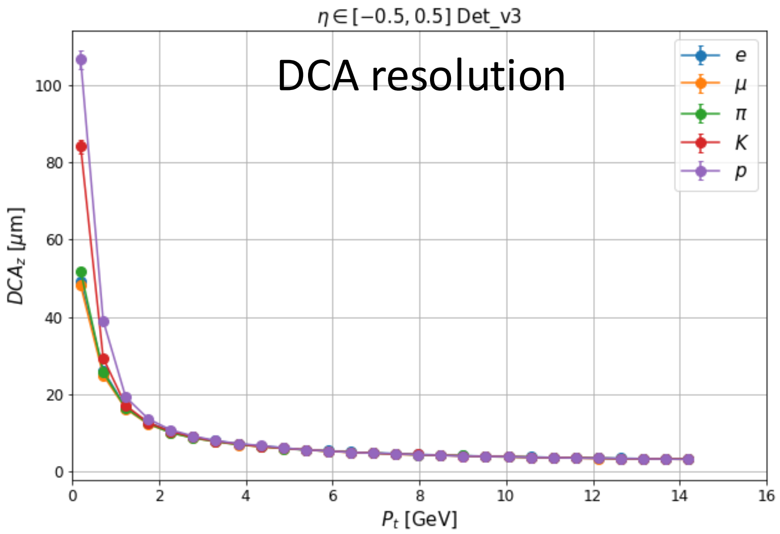

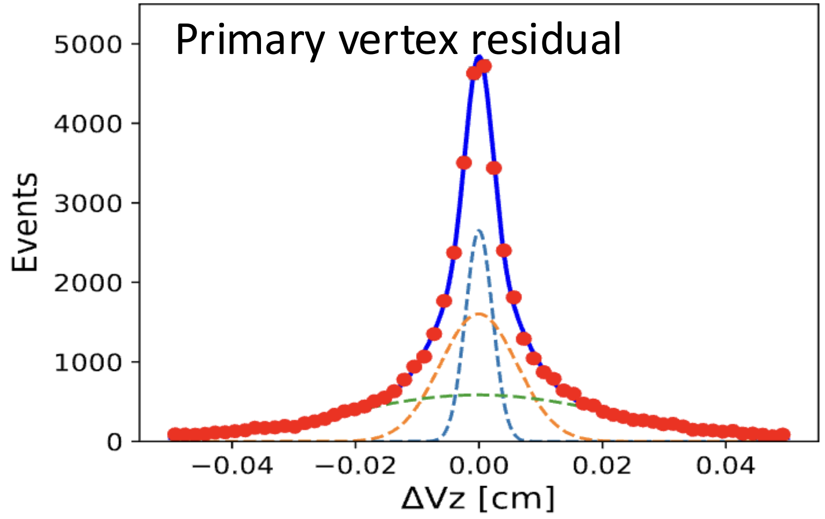

Spectrometer of EicC

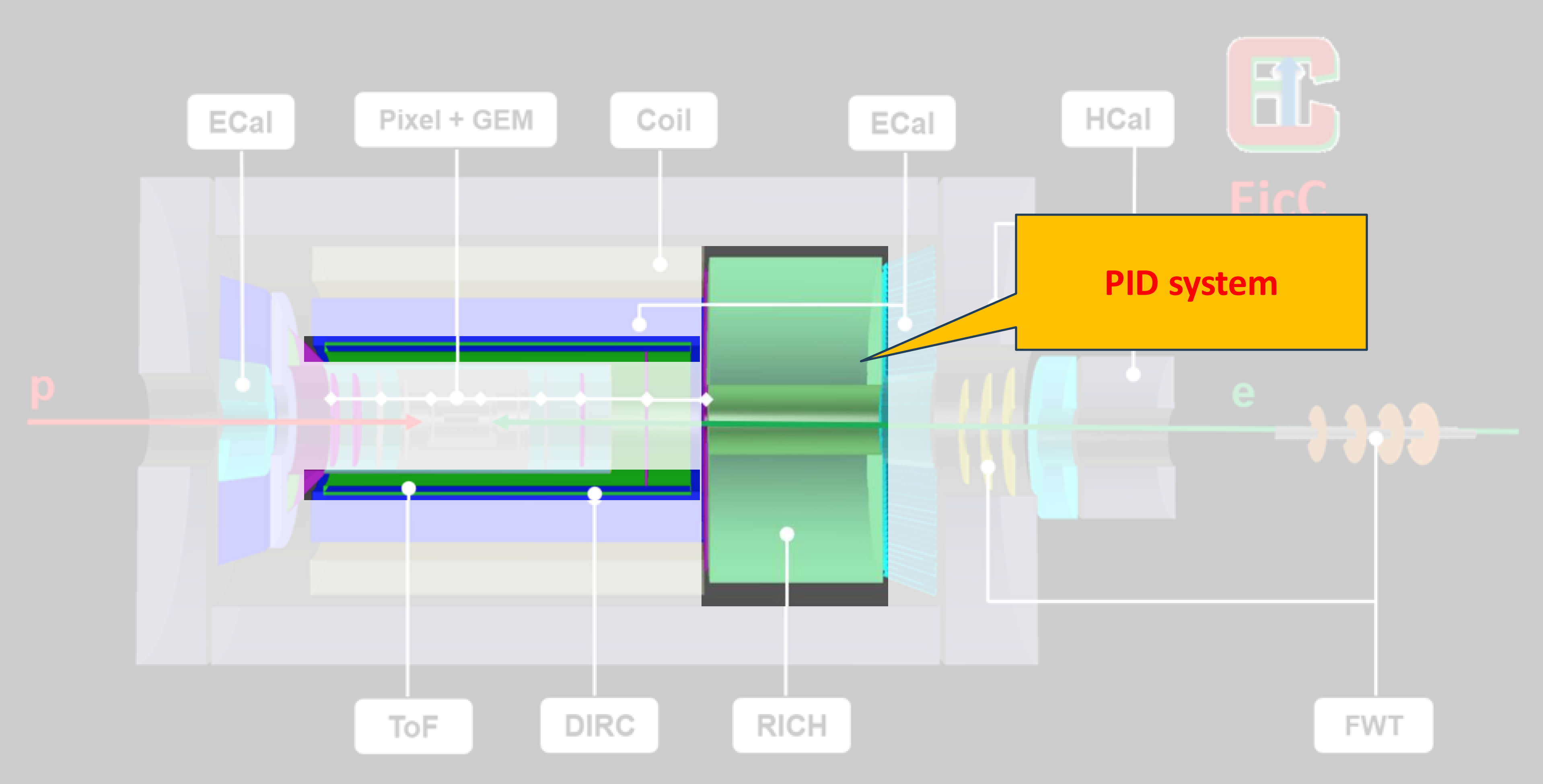

- Baseline design of EicC: 3.5 GeV electron beam and 20 GeV proton beam,
- Mian parts of the spectrometer: Vertex, Tracking, PID, Calorimeter, FWT, …,

Barrel DIRC for PID

Detector of Internal Reflection Cherenkov lights (DIRC):

DIRC achieve PID through reconstructing their **Cherenkov angles**, by measuring the **transit time** and **exit position/angle** of Cherenkov photons induced by different particles.

- Consisted of fused silica(n=1.47) as Cherenkov radiator and MCP-PMTs as photosensor array
- Compact structure as barrel detector
- Achieve 3σ π/K separation up to 6 GeV/c with angle resolution ~ 1mrad

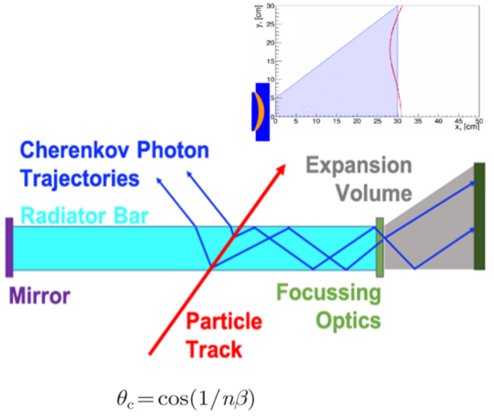

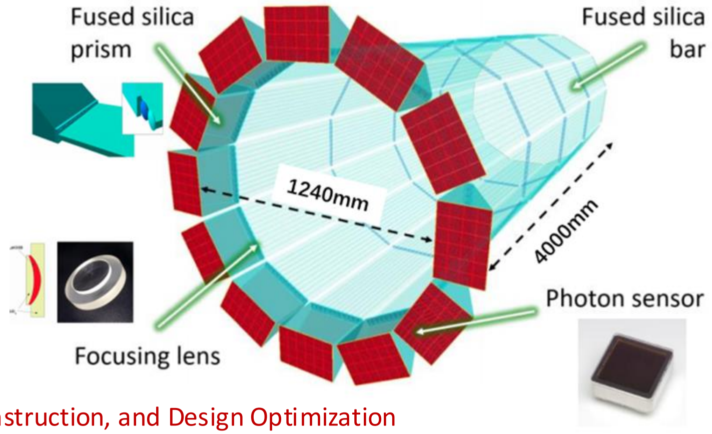

Reference from “Simulation, Reconstruction, and Design Optimization for the PANDA Barrel DIRC”, 2016

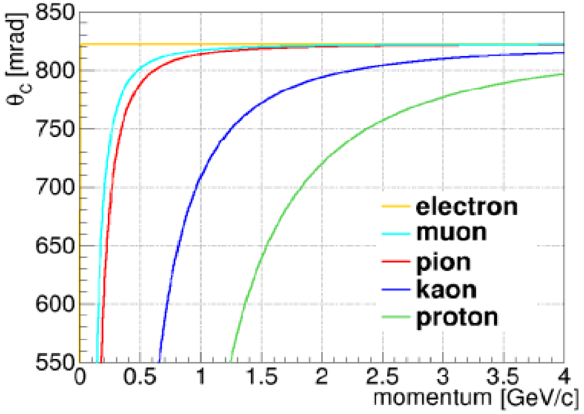

refractive index of synthetic fused silica **with n = 1.47**

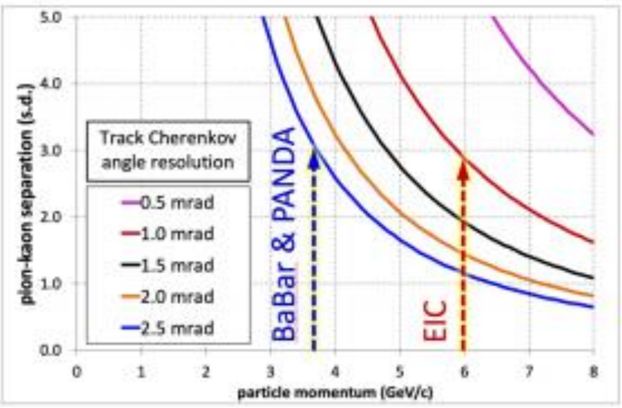

Reference from PANDA & EIC

DIRC Prototype setup

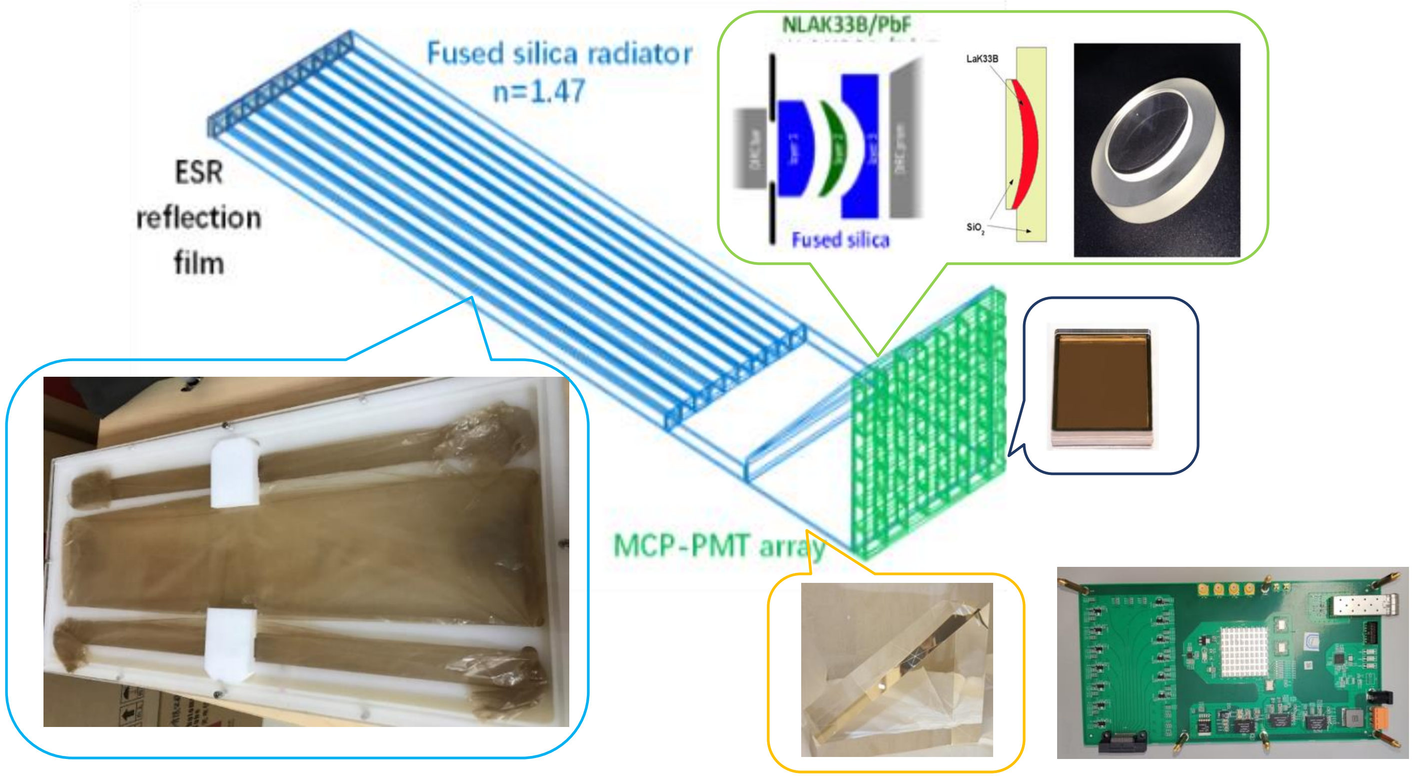

Hamamastu
R10754 (available)

北方夜视 N6021

DIRC protype consisted of

- Fused silica radiator (HERAEUS SUPRASIL) ,
- Optical focus system
- MCP-PMT array. Timing resolution ~ 10ps, developed by USTC-STCF group.

mRICH: Lens-based Focusing Aerogel Detector Design

- Modular RICH is a Cherenkov detector based on aerogel radiator.
- It uses a Fresnel lens to generate focusing effect to improve position resolution.
- It has compact and flexible structure, and PID power with large momentum coverage.

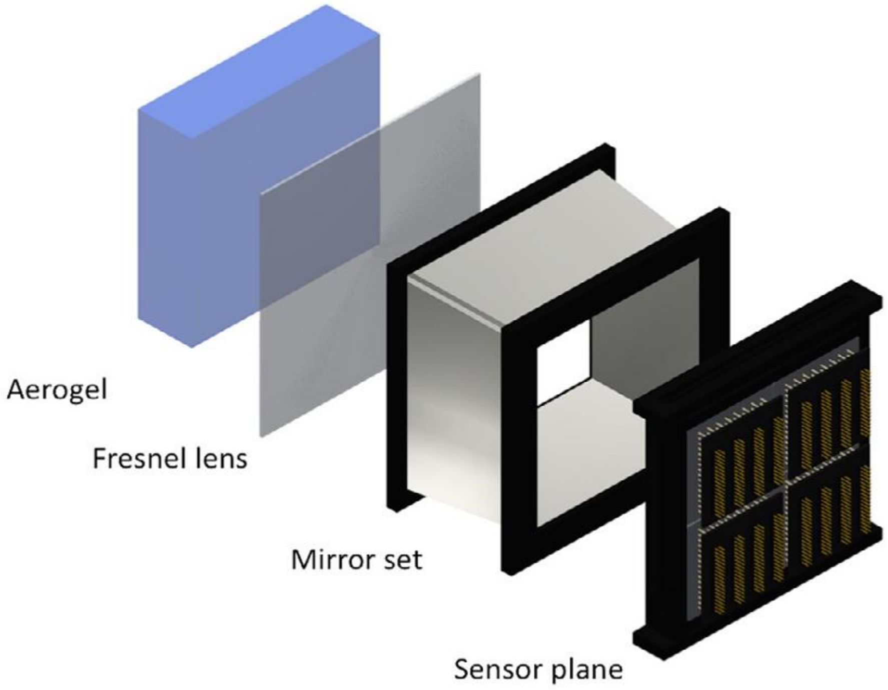

Lens-Based mRICH Design

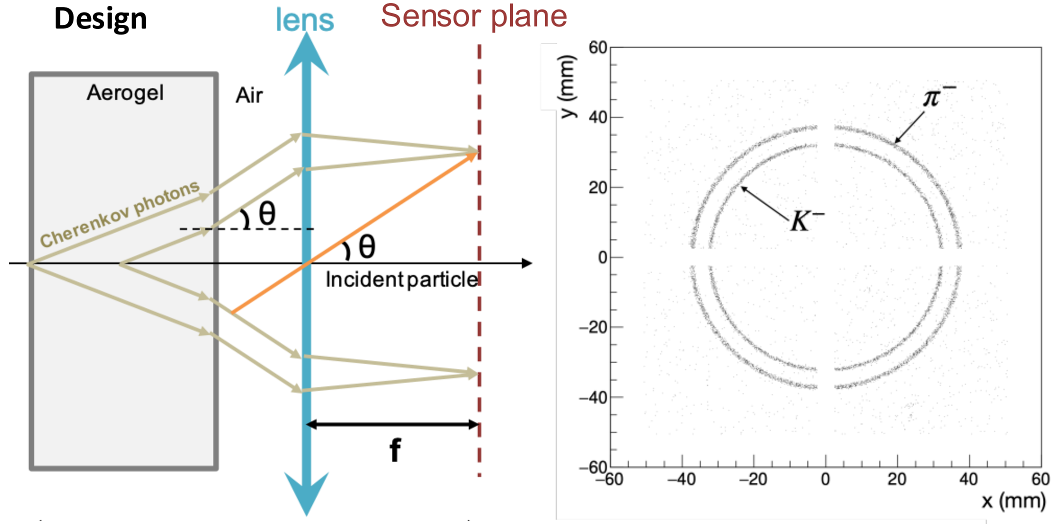

focal length 7.62cm (3”)

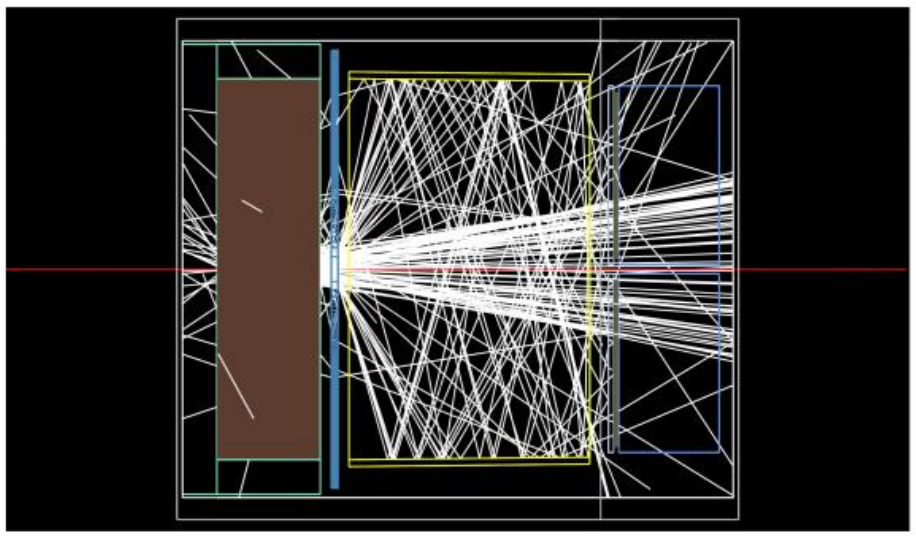

mRICH Design and Simulation

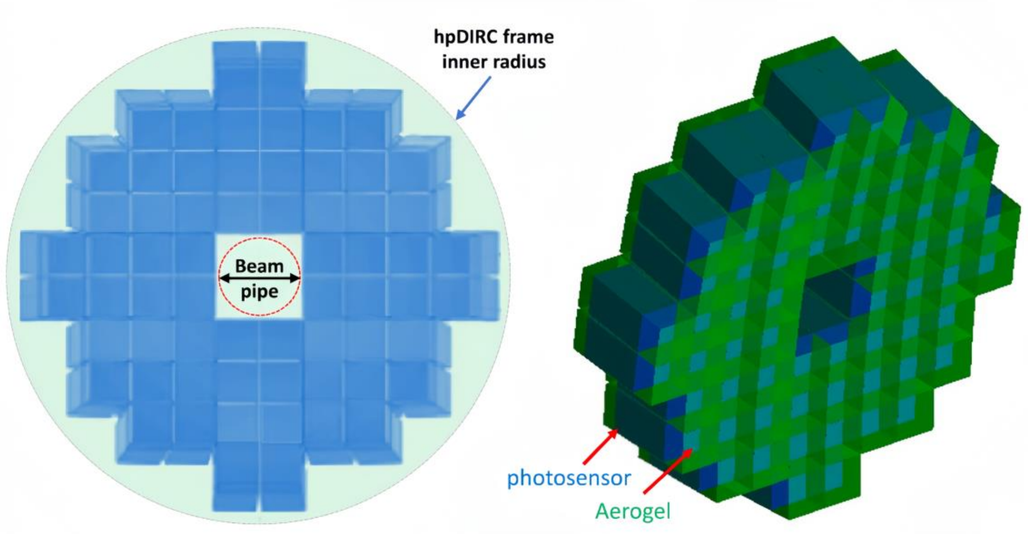

- Composed of 64 aerogel modules (located at z=1080 ~ 1380 mm, radius 100 ~ 670 mm);
- The cross section of each module is 108 × 108 mm^2, with a thickness of 25 ~ 35 mm;
- The center of each module is at z=-1230 mm and tilted towards the collision center point;
- Fresnel lens focal length L=76.2 mm (3 inches, n=1.47, Edmund Optics).

- pi/K separation up to 9 GeV/c at best
- e/pi separation up to 2 GeV/c at best

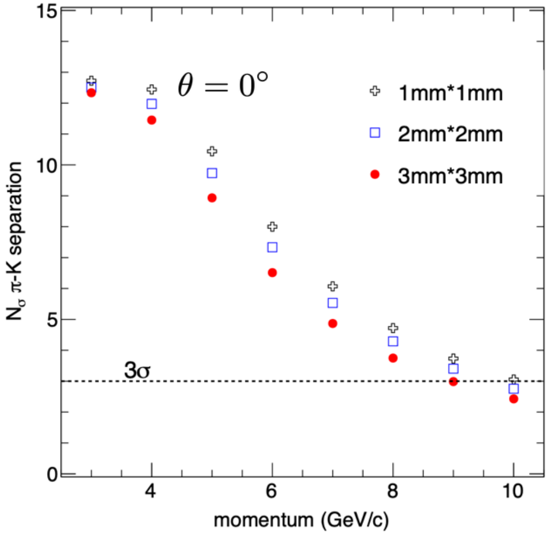

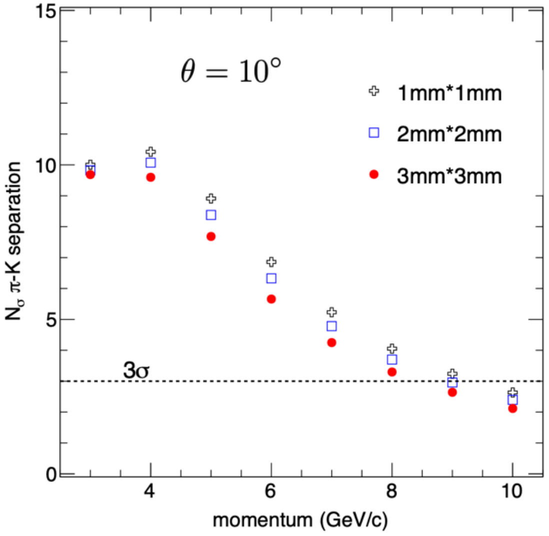

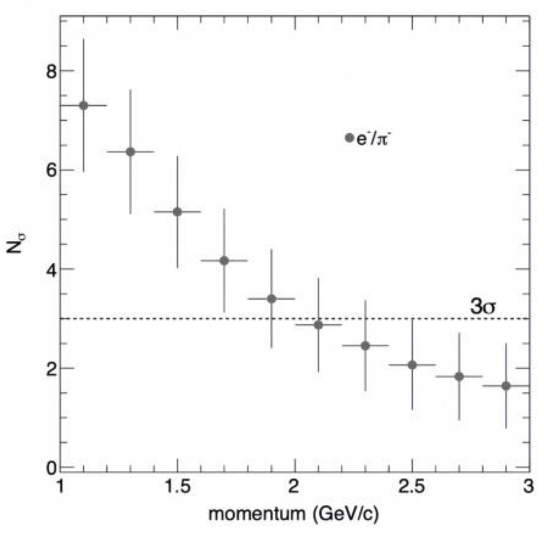

- Separation power decrease with increasing polar angle
- 3 sigma separation up to 9 GeV/c when particle launched at the center of aerogel
- 3 sigma separation up to 8 GeV/c when particle launched at 10 degrees

Spectrometer of EicC

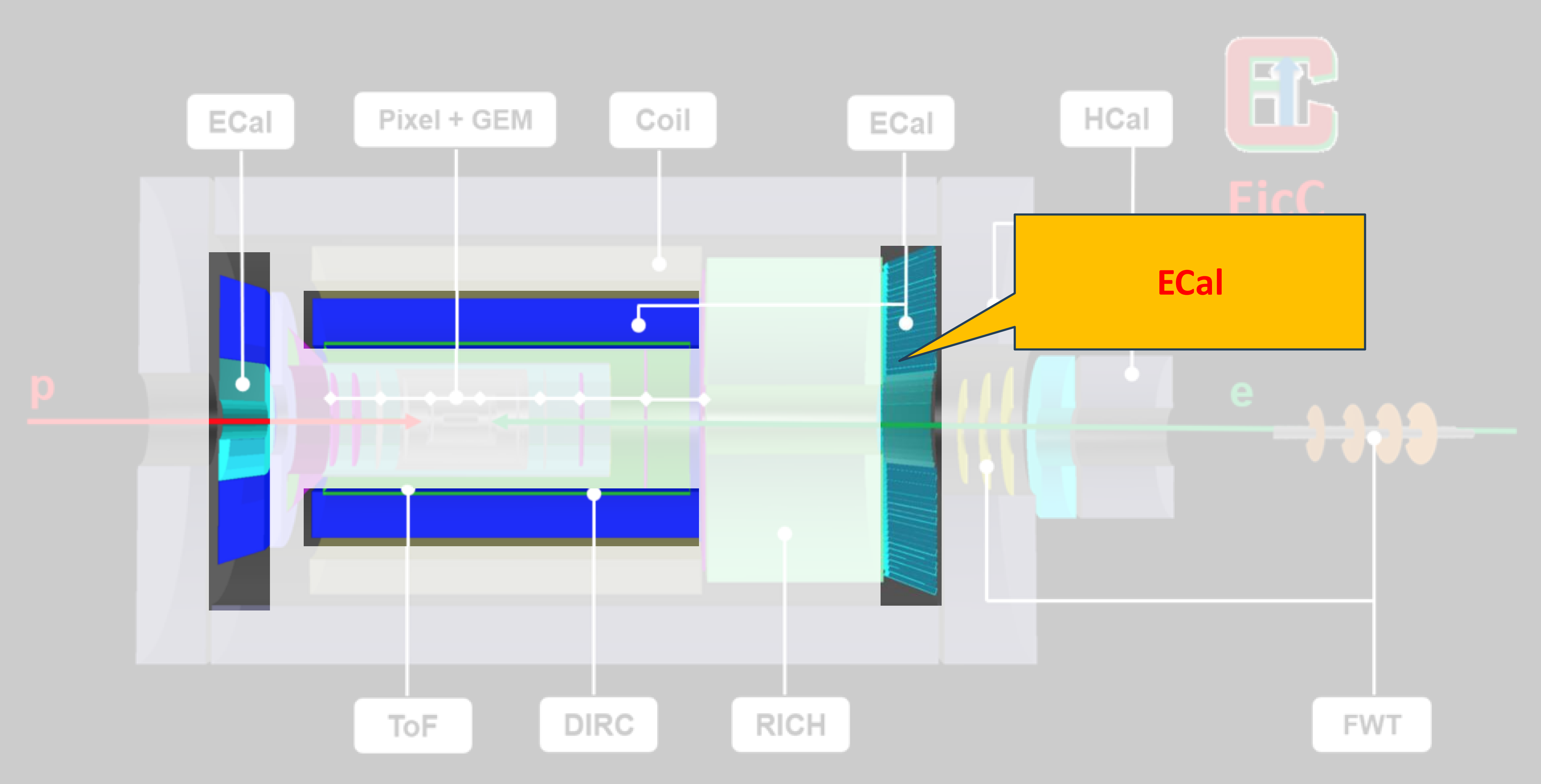

- **Baseline design of EicC: 3.5 GeV electron beam and 20 GeV proton beam,**
- **Mian parts of the spectrometer: Vertex, Tracking, PID, Calorimeter, FWT, ...,**

Ecal Design in Simulation

- General design of whole Ecal Detector.
- Cesium Iodide (CsI) crystal is applied in e-endcap, Shashlik style is applied in both barrel and ion-endcap
- **The actual distances** of the two endcaps to IP depend on the available space of the EicC design

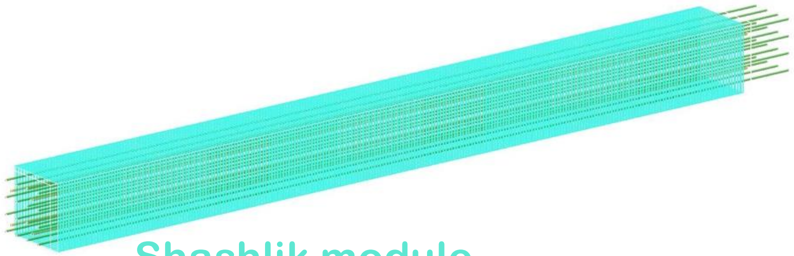

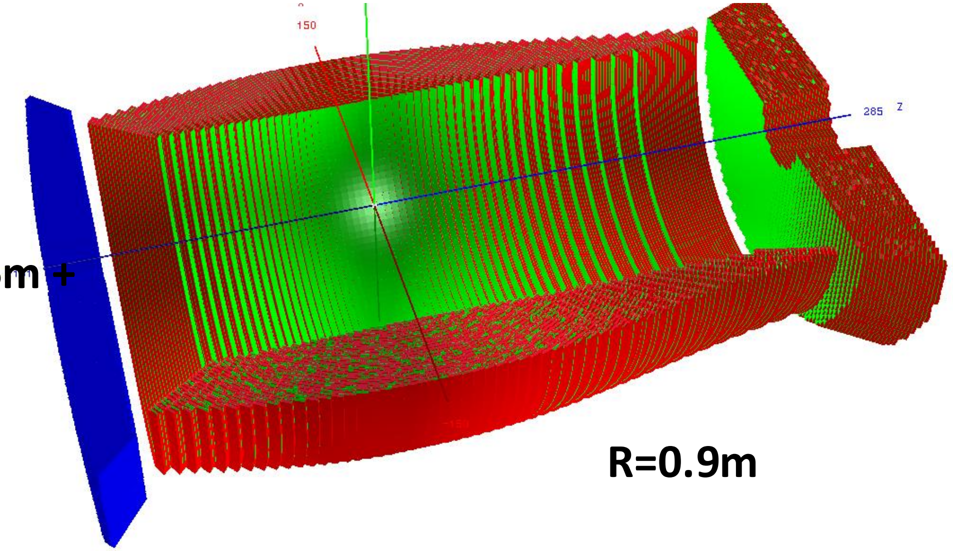

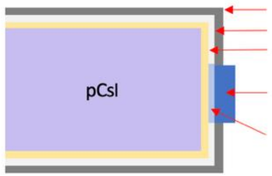

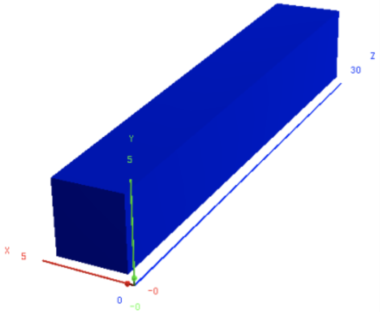

	EMC	type	z/r[m]	Length[cm],X_0	Coverage[cm]	pseudorapidity	Tower size
EicC	e-endcap	**CsI**	**Z=-1.5**	30, $16X_0$	15.0<r<128	(-3.0, -1.0)	4.0*4.0(front)
	barrel	**Shashlik**	**R=0.9**	45, $16X_0$	-105.8<z<187.5	(-1.0, 1.5)	4.0*4.0 (front)
	Ion-endcap	**Shashlik**	**Z=2.4**	45, $16X_0$	24.0<r<113	(1.5, 3.0)	

Module (7x7) array simulation result

Ye Tian (IMP)

Shashlik simulation result

Energy resolution

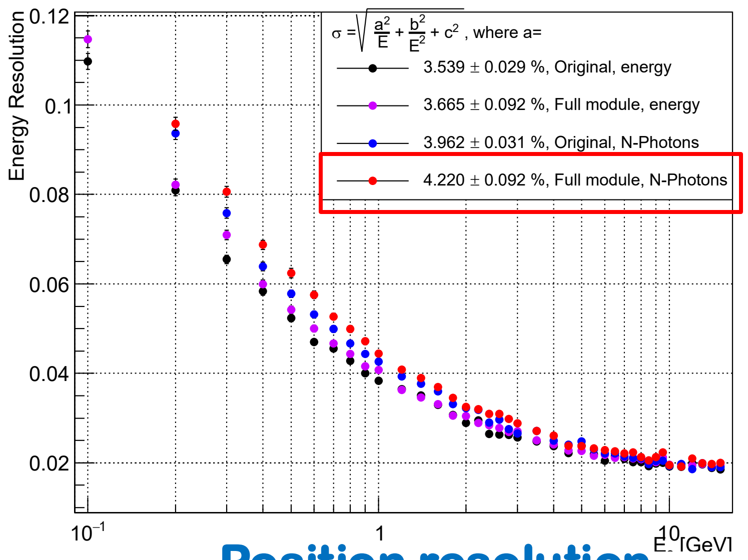

Position resolution

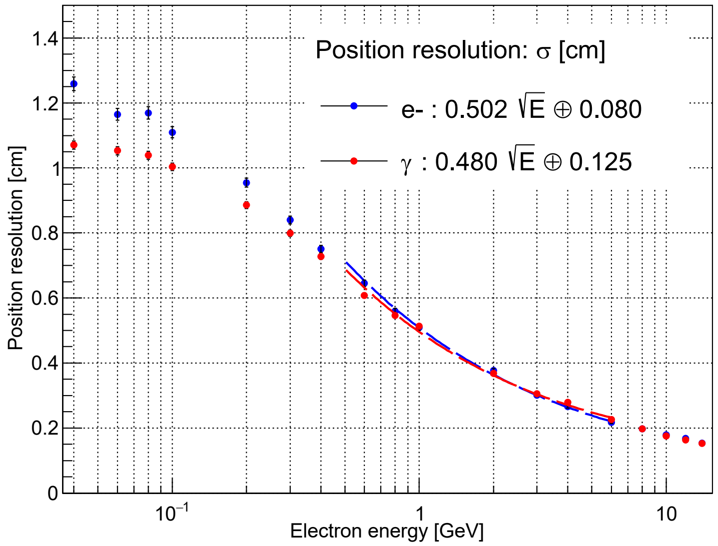

CsI simulation result

Energy resolution

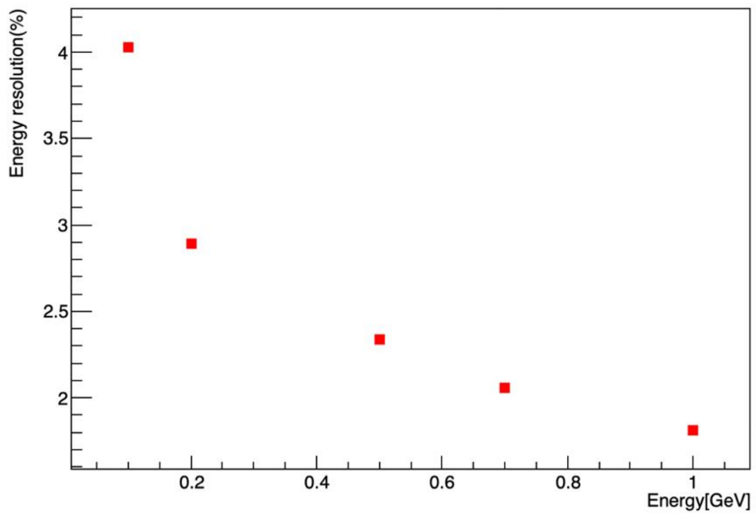

Position resolution

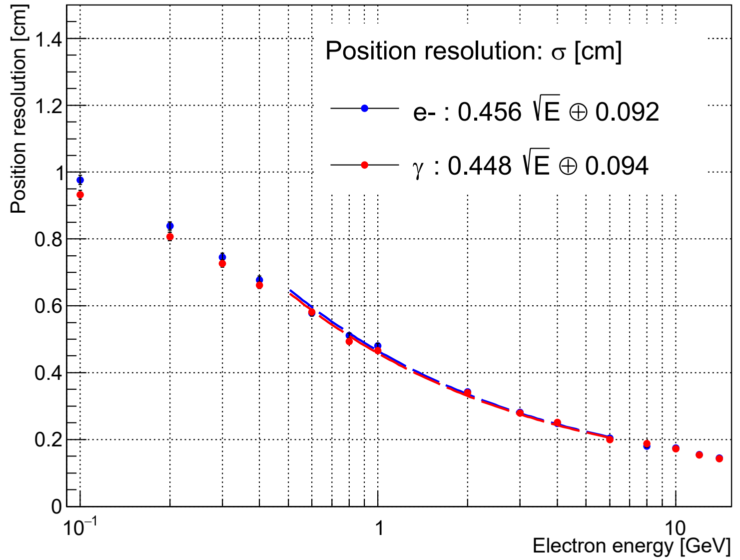

Shashlik ECal cosmic ray test result

Ye Tian (IMP)

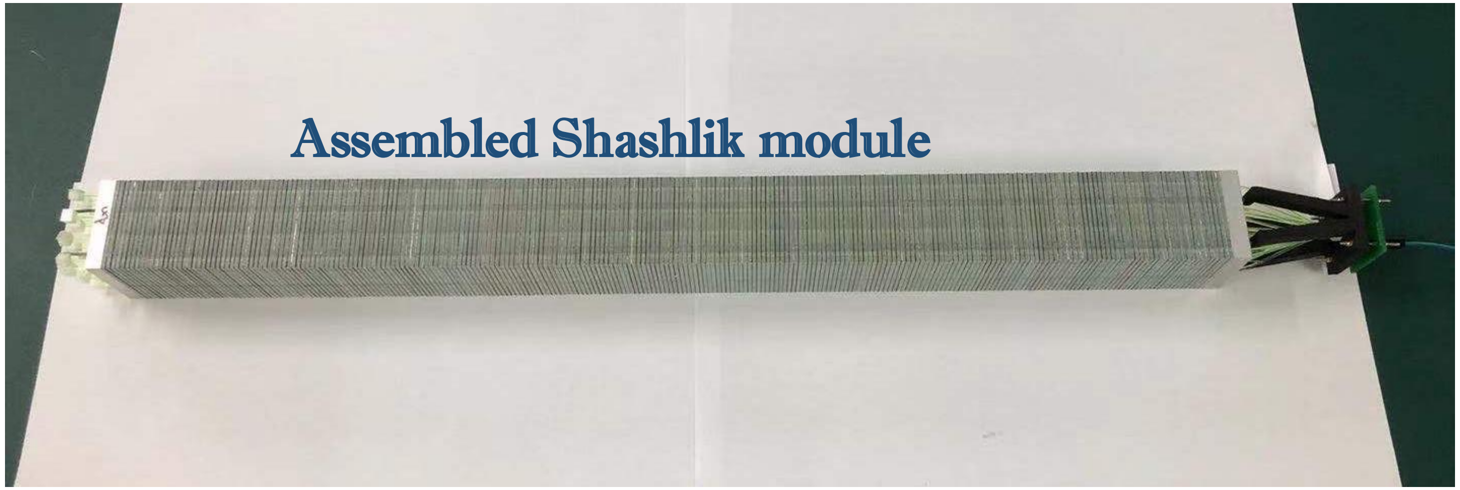

Horizontal test setup

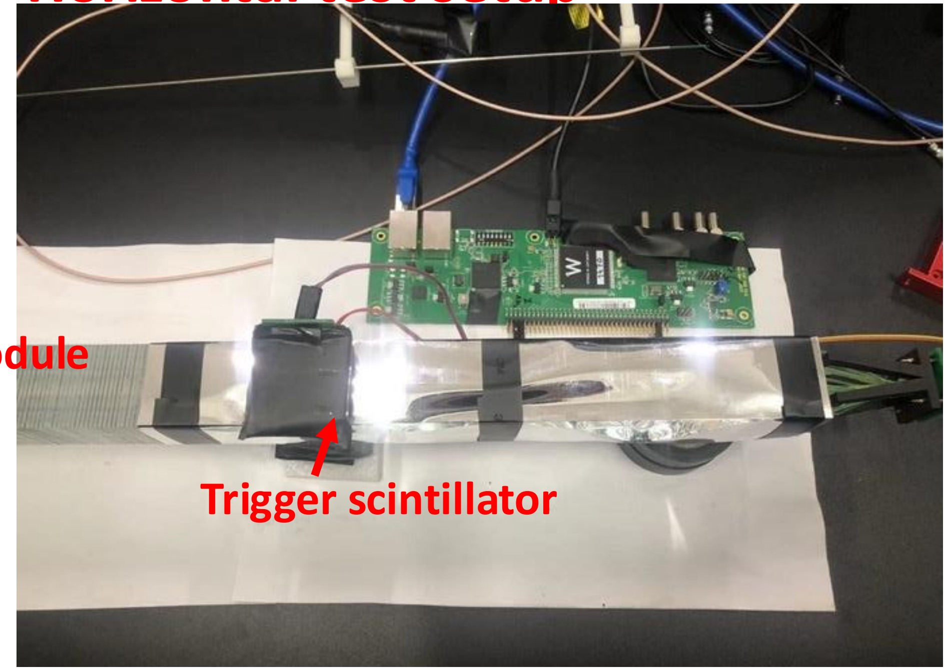

Shashlik module measuring with cosmic ray

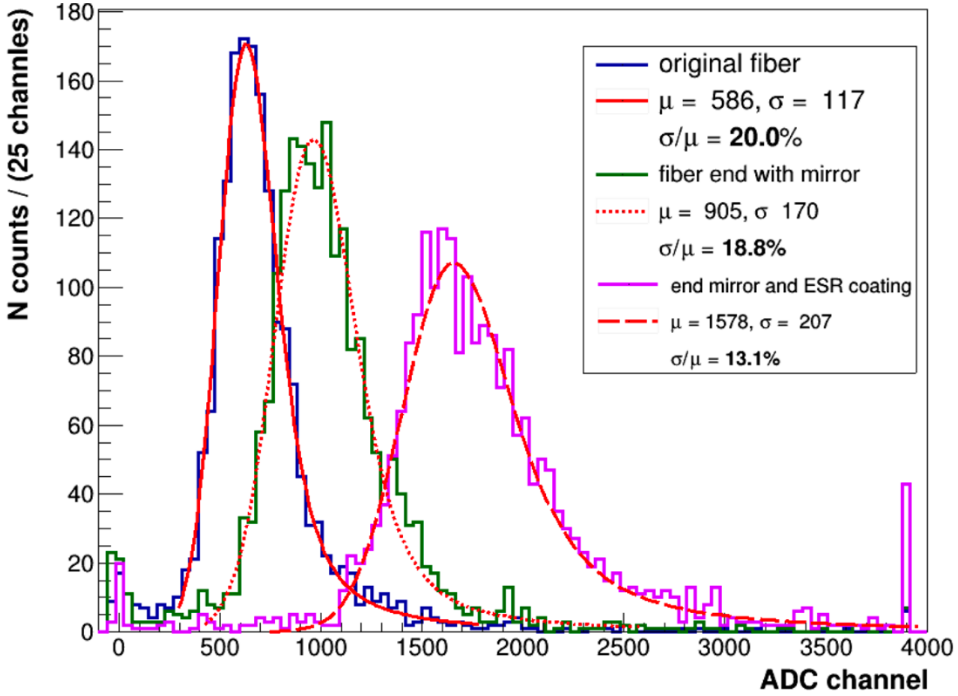

The far forward detector

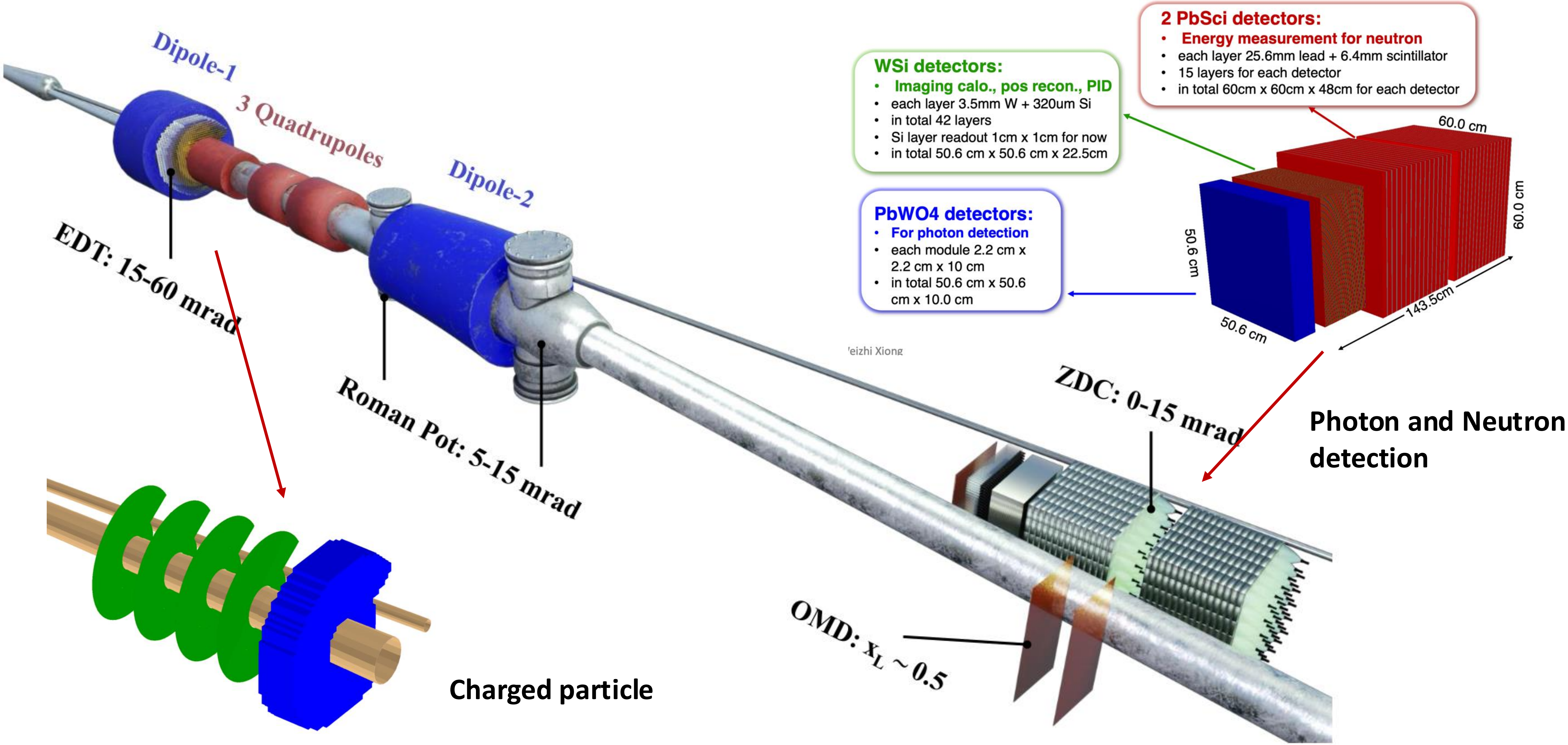

Luminosity and polarization monitor

- Luminosity monitor and polarimetry are largely independent and essentially supportive "experiments"

- Relatively simpler subsystems but complex requirement overall e.g. coordination with accelerator, specific calorimeter and DAQ systems, etc.

- Geant4 simulation is ongoing

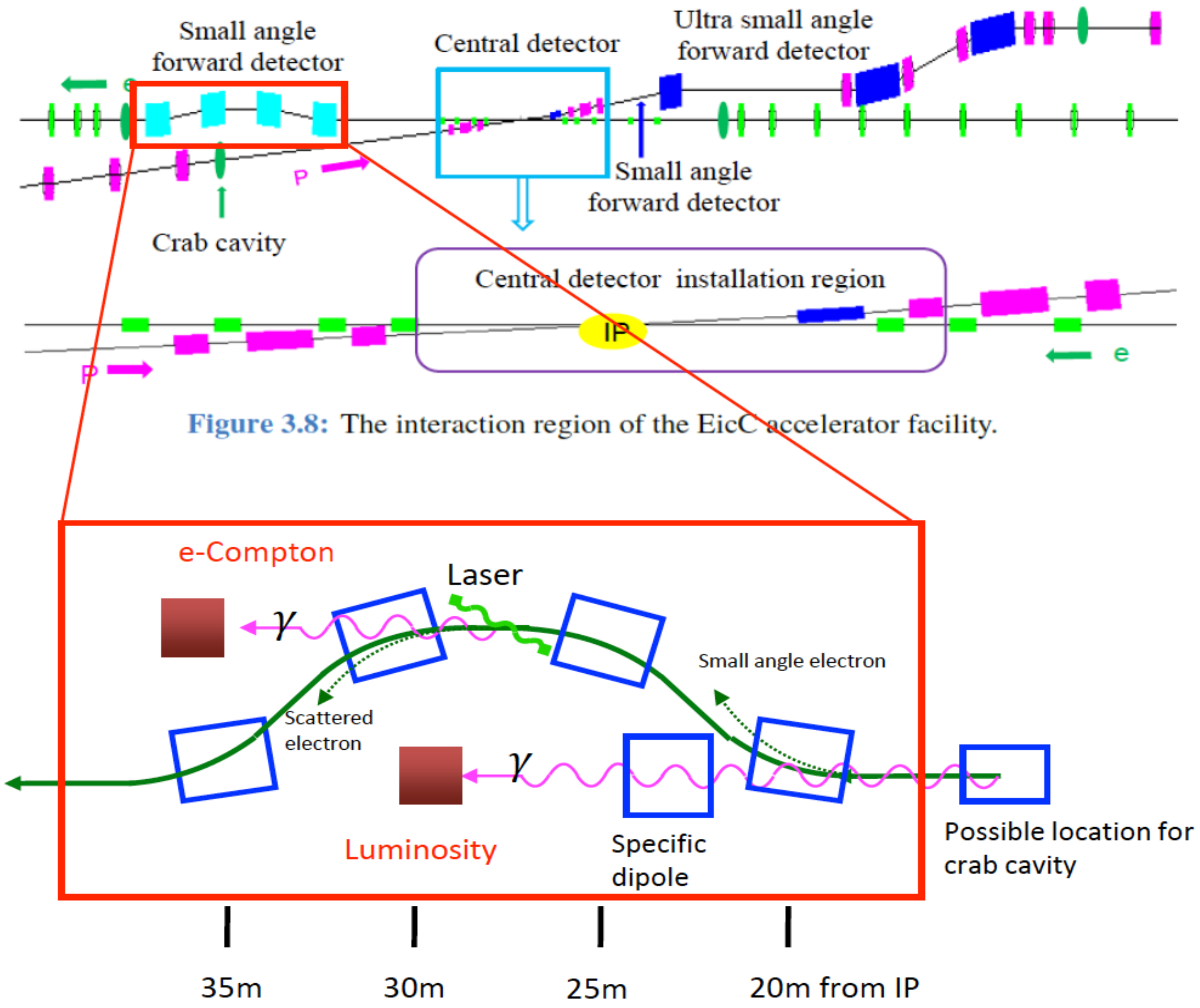

Lab developement

Clean rooms of ISO6 and ISO7 (in total of 200 m^2) for detector assembling @ lanzhou

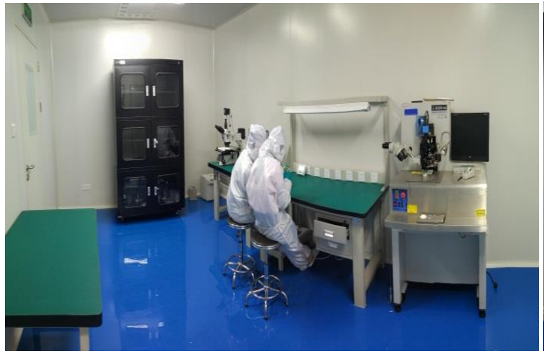

~200 m^2 lab in Huizhou
Budget: ~2M/per year from IMP

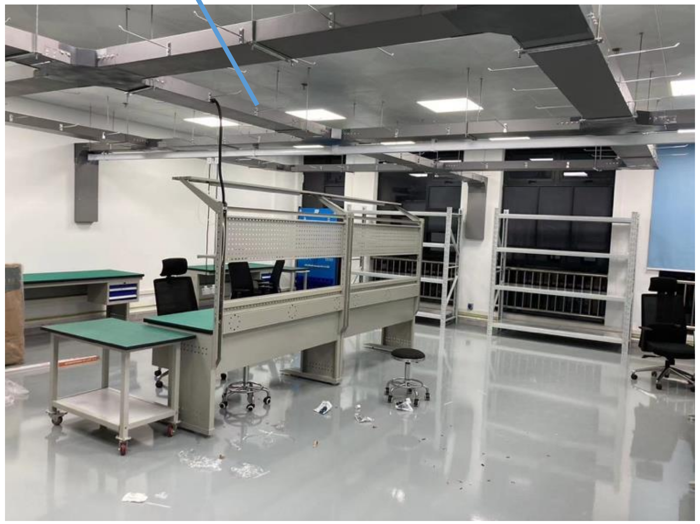

Preliminary Timeline of EicC

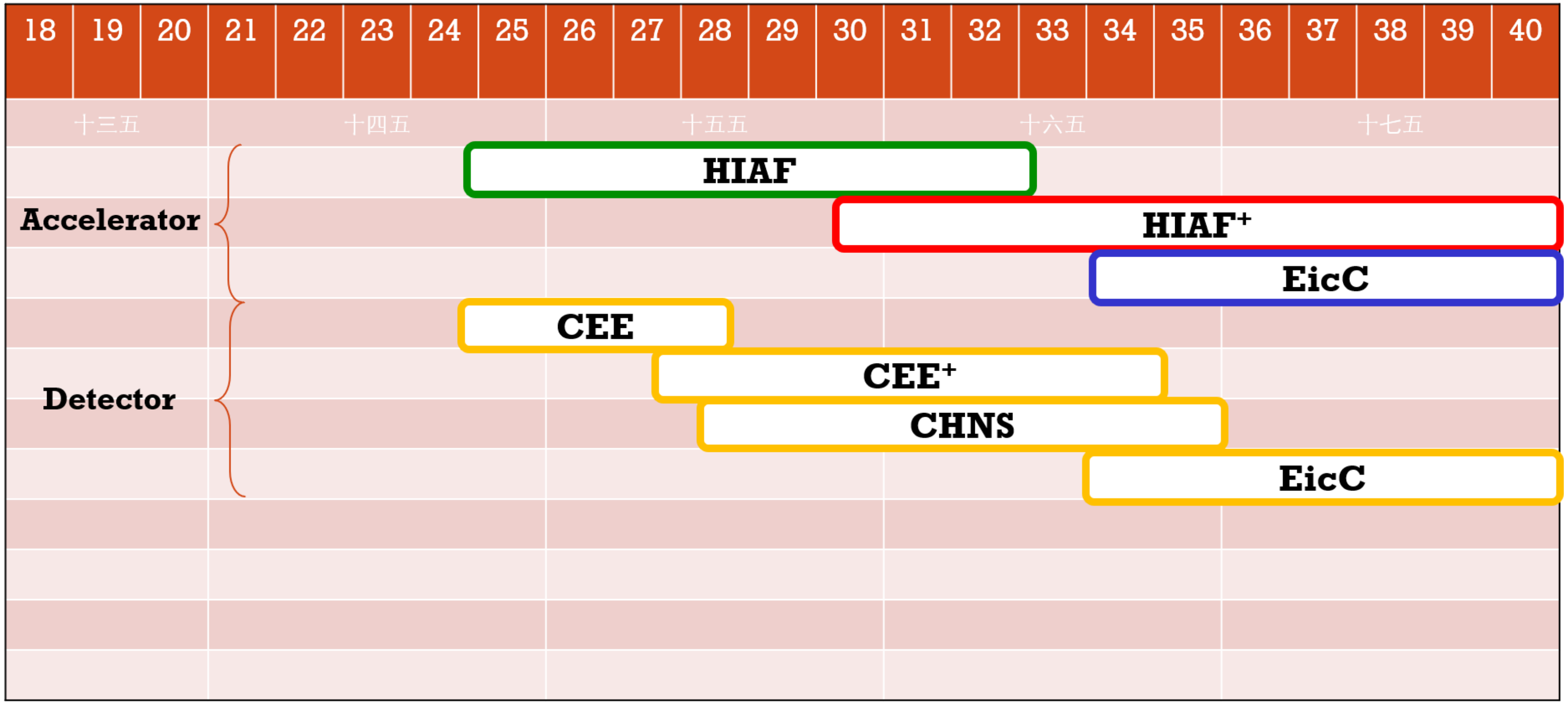

- HIAF is half way through its construction,
- 2021: EicC white paper published,
- 2024: Aim to finish the Conceptual Design Report (CDR) of EicC,
- 2026-2030: Hope to get support by the next five-year plan.

Summary

- An electron-ion collider has been proposed in China, based on the further upgrade of HIAF
- Moderate energy (electron beam 3.5 GeV, proton beam 20 GeV) covers the region (x) between us-EIC and JLab
- High precision measurements of nucleon structures
- Many interesting physics topics are under development and studying
- Research and development of the EicC detectors are ongoing,
- The Concept Design Report (CDR) is expected in 2024.

Thanks!

Office area in Huizhou, Guangdong ready to be used

Backup

Key features of Eic

➢Complementary to JLab@12GeV and US-EIC:

- ✓ Luminosity: $10^{33} cm^{-2} s^{-1}$;
- ✓ Polarization: electrons →70%, ^2D & ^3He

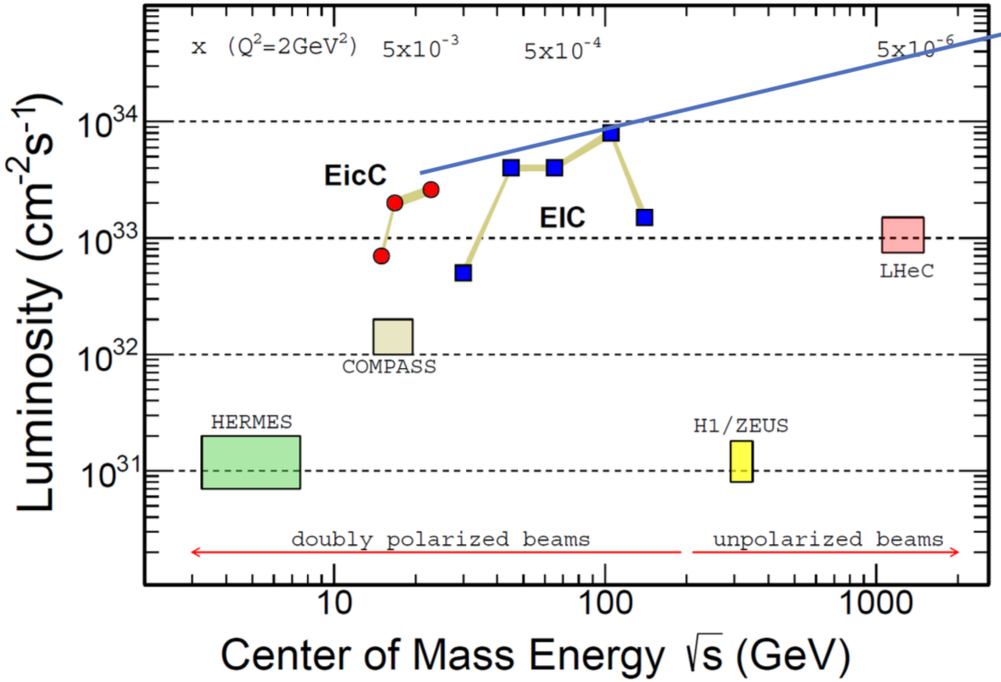

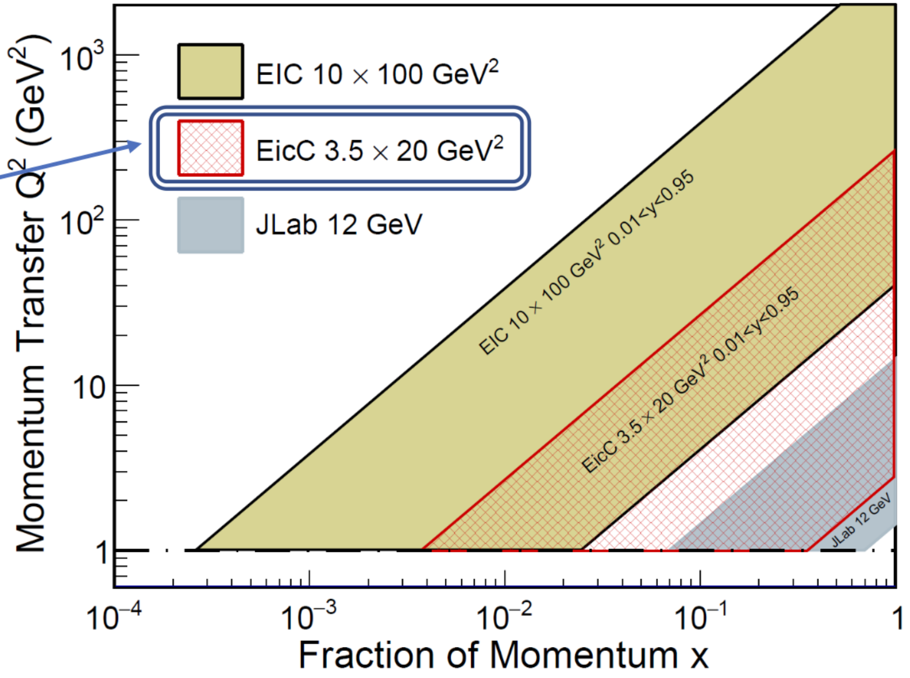

$\sqrt{s} \sim 17$GeV, $2\text{x}10^{33}$/s/cm^2

◆ Some overlap with JLab@24GeV

Spin decomposition

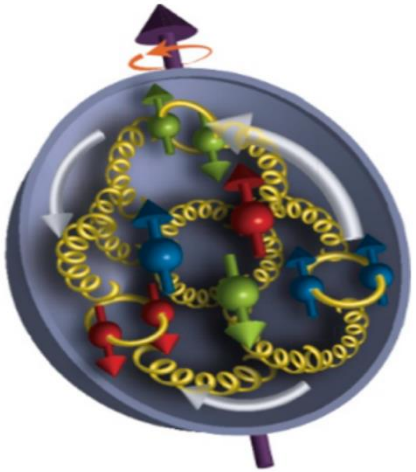

$$\frac{1}{2} = \frac{1}{2}\Delta\Sigma(\mu) + \Delta G(\mu) + L_{Q+G}(\mu)\,,$$

quarks gluon orbital angular momenta

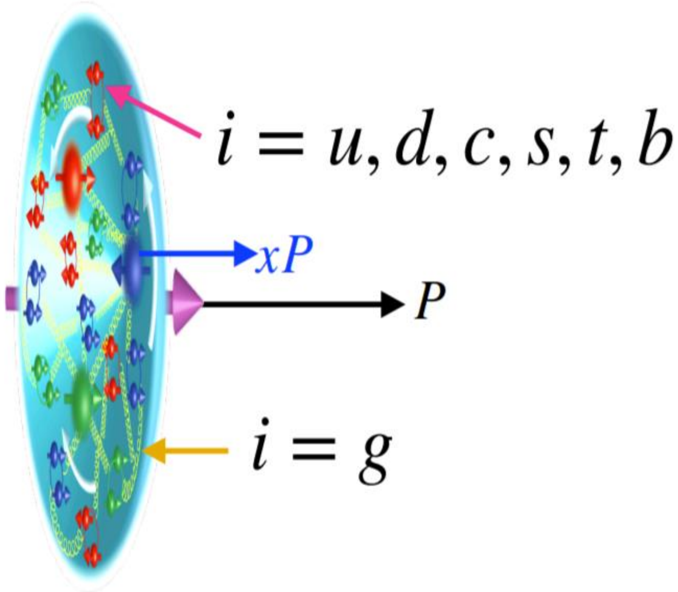

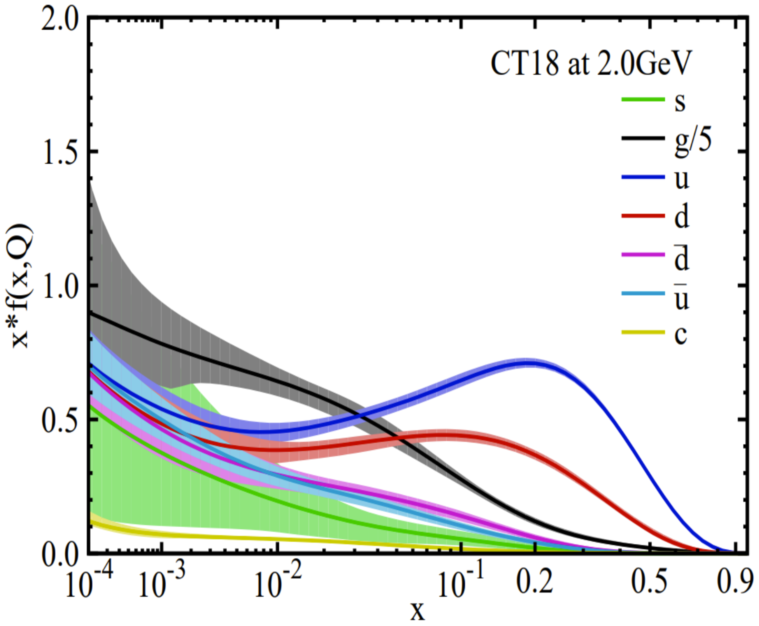

- ➢ By DIS, we can measure the nucleon parton distribution function in momentum space: F(x)
- ➢ Similarly, to measure the $\Delta\Sigma(\mu)$, we need to know the parton distribution function in spin space: g(x)

Structure functions and PDFs : Polarized case

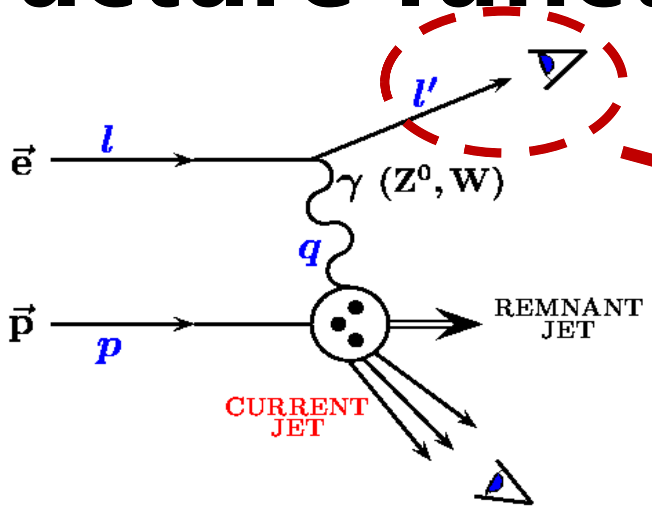

Only scattered leptons are detected

Experimental observables

$$\frac{1}{2}\left[\frac{d^2\sigma^{\rightleftarrows}}{dx\,dQ^2} - \frac{d^2\sigma^{\rightrightarrows}}{dx\,dQ^2}\right] \simeq \frac{4\pi\,\alpha^2}{Q^4} y\,(2-y)\,g_1(x,Q^2)$$

beam/target helicity flips

Quark-Parton Model QPM

PDFs

Polarized pdfs

Helicity distribution

$\Delta q = q^{\uparrow}(x) - q^{\downarrow}(x)$

$$g_1(x) = \frac{1}{2}\sum_q e_q^2 \Delta q(x).$$

Flavor decompositions

- With pure γ exchange in inclusive DIS:

$$g_1^P = \frac{1}{2}\left(\frac{4}{9}(\Delta u + \Delta\bar{u}) + \frac{1}{9}(\Delta d + \Delta\bar{d}) + \frac{1}{9}(\Delta s + \Delta\bar{s})\right)$$
$$g_1^n = \frac{1}{2}\left(\frac{1}{9}(\Delta u + \Delta\bar{u}) + \frac{4}{9}(\Delta d + \Delta\bar{d}) + \frac{1}{9}(\Delta s + \Delta\bar{s})\right)$$

Hmm … No third kind of nucleon … No...

- Assumption: SU(3) flavor symmetry
  - ✓ Additional inputs from β-decay of neutron and hyperons

$\Delta u + \Delta d - 2\,\Delta s$ $\quad\quad$ $\Delta u + \Delta d$

A way out:

SIDIS measurements: with the initial quark flavor tagged
Fragmentation Functions needed

Probing gluon distributions

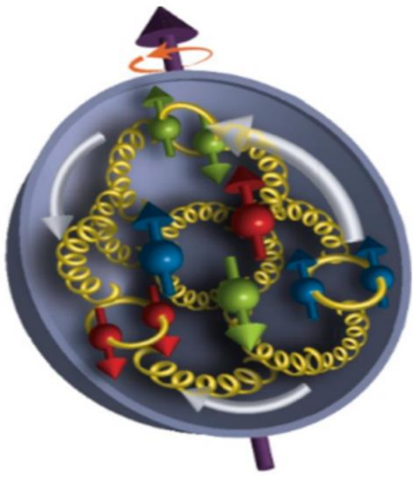

$$\frac{1}{2} = \frac{1}{2}\Delta\Sigma(\mu) + \Delta G(\mu) + L_{Q+G}(\mu)\,,$$

quarks gluon orbital angular momenta

- Heavy-flavor quarks produced at leading-order via boson-gluon fusion
- Investigate charm production + constraints to gluon (n)PDF
  - High-x_B charm production offers more constraint w.r.t. inclusive-only measurements

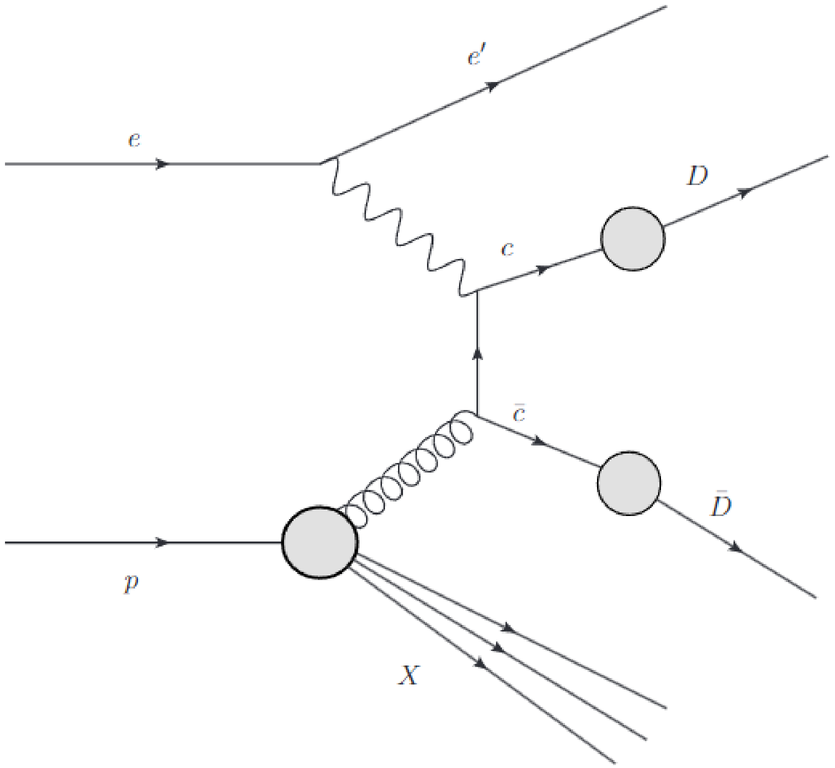

Impact on the proton gluon PDF

- Impact on the unpolarized proton gluon PDF g(x, Q2) using reweighting techniques.
- We focus on the most recent CTEQ PDF set .

In the context of collinear factorization, the structure functions can be computed as a convolution of (p)PDFs $(\Delta)f_j$ and perturbative coefficient functions $(\Delta)c_{k,j}$:

$$F^c_{[1,2]}(x, Q^2) = \sum_{j=g,q,\bar{q}} \int_x^{z_{\max}} \frac{dz}{z} f_j\left(\frac{x}{z}\right) c_{[1,2],j}(z, Q^2), \quad (7)$$

$$g^c_1(x, Q^2) = \sum_{j=g,q,\bar{q}} \int_x^{z_{\max}} \frac{dz}{z} \Delta f_j\left(\frac{x}{z}\right) \Delta c_{1,j}(z, Q^2), \quad (8)$$

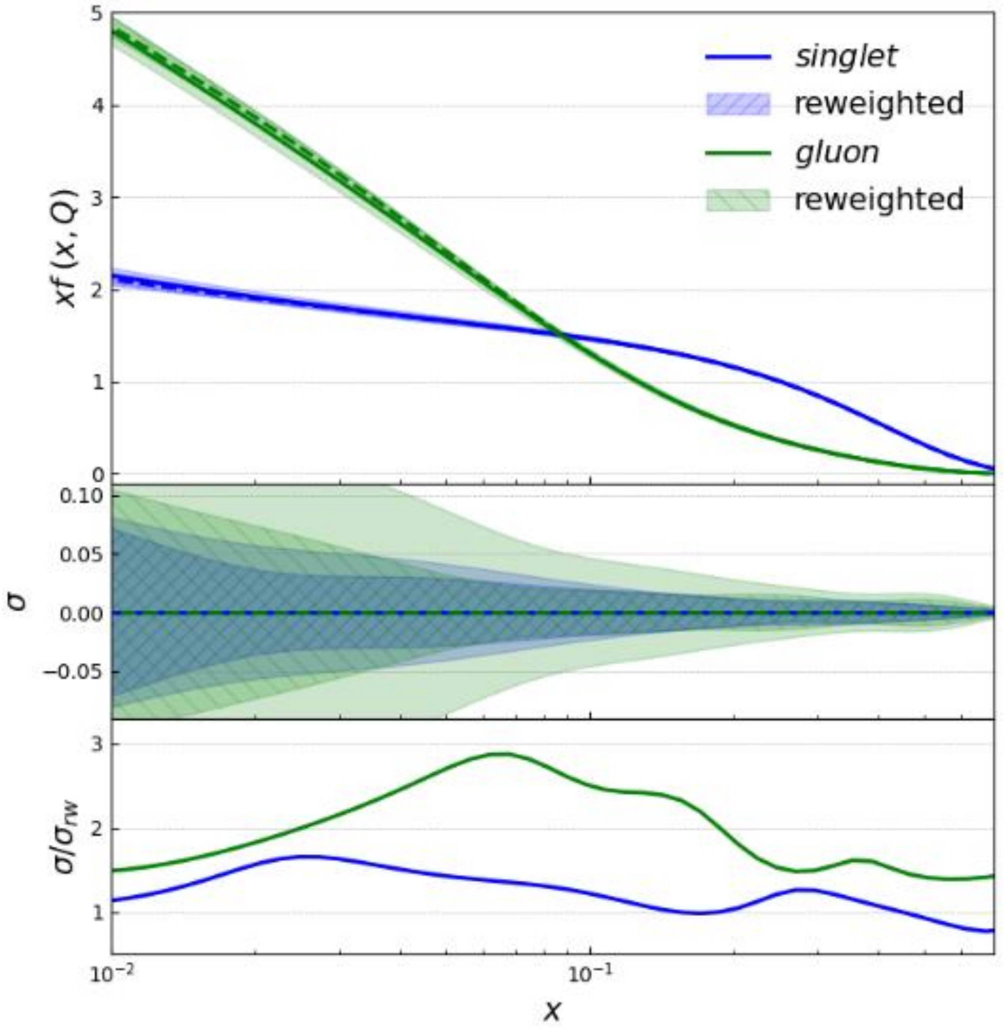

Impact on CTEQ singlet Σ and gluon g PDFs using a NLO computation.

Gluon helicity distribution

One can perform double spin asymmetry ALL measurements in the e+p → e′ +D^0 +X process to access the gluon helicity distribution:

$$A_{LL}^{\vec{e}+\vec{p}\to e'+D^0+X} = \frac{1}{P_e P_p}\frac{N^{++} - N^{+-}}{N^{++} + N^{+-}},$$

$$= \frac{\Delta g(x,Q) * f(g \to D\hat{}0\,)}{g(x,Q) * f(g \to D\hat{}0\,)} = \Delta g/g$$

With lower center-of-mass energy, the EicC will push the measurement in the relatively high-x region, where Δg/g is supposed to be larger compared to the small-x region.

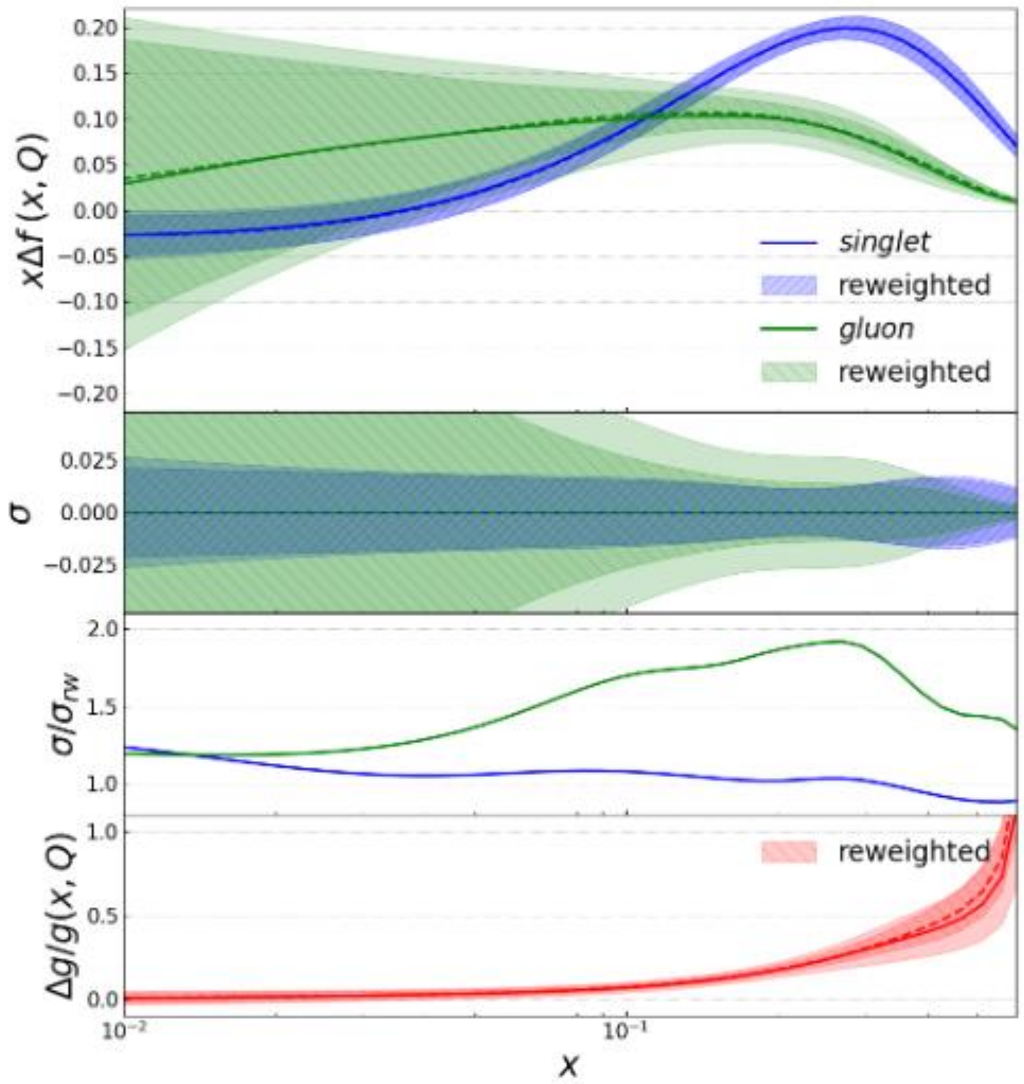

The TMDs

PDF 1D

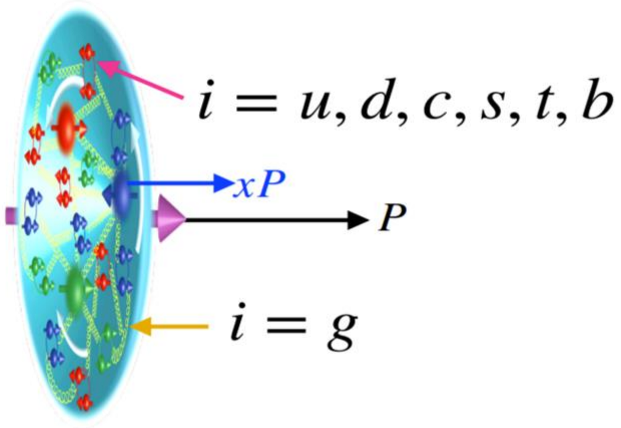

$xf_1^u(x)$

TMD PDF 3D

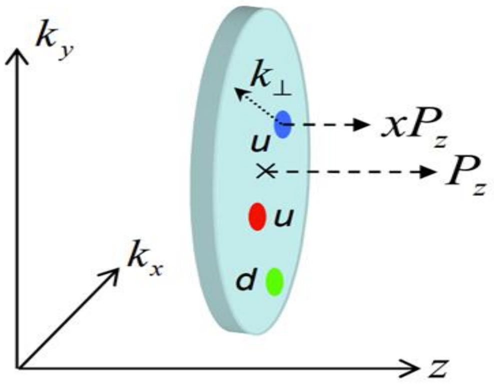

$xf_1^u(x, p_T^2)$

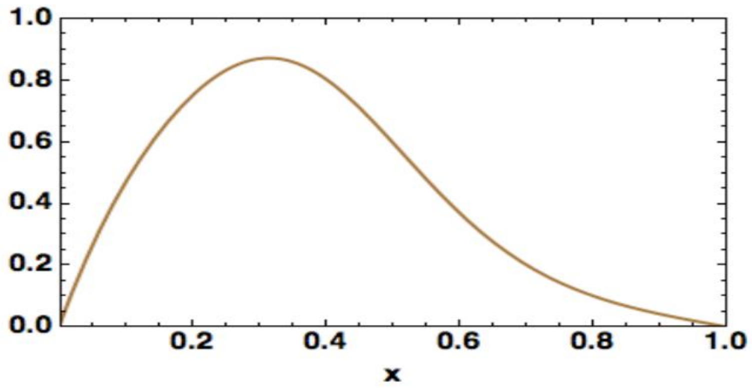

Standard collinear PDF

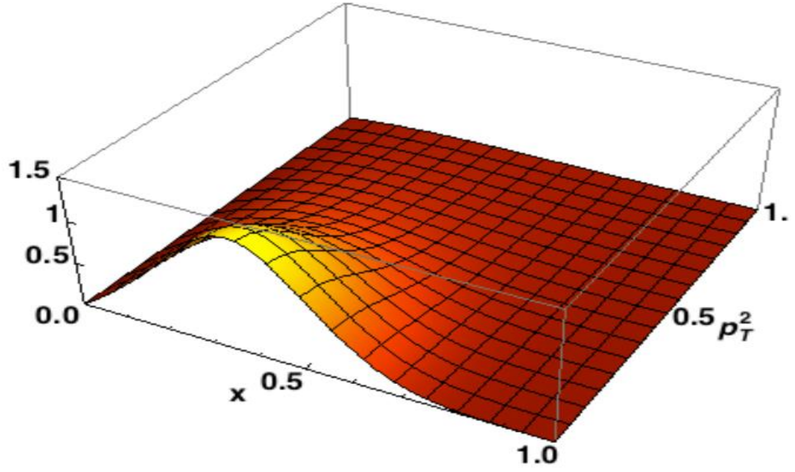

TMD

A. Bacchetta, F. Conti, M. Radici, Phys.Rev. D78 074010 (2008)

Separation of Collins, Sivers and Pretzelosity through azimuthal angular dependence

$$A_{UT}(\varphi_h^l, \varphi_S^l) = \frac{1}{P}\frac{N^{\uparrow} - N^{\downarrow}}{N^{\uparrow} + N^{\downarrow}}$$

$$= A_{UT}^{Collins}\sin(\phi_h + \phi_S) + A_{UT}^{Sivers}\sin(\phi_h - \phi_S)$$

$$+ A_{UT}^{Pretzelosity}\sin(3\phi_h - \phi_S)$$

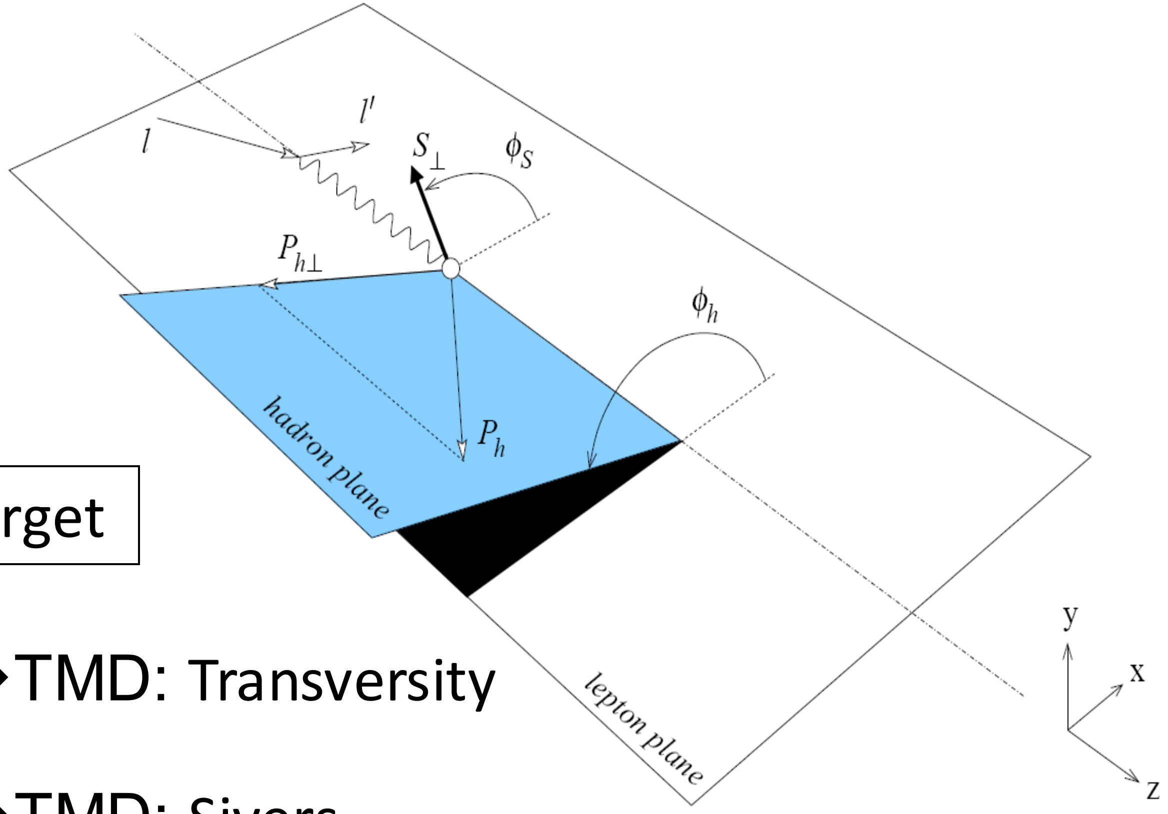

UT: **U**npolarized beam + **T**ransversely polarized target

$$A_{UT}^{Collins} \propto \langle \sin(\phi_h + \phi_S) \rangle_{UT} \propto h_1 \otimes H_1^\perp$$ →TMD: Transversity

$$A_{UT}^{Sivers} \propto \langle \sin(\phi_h - \phi_S) \rangle_{UT} \propto f_{1T}^\perp \otimes D_1$$ →TMD: Sivers

$$A_{UT}^{Pretzelosity} \propto \langle \sin(3\phi_h - \phi_S) \rangle_{UT} \propto h_{1T}^\perp \otimes H_1^\perp$$ →TMD: Pretzelosity

J/Psi production at EicC

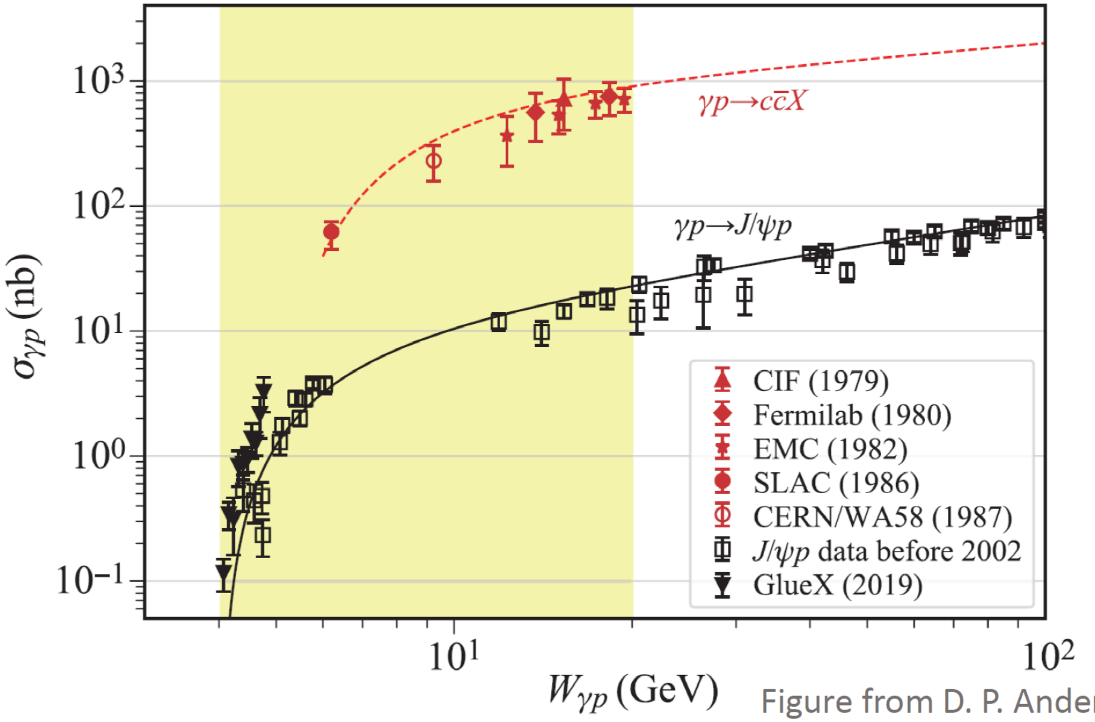

Figure from D. P. Anderle et al. Front.Phys.16(2021)64701

For W=10-20 GeV,

- Photoproduction: $\sigma(\gamma p \to J/\psi p) \sim O(10\text{ nb})$, (no resonant enhancement considered), $\sigma(\gamma p \to c\bar{c}X) \sim 50\sigma(\gamma p \to J/\psi p)$
- Leptoproduction: cross sections are roughly two orders of magnitude (α) smaller
- For an integrated luminosity of 50 fb^{-1}, no. of J/ψ is $\sim O(10^7 - 10^8)$; many more open-charm hadrons D and Λ_c

J/ψ production at EicC

- J/ψ production is important to study
  - Multi-quark states (Pc)

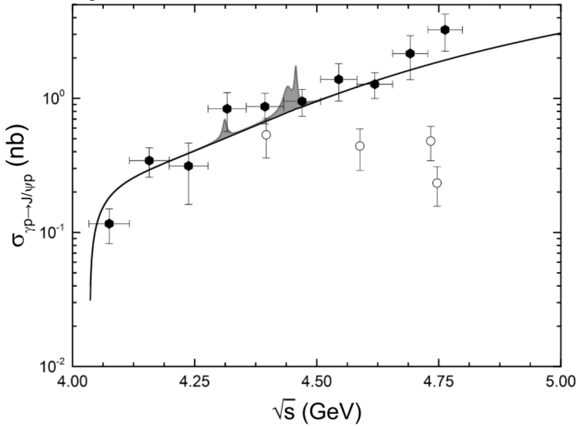

  - Kinematic effect (CUSP)

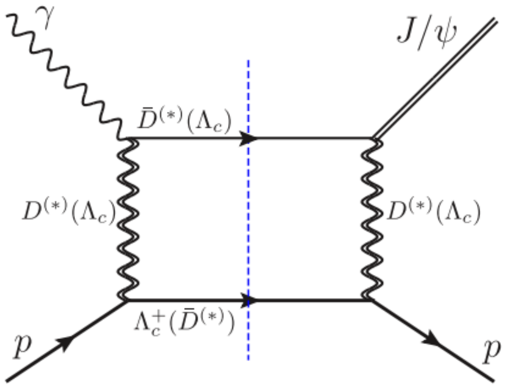

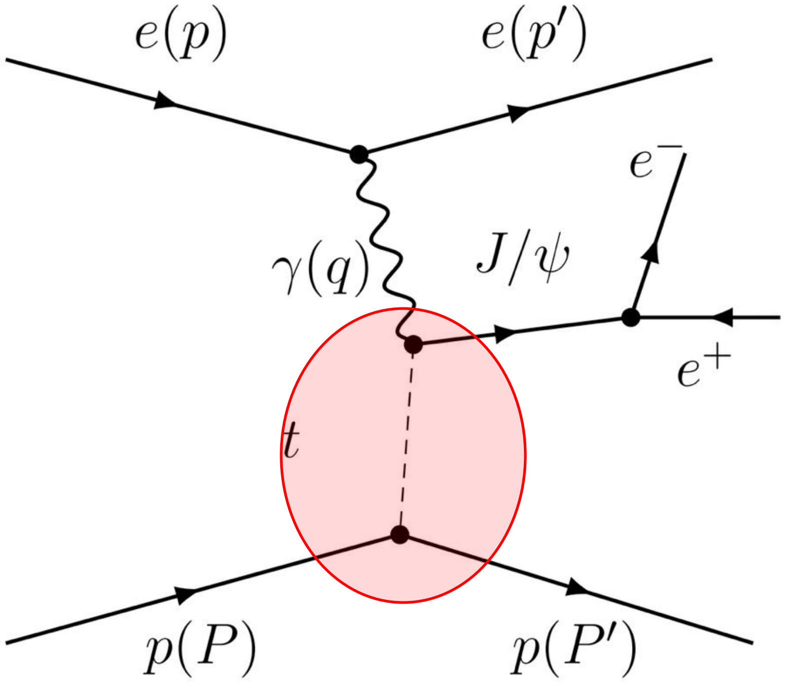

ep →epJ/ψ → e^+e^- or ($\mu^+\mu^-$)

Simulation setup

Detection efficiency

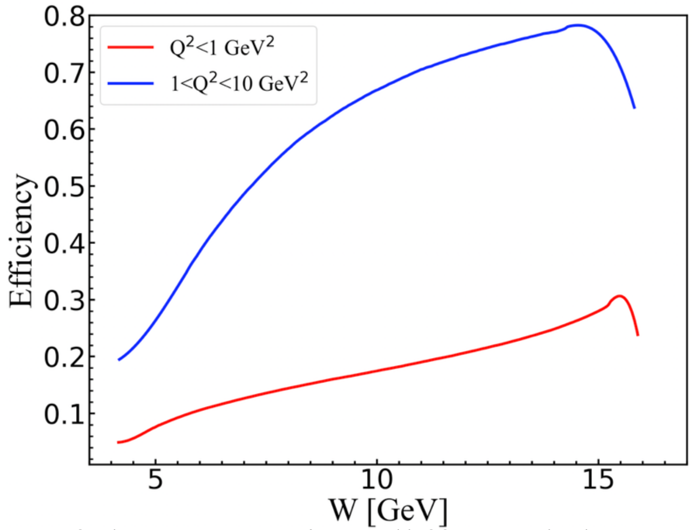

- We adopt eSTARLight event generator with two improvements at near-threshold
- With the input of t-dependent photoproduction cross sections, the differential cross section of exclusive meson electroproduction:

$$\frac{d\sigma_{ep\to eVp}}{dQ^2dydt} = \Gamma_T(1+\epsilon R_L)f(Q^2)\frac{d\sigma_{\gamma p\to eVp}}{dt}$$

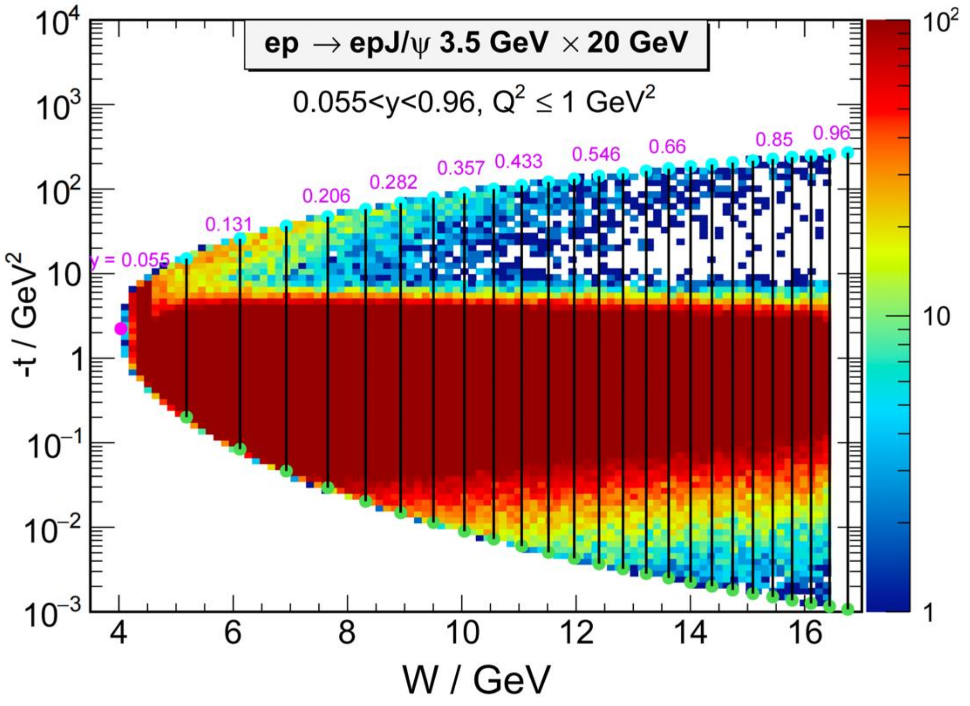

t dependence of the $\gamma p \to J/\psi p$ differential cross section as indicated on the figure.

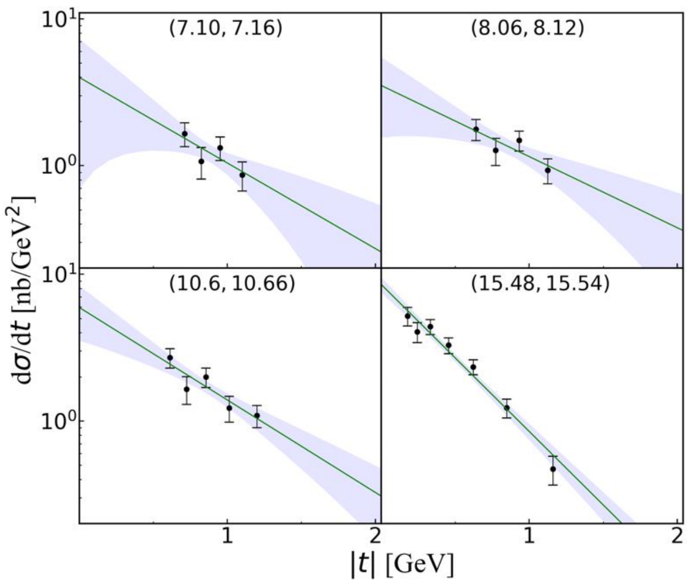

Upsilon production at EicC

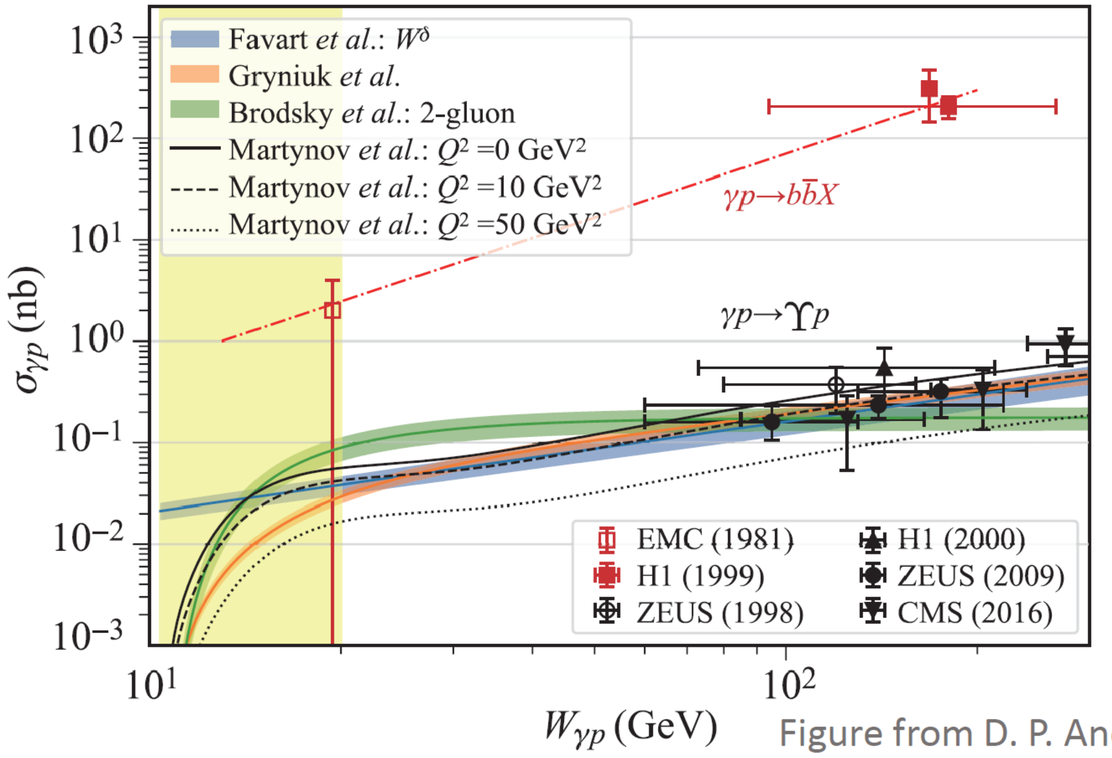

Figure from D. P. Anderle et al. Front.Phys.16(2021)64701

For W=15-20 GeV,

- Photoproduction: $\sigma(\gamma p \to \Upsilon p) \sim O(10 \text{ pb})$ (no resonant enhancement considered), $\sigma(\gamma p \to b\bar{b}X)$ is about two orders higher
- Electroproduction: roughly two orders of magnitude (α) smaller, $\sim O(0.1 \text{ pb})$
- For an integrated luminosity of 50 fb^{-1}, no. of Υ is $\sim O(10^4)$;

Exotic states production at EicC

- Cross section estimates for exclusive reactions assuming VMD (highly model-dependent)

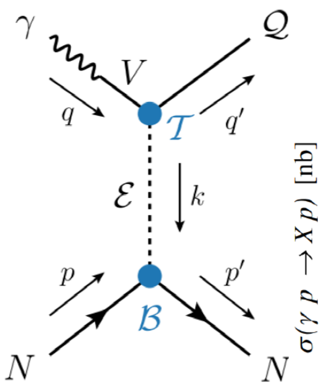

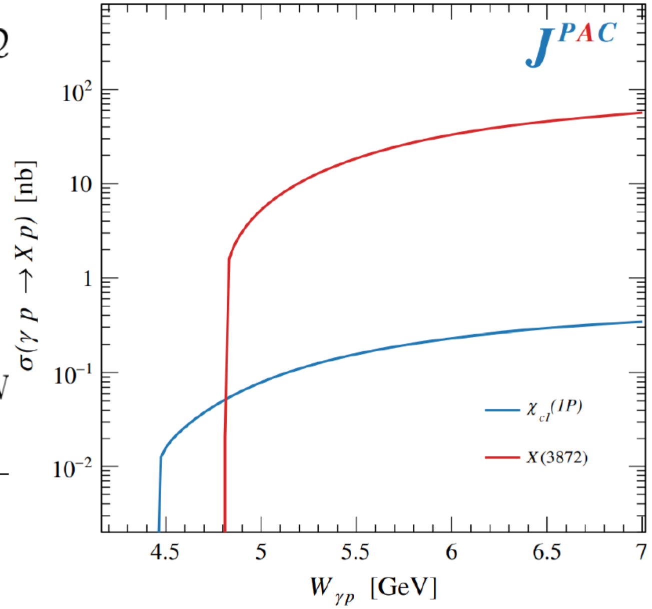

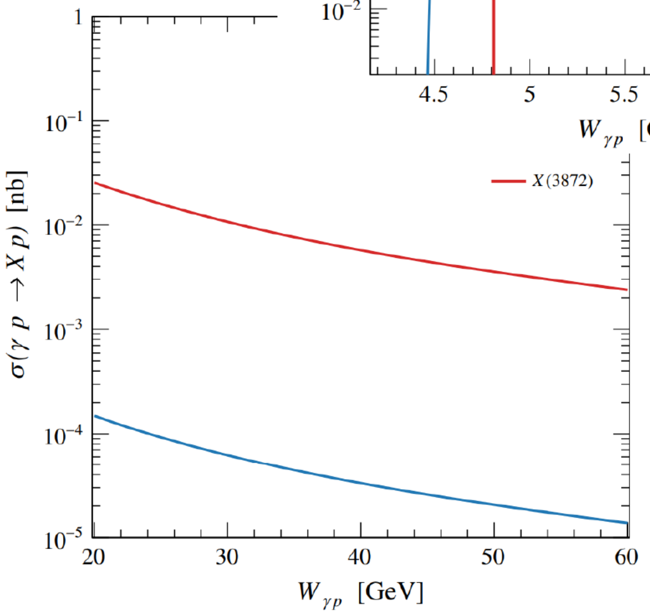

- Estimated events for EicC (50 /fb)

Exotic states	Production/decay processes	Detection efficiency	Expected events
$P_c(4312)$	$ep \to eP_c(4312)$ $P_c(4312) \to pJ/\psi$ $J/\psi \to l^+l^-$	~30%	15–1450
$P_c(4440)$	$ep \to eP_c(4440)$ $P_c(4440) \to pJ/\psi$ $J/\psi \to l^+l^-$	~30%	20–2200
$P_c(4457)$	$ep \to eP_c(4457)$ $P_c(4457) \to pJ/\psi$ $J/\psi \to l^+l^-$	~30%	10–650
$P_b(\text{narrow})$	$ep \to eP_b(\text{narrow})$ $P_b(\text{narrow}) \to p\Upsilon$ $\Upsilon \to l^+l^-$	~30%	0–20
$P_b(\text{wide})$	$ep \to eP_b(\text{wide})$ $P_b(\text{wide}) \to p\Upsilon$ $\Upsilon \to l^+l^-$	~30%	0–200
$\chi_{c1}(3872)$	$ep \to e\chi_{c1}(3872)p$ $\chi_{c1}(3872) \to \pi^+\pi^- J/\psi$ $J/\psi \to l^+l^-$	~50%	0–90
$Z_c(3900)^+$	$ep \to eZ_c(3900)^+n$ $Z_c^+(3900) \to \pi^+ J/\psi$ $J/\psi \to l^+l^-$	~60%	90–9300

JPAC, PRD102(2020)114010

Proton mass study

Mass decomposition [Ji, 95]

$$M = \underbrace{M_q + M_m}_{\text{Quark}} + \underbrace{M_g + M_a}_{\text{Gluon}}$$

M_q : quark energy
M_m : quark mass (condensate)
M_g : gluon energy
M_a : trace anomaly

- M_q and M_g constrained by PDFs.
- M_m via πN low energy scattering.
- M_a via threshold production of J/Ψ (8.2 GeV; JLab) and Υ (12 GeV);
- Threshold requires low CoM energy. (Low y at EIC).
- Complementarity between EicC (and EIC) and lattice. Guideline

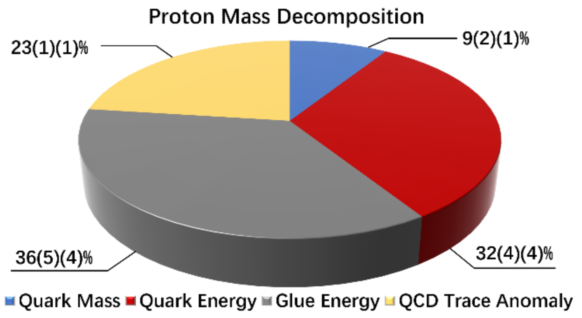

Lattice QCD calculation by Yang et al, 2018

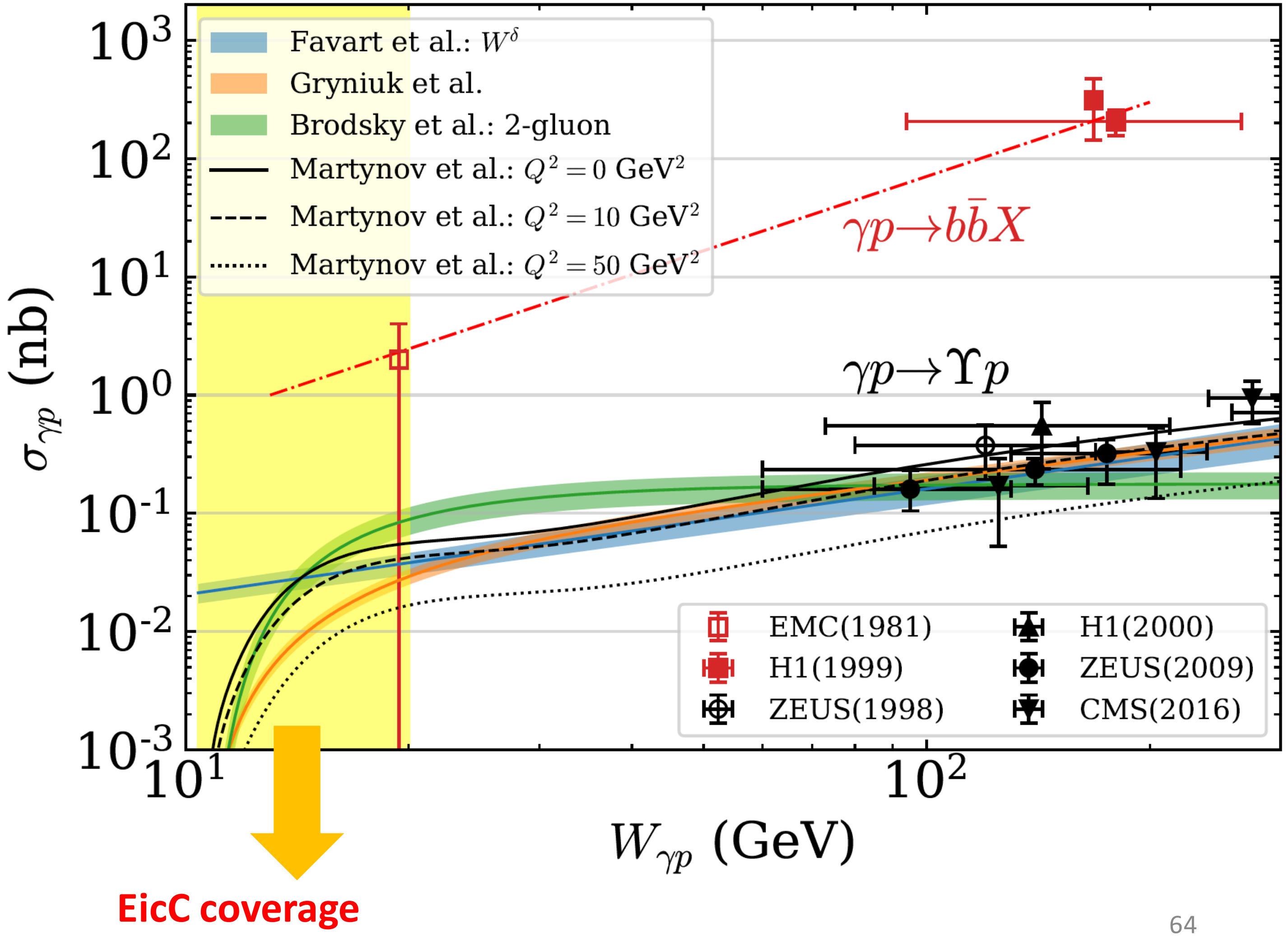

Luminosity and polarization monitor

- Luminosity monitor and polarimetry are largely independent and essentially supportive “experiments”
- Relatively simpler subsystems but complex requirement overall e.g. coordination with accelerator, specific calorimeter and DAQ systems, etc.
- Geant4 simulation is ongoing

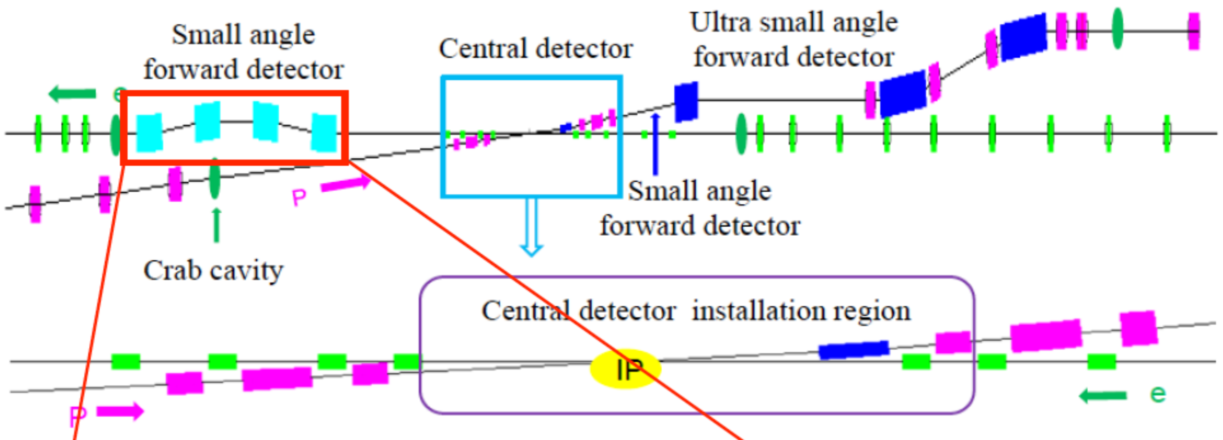

Figure 3.8: The interaction region of the EicC accelerator facility.

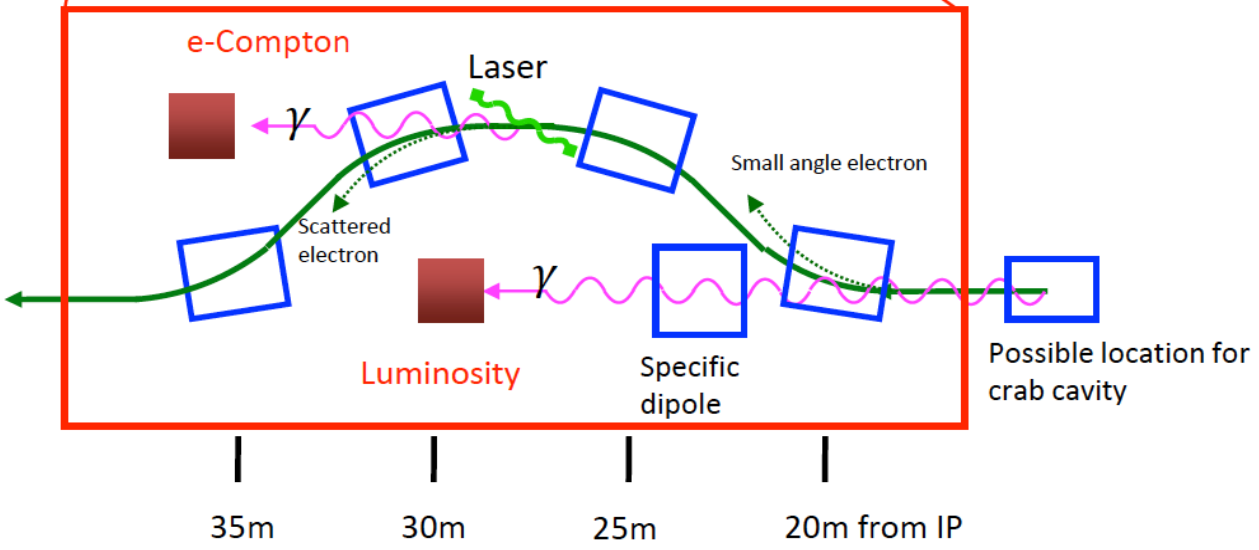

Cosmic Ray Platform

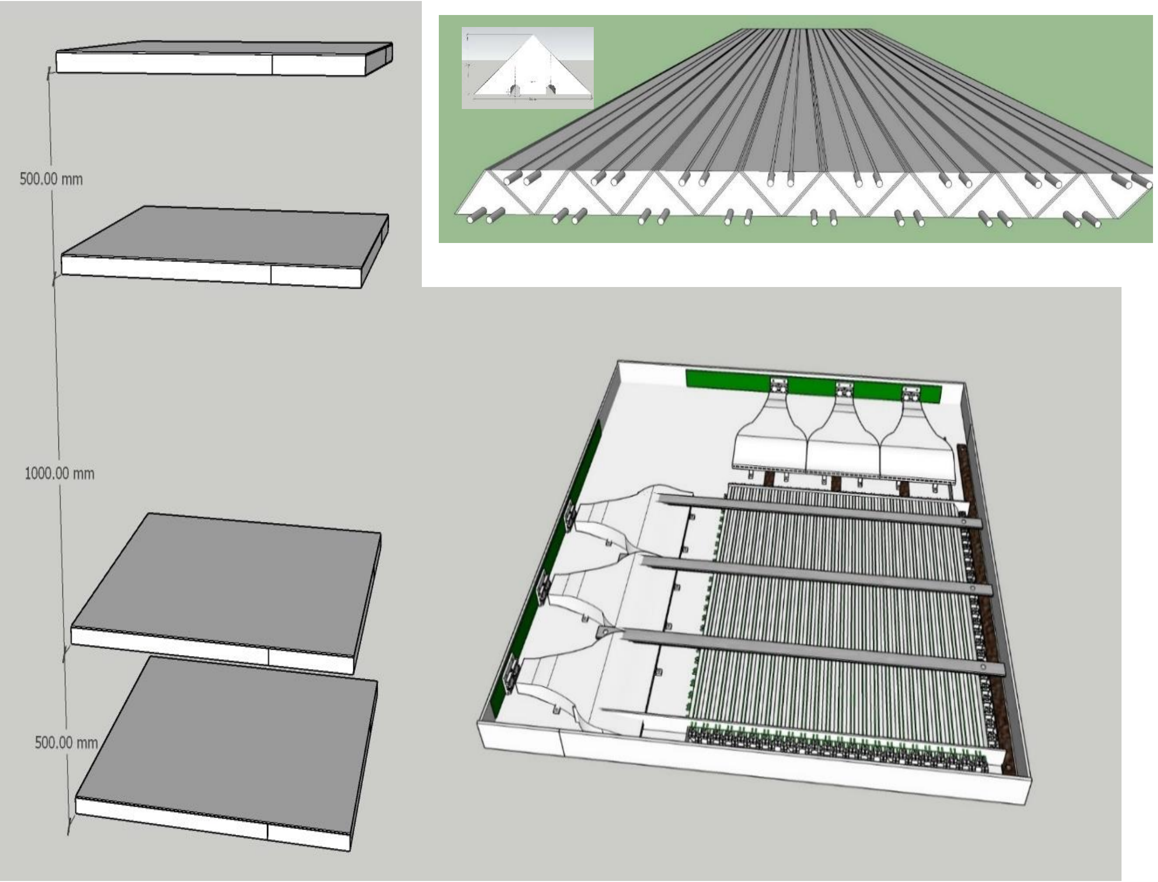

*Cooperation with the EicC USTC group

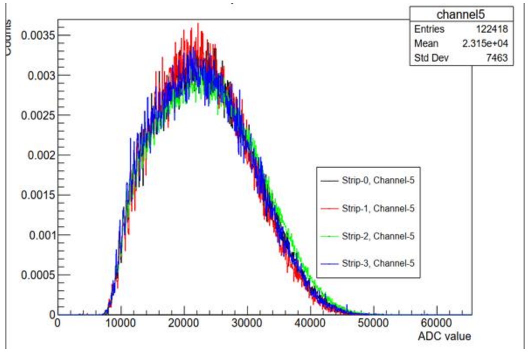

不同批次闪烁体的发光效率

- 宇宙线测试平台：闪烁体 + SiPM, 8 layer (4 layer for x, y each), 探测面积 50cm x 50cm
- One layer：3 module + 1 electronics
- One module：16块EJ-200 + 32根光纤 + 8 SiPM
- 位置分辨~1mm, 时间分辨<100ps

Barrel DIRC Concept Design

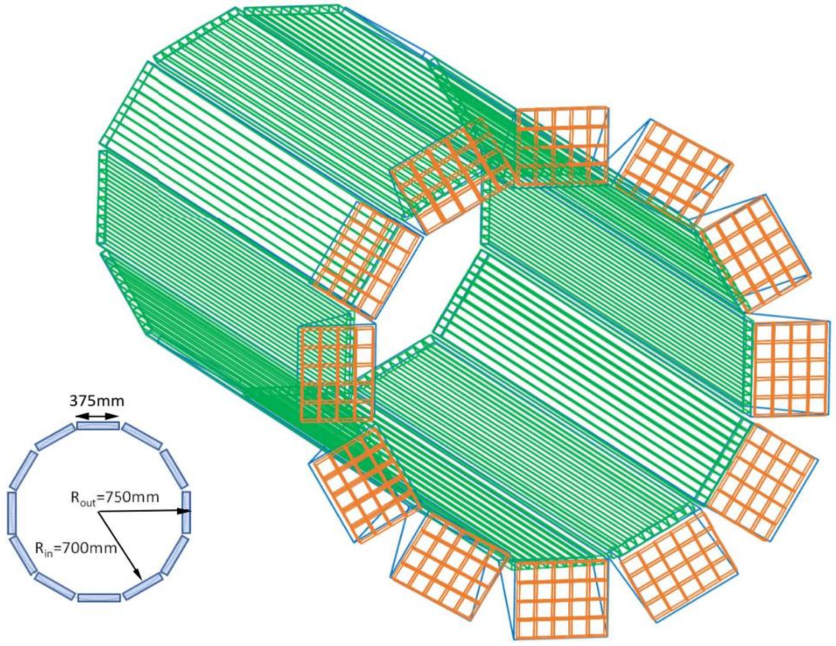

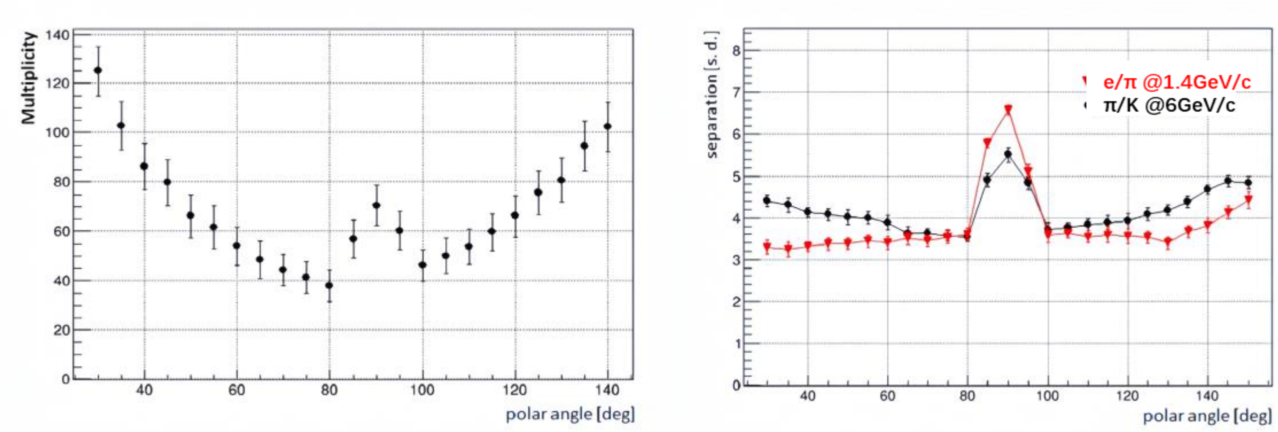

- Quartz radiator bar: 15mm x 17mm x 3300mm
- Expansion volume(EV): 208mm x 340mm x 300mm
- MCP-PMT: Hamamatsu R10754 (pixel size: 5.2mm x 5.2mm) or Photek MAPMT253 (pixel size: 1.6mm x 1.6mm)
- Tray box size: 50mm x 320mm x 4000mm with 6 bar+EV
- 12 trays forms a barrel detector with a minimum radius R = 0.7m
- Focusing: spherical 3-layer lens (Fused silica N-LAK33B) curvature radius: 30cm, Thickness: 10mm

Definition of measured DIRC angular resolution:

$$\sigma_{\theta_c}(\text{photo}) = \sqrt{\sigma_{chrom}^2 + \sigma_{foc}^2 + \sigma_{bar}^2 + \sigma_{trans}^2 + \sigma_{rec}^2}$$

- σ_{chrom}: the dispersion contribution of the quartz radiator (wavelength: 300-700 nm)
- σ_{foc}: error from the optical focusing lens and the pixel size of photosensors
- σ_{bar}: the influence of radiator thickness (flatness) on photon yield and transmission efficiency;
- σ_{trans}: transit fluctuation due to the roughness of the radiator
- σ_{rec}: error from incident particle tracking

dRICH: RICH with “dual” radiators

Dual RICH contains “dual” radiators with different refractive index, which largely expands its PID momentum coverage. The C_2F_6 gas and aerogel are ideal dual radiator options for the π/k identification in large momentum region. The particle passes through the aerogel and the gas sequentially, the induced Cherenkov radiation is focused by the spherical reflector (gray) and forms a halo image at the focal plane, finally readout by the photosensor array. “dual” radiators.

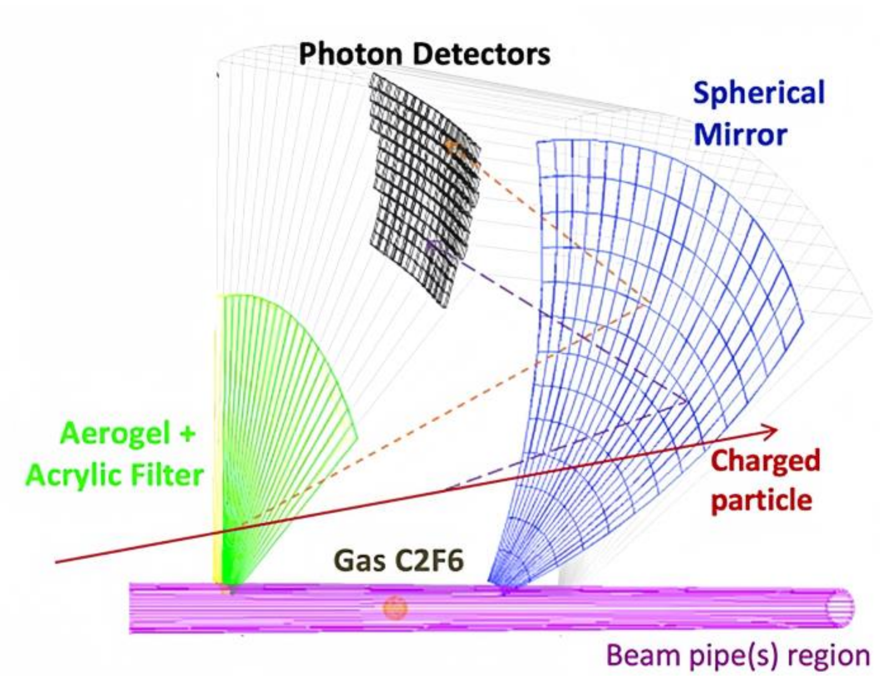

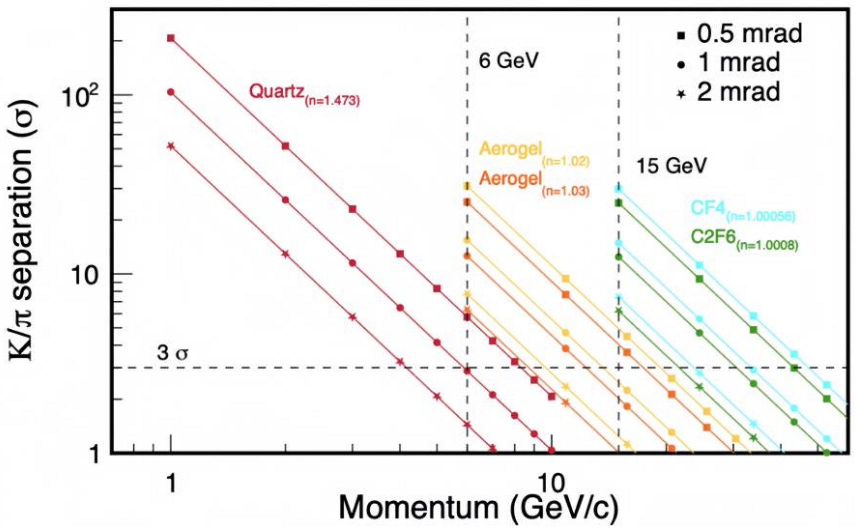

Radiator	Index	Threshold (GeV/c) e	π	k	P
Fused Silica(DIRC)	1.473	0.00047	0.13	0.46	0.87
Aerogel(mRICH)	1.03	0.00213	0.58	2.06	3.92
Aerogel(dRICH)	1.02	0.00254	0.69	2.46	4.67
C_2F_6(dRICH)	1.00080	0.0128	3.49	12.34	23.45
CF_4(dRICH)	1.00056	0.0153	4.17	14.75	28.03
C_4F_{10}(RICH)	1.00014	0.0305	8.34	29.50	56.07

dRICH Design and Simulation

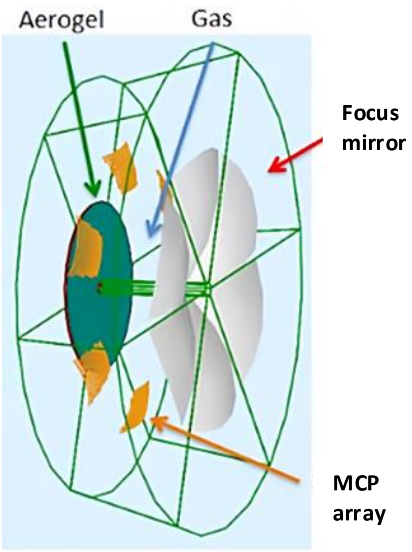

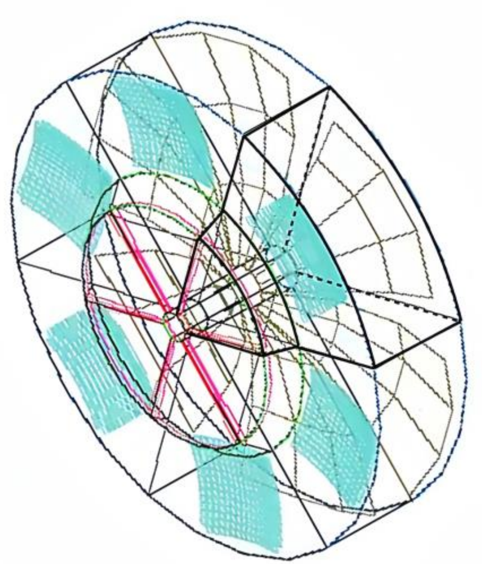

Geometric:
– Length: 2160 mm
– Inner radius: 100 mm
– Outer radius: 1500 mm
– Coverage angle 5-25 degrees

Cherenkov radiator:
– Refractive index: n = 1.03/1.02 (aerogel, 400 nm); n = 1.0008 (C_2F_6)
– Thickness of radiant body: L = 40-50 mm (aerogel), 1600-2000 mm (C_2F_6)

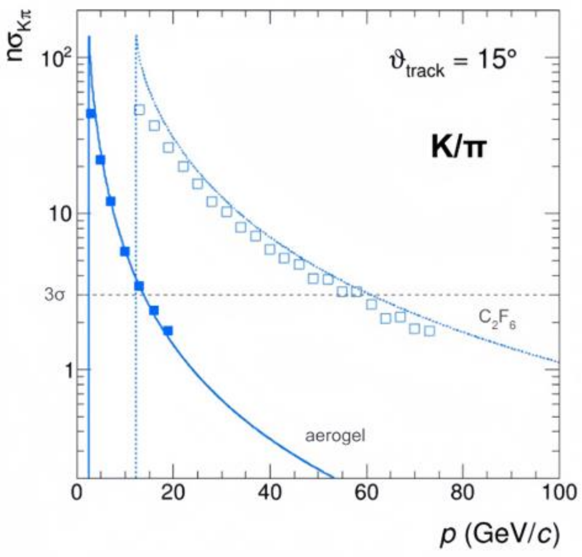

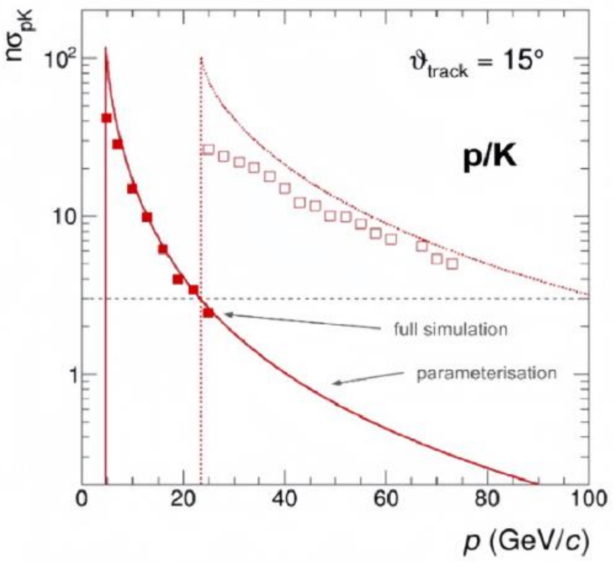

In GEANT4 simulation, the reflectivity of the spherical mirror is set to be 50%, the quantum efficiency of the photosensor is 20%, and its pixel size is 3mm × 3mm. Approximately 60 photons are generated by the aerogel radiator per track. Considering the detection efficiency of the photosensor array, the actual measured number is 3 ~ 5pe. Meanwhile, approximately 200 photons are generated in the gas, with an actual measured number of 30 ~ 40 pe.